jWe thank the referees for their reviews. To facilitate the review process we have copied the reviewer comments in black text. Our responses are in regular blue font. We have responded to all the referee comments and made alterations to our paper (**in bold text**).

Anonymous Referee #1

R1.0) This paper describes a modeling study aimed at understanding the relative role of different oxidants within "oxidation flow reactors" (OFRs), flow tubes that have recently seen a lot of attention in atmospheric chemistry as a way to rapidly expose organic species to the equivalent of hours to days of oxidation. The aim is to assess the extent to which non-tropospherically-relevant oxidation processes may occur within such reactors. The authors conclude that under the vast majority of conditions (especially in field studies), OH oxidation dominates over photolysis and initiation by other oxidants, pointing to its utility as an "OH-only" aging reactor.

R1.1) The chemical modeling is quite comprehensive, and the paper makes a very compelling case for the dominance of OH oxidation for the range of compounds examined. However, this range is also the main limitation of the study – the modeling largely covers lightly-oxidized species only. Hydrocarbons and mono-substituted oxygenates are explored fairly well, but the more oxidized, multifunctional species are not. Such species are significant for two reasons: (1) they are major players in chemistry related to multi-day oxidation processes and secondary organic aerosol (SOA) formation, the main targets of OFR studies, and (2) such multifunctional species are likely to photolyze much more readily than the less-oxidized compounds covered in this work. Thus this work really only shows that OH dominates over photolysis for the oxidation of hydrocarbons and first-generation oxidation projects, but not necessarily for later-generation species. As a result, many of the strongly-worded conclusions in the manuscript, involving the dominance of OH reactions, simply might not be valid after 1-2 generations of oxidation. Specific concerns related to these multifunctional species are:

- R1.1.1) A few di-functional species are included (some C2-C4 species), but nothing like the sort of multi-substituted molecules that models predict to be in SOA (e.g., Johnson et al., Env. Chem 1, 150-165, 2004; Camredon et al., Atmos. Chem. Phys. 7, 5599– 5610, 2007) or have been recently measured using CIMS techniques. In fact even the O/C ratios of aerosol generated within the PAM (e.g., Ortega, Lambe papers) would suggest one functional group for each 1-3 carbon atoms. For these molecules, there is a good chance that several of them will be located on adjacent carbon atoms, potentially leading to conjugated systems with much higher cross sections than from any of the individual functional groups. (The C-C bonds in between these functional groups may also be weakened, increasing dissociation quantum yields.)

We agree that conjugated or multifunctional molecules may have higher absorption cross-sections. However, we believe that species with high absorptivity due to multiple functional groups are also likely to have low photolysis quantum yields, and hence that these species may photolyze at moderate rates, even if they absorb light efficiently. In addition, conjugated species

also have high reactivity toward OH, resulting in an estimated relative importance of their photolysis that is not higher than for the species discussed in the ACPD paper. To discuss these two types of species (multifunctional and conjugated) in detail, we have modified the text at P23555/L8 (this and all other page / line numbers refer to the ACPD version) to read:

"**Unsaturated carbonyls may have much higher absorption cross-sections if their C=C bonds are conjugated with carbonyls. However, according to our following analysis, conjugated unsaturated carbonyl compounds do not often cause problems of non-tropospheric photolysis at 254 nm. Carbonyls have π–π* and n–π* transitions. The former corresponds to high cross-section (typically >10^{-18} cm^2) and typically occurs around or below 200 nm. The latter is forbidden, and thus has weak absorption (cross-section on the order of 10^{-19} cm^2 or lower), and typically occurs around or above 300 nm (Turro et al., 2009). Conjugation usually does not substantially enhance the absorption of n–π* transition, but it does for π–π* transitions (Turro et al., 2009). As a result, through conjugation, the only reason why cross-sections of carbonyls at 254 nm may be elevated above 10^{-18} cm^2 is the red-shift of the maximum absorption wavelength of their π–π* transitions due to conjugation. According to Woodward's rules (Pretsch et al., 2009) and available cross-section data of α,β-unsaturated carbonyls in Keller-Rudek et al. (2015), a conjugation of at least 3–4 double bonds is required for the excitation at 254 nm to dominantly correspond to π–π* transition. Conjugated oxidation intermediates containing at least 3–4 double bonds including C=C bond(s) are virtually impossible to form from aliphatic hydrocarbon oxidation in OFRs. Nevertheless, such intermediates may form via ring-opening pathways of aromatic oxidation (Calvert et al., 2002; Atkinson and Arey, 2003; Strollo and Ziemann, 2013). E,E-2,4-hexadienedial may be regarded as an example of this type of intermediates. Even under assumption of a unity quantum yield, its fraction of photolysis at 254 nm is not much higher than that of aromatic precursors (Fig. 2). Therefore, 254 nm photolysis of conjugated intermediates should not be problematic as long as safer experimental conditions are adopted.**

To our knowledge, the only exception that has strong absorption at 254 nm due to conjugation with <2 double bonds are β-diketones, which may be formed in aliphatic hydrocarbon oxidation, particularly that of long-chain alkanes (Ziemann and Atkinson, 2012). The peculiarity of β-diketones is that their enol form may have a highly conjugated ring structure due to very strong resonance (Scheme S1), and hence cross-sections of the order of 10^{-17} cm^2 at 254 nm (Messaadia et al., 2015). However, even under the assumption of unity quantum yield, the fractional contribution of 254 nm photolysis of acetylacetone (representative of β-diketones) is only slightly larger than for aromatic VOCs (Fig. 2), since its enol form also contains a C=C bond leading to very high reactivity toward OH. Furthermore, we argue that the actual probability that a concrete structural change (in number and type of functional groups, O/C ratio, average C oxidation state etc.) of β-diketones resulting from photoexcitation at 254 nm may be low. As their excitation at 254 nm corresponds to π–π* transition, their rigid ring structure likely hinders cyclic structural change at the 1st singlet excited state ($S_1(\pi,\pi^*)$) while the biradical structure of the 1st triplet state ($T_1(\pi,\pi^*)$) may favor H-shift between two O

atoms, which ends up with the same/similar structure than prior to the H-shift (Scheme S1). Also, the excitation of β-diketones at 254 nm may also lead to charge transfer complex formation via direct excitation and/or radiationless transition from a local excited state (Phillips and Smith, 2015), which is likely to result in low quantum yields, as discussed in detail below.

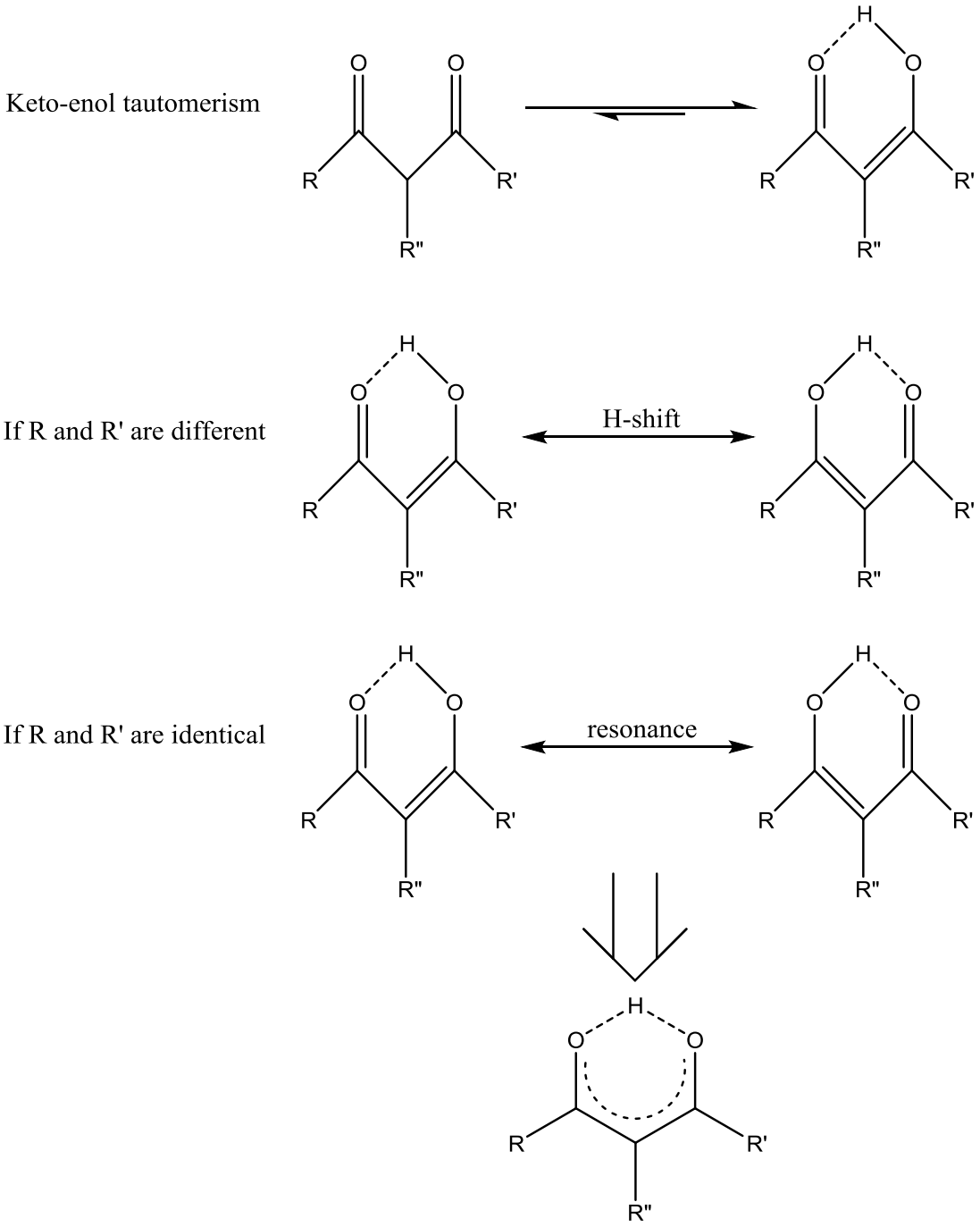

Scheme S1. Keto-enol tautomerism of β-diketone, and H-shift between O atoms or resonance of the enol form. Note that the tautomerism is generally favorable toward the enol form (Burdett and Rogers, 1964) and that the enol form, particularly its resonance, results in an extensive conjugated ring structure, which may have high absorptivity.

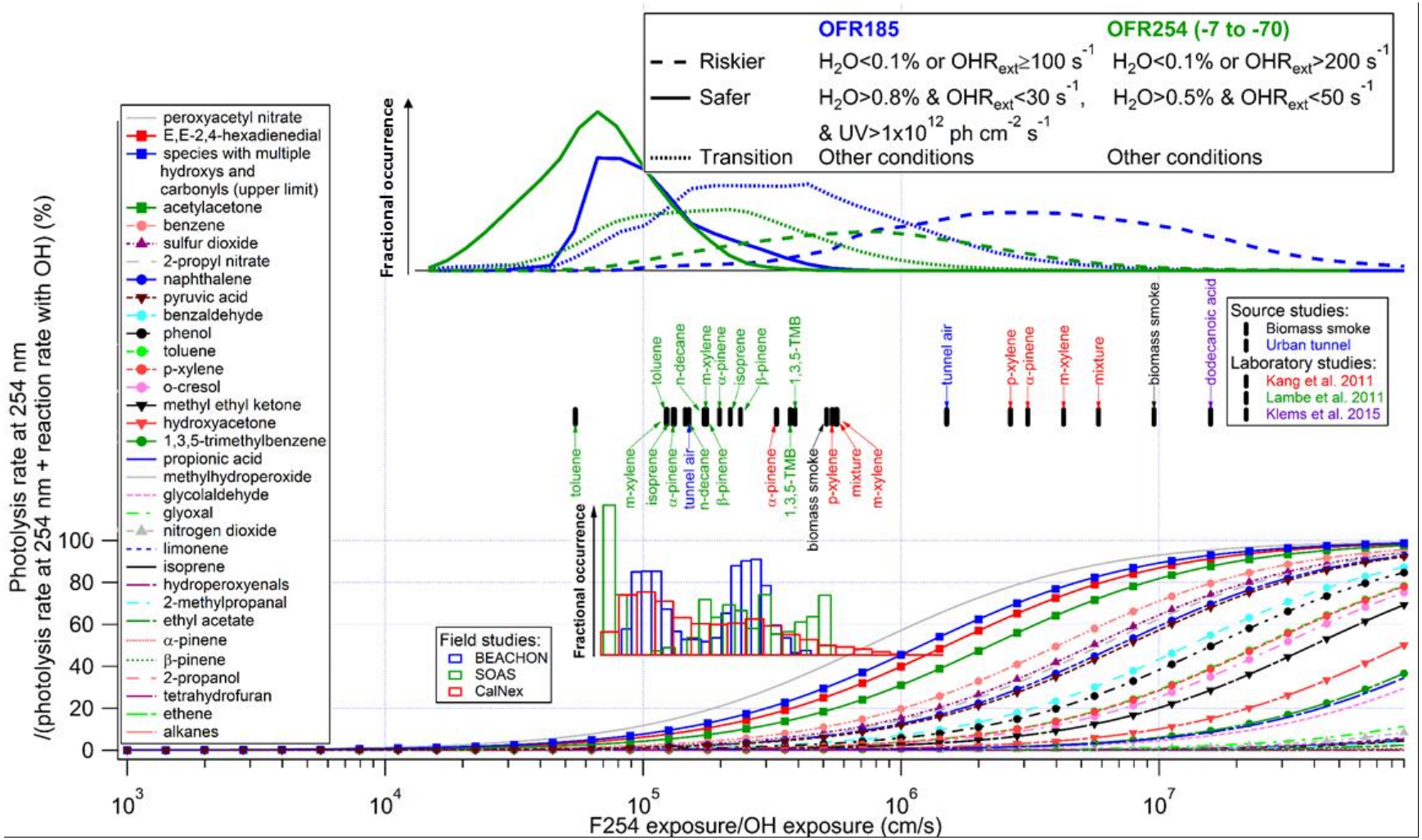

Figure 1. Same format as Fig. 1, but for the fractional importance of the photolysis rate at 254 nm vs. the reaction rate with OH as a function of the ratio of exposure to 254 nm (F254) and OH. The modeled frequency distributions of ratios of 254 nm photon exposure to OH exposure under riskier, safer, and transition conditions for OcFR185 and OFR254 (-7 to -70) are also shown. The curves of saturated carbonyl compounds and possible highly absorbing oxidation intermediates are highlighted by downward triangles and squares, respectively. The insets show histograms of model-estimated F254/OH exposures for three field studies where OFR185 was used to process ambient air. In addition to source studies of biomass

smoke (FLAME-3) and urban tunnel (Tkacik et al., 2014), F254 exposure/OH exposure ratios in two laboratory studies (Kang et al., 2011; Lambe et al., 2011) are shown in the upper inset. Colored tags indicate species used in the laboratory experiments. The lower and upper limits of F254 exposure/OH exposure ratios in the experiments with a certain source in a certain study are denoted by tags below and above the markers, respectively.

In addition to conjugated species, Phillips and Smith (2014, 2015) reported a new type of highly absorbing species that may be formed from VOC oxidation. Although their studies were conducted in the condensed phase, it is likely that the main conclusions of these studies are generally transferable to the gas-phase conditions, since no long-range interactions, which do not exist in normal gases, were involved in these studies. Phillips and Smith (2014, 2015) investigated the photoabsorption enhancement of multifunctional oxygenated species in SOA and found that the high absorptivity of these species can largely be explained by transitions toward the electronic states of charge transfer complex formed between hydroxyl groups (donor) and neighboring carbonyl groups (acceptor). They also pointed out that charge transfer complexes of this kind have a continuum of states whose energy levels range from that of local excited states (radiative transition wavelength <300 nm) to very low levels (radiative transition wavelength >600 nm). The latter are insufficient to cause common photochemical reactions. Relaxation through a continuum of states is usually ultrafast according to Fermi's golden rule (Turro et al., 2009), likely leading to low quantum yields of chemical reactions. The low quantum yields may be seen even from species with only one hydroxyl and one carbonyl: the photolysis of 3-hydroxy-3-methyl-2-butanone and 4-hydroxy-2-butanone at wavelengths down to 270 nm has quantum yields around only 0.1 (Bouzidi et al., 2014, 2015). Although measurements of photolysis quantum yield for multifunctional species are challenging and rare, it is reasonable to expect even lower quantum yields for larger and/or highly substituted (by hydroxyl and carbonyl) species, since larger species have more degrees of freedom for relaxation of excited molecules, and more and/or larger complex sites generally lead to more efficient relaxation through a continuum of states, in accordance with common photophysical sense (Sharpless and Blough, 2014). Therefore, even though species with a number of hydroxyls and carbonyls are formed in VOC oxidation and absorb >1 order of magnitude more efficiently at 254 nm than mono- and difunctional species, they may still have low effective photolysis rates because of low quantum yields.

For this type of species, we estimate an upper limit of the fractional importance of their photolysis at 254 nm. Molar absorption coefficients of charge transfer transitions of organic molecules are usually ~10^3–$1x10^4$ L mol^{-1} cm^{-1}, i.e., cross-sections of ~$3.9x10^{-18}$–$3.9x10^{-17}$ cm^2 (Foster, 1969). Based on that, it is reasonable to estimate an upper limit of absorption cross-sections of charge transfer transitions of $5x10^{-17}$ cm^2. On the other hand, photolysis quantum yields of multifunctional species are unlikely to be larger than that of species with only one carbonyl and one hydroxyl, i.e., ~0.1 (see discussion above). We thus take 0.1 as an upper limit of photolysis quantum yields. Besides, $6x10^{-12}$ cm^3 $molecule^{-1}$ s^{-1} can be a conservative estimate of rate constants of multifunctional oxygenated species with OH, as it is roughly an average value for ketones (Atkinson and Arey, 2003), and the enhancement of H-abstraction by hydroxyl groups (Kwok and Atkinson, 1995; Ziemann and Atkinson, 2012) and the fast abstraction of aldehydic H atoms (Atkinson and Arey, 2003) are completely neglected. With the three estimates combined, the estimated maximum fractional contribution from photolysis at 254 nm to

the fate of multifunctional species is close to that of E,E-2,4-hexadienedial and acetylacetone.

The problem of photolysis of oxidation intermediates at 185 nm is unlikely to be worse than at 254 nm. According to available UV spectra of carbonyl compounds in Keller-Rudek et al. (2015), 185 nm is almost always located within the π–π* transition band, whose maximum cross-section is on the order of 10^{-17} cm^2. Even if all types of radiative transitions at normal radiation intensity are considered, an approximate upper limit of absorption cross-sections is ~10^{-16} cm^2 (Evans et al., 2013). However, UV intensity at 185 nm in the OFR185 mode is ~100 times lower than that at 254 nm (Li et al., 2015). The photolysis rate of oxidation intermediates at 185 nm should thus be generally smaller than at 254 nm.

Therefore, in summary, photolysis of oxidation intermediates are, to our knowledge, conservatively estimated to be of limited importance relative to their reactions with OH, as long as the experimental conditions are in the safer range. Although studies on photolysis quantum yields of oxidation intermediates are very sparse, we reason, based on the existing studies on this topic and common photophysical and photochemical rules, that the photolysis quantum yields of these species may be lower than the values assumed in this study (e.g., 1 for E,E-2,4-hexadienedial and acetylacetone and 0.1 for multifunctional species). As a result, actual rates and relative importance of photolysis might be significantly smaller than the upper limits estimated in our study."

We have also inserted the following paragraph in P23554/L7:

"**Oxidation intermediates may also photolyze at 185 nm. However, their photolysis is unlikely to be significant when OFR is not operated at low H_2O and/or high OHR_{ext}. To clarify this issue, a detailed discussion about the photolysis of oxidation intermediates at 254 nm is required as a premise. We thus discuss oxidation intermediate photolysis at both 185 and 254 nm in Section 3.1.3.**"

We have also modified the text in P23555/L23 to read:

"**Note that photolysis of oxidation intermediates also needs to be taken into account. If multifunctional species, β-diketones, and extensively conjugated species are photolyzed as shown in Fig. 2, these photolyses would be significant in some previous source and laboratory studies examined here, as they were conducted at relatively low H_2O and/or high OHR_{ext}. To our knowledge, none of these studies reported a significant photolysis of oxidation intermediates. Klems et al. (2015) attributed large amounts of fragmentation products detected in their OFR experiments with dodecanoic acid to photolysis of peroxy radicals. However, these products may also be at least partially accounted for by photolysis of carbonyls leading to carbon-chain cleavage via Norrish reactions (Laue and Plagens, 2005). The OFR used by Klems et al. (2015) has a different design from the PAM, which is regarded as the base design in this study. Their reactor employs a light source**

stronger than the PAM's highest lamp setting, with UV at 254 nm estimated to be ~3x10^{16} photons cm^{-2} s^{-1} (~4 times the value at the highest lamp setting of the PAM OFR) based on the lamp power and the reactor geometry. Such high UV may even result in significant photolysis of saturated carbonyl intermediates, which are very likely formed in the oxidation of long-chain alkane-like dodecanoic acid."

We also modify the text P23566/L7 to read:

"**In laboratory experiments, running OFRs under safer conditions ensures a minor contribution of non-tropospheric photolysis, based on the current knowledge of oxidation intermediate photolysis (Fig. 2). This also reduces the relative contribution of ozonolysis to VOC fate. However, when more information becomes available about photoysis quantum yields of oxidation intermediates (vs. the upper limits assumed here), there may be additional flexibility to include ozonolysis while excluding non-tropospheric VOC consumption. As the precursor composition is usually relatively simple in laboratory experiments, it is sufficient to ensure the insignificance of non-tropospheric consumption of only the precursor(s) and possible intermediates (usually oxygenated species), rather than for a large variety of VOC precursors and intermediates. For example, in the case of quantum yields significantly lower than used in the present work, we may perform OFR254-70 experiments with a large amount of biogenics at medium H_2O and UV. In this case, a tropospheric O_{3exp}/OH_{exp} ratio can be obtained without major side effects, because the fractional contribution of photolysis of possible intermediates is still minor due to low quantum yields. On the other hand, OFR experiments with some anthropogenic VOCs, such as alkanes, can just be conducted at high H_2O and low OHR_{ext} to avoid the contribution of all non-OH reactants, since ozonolysis of alkanes is negligible even at a tropospheric O_{3exp}/OH_{exp}.**"

- R1.1.2) Some broad generalizations are made about the photolysis of nitrates and peroxides (e.g., page 23555 line 5). However only one nitrate (with 3 carbon atoms) and one peroxide (with 1 carbon atom) were actually studied. (PAN has a peroxynitro group - given it has no C-O-N bonding moiety, it is not truly a nitrate – and hydroperoxyenal cross sections have never actually been measured, but rather only estimated based on cross sections of similar but nonperoxidic species.) Larger or more functionalized species may well exhibit very different photolytic behavior.

We already stated in the ACPD manuscript that "we include one or two representative species for a category of species with certain functional group(s)" in Section S1. This does not mean that we made broad generalizations based on the data of only one species but that we selected for graphical display 1–2 species whose data are representative enough for the category. In fact, we did include the photolysis of 4 additional nitrates (methyl nitrate, ethyl nitrate, 1-propyl nitrate, and 1-butyl nitrate) in Fig. 6. We did also find UV spectra of more or larger nitrates (e.g., 2-butyl nitrate, 2-pentyl nitrate, 3-pentyl nitrate, cyclopentyl nitrate, 3-methyl-1-butyl nitrate, and 1-pentyl nitrate) in Keller-Rudek et al. (2015), but did not include them in Fig. 6 to avoid clutter,

since the UV-Vis spectra of most simple organic nitrates, with the nitrate group dominating the absorption, are very similar.

We agree that PAN is not a nitrate, and have replaced “nitrate(s)” with “nitrate(s) and peroxynitrate(s)” throughout the manuscript whenever necessary.

We agree that the proxy of hydroperoxyenals used in the ACPD version (E-2-hexanal) was nonperoxidic. The absorption of hydroperoxyenals at 254 nm should have the contribution from hydroperoxy group (cross-section of methylhydroperoxide at 254 nm: 3.23×10^{-20} cm^2), which is likely larger than the cross-section of the nonperoxidic proxy at 254 nm (~2×10^{-21} cm^2). We thus replaced the 254 nm cross-section of hydroperoxyenals used in the ACPD version with that of methylhydroperoxide. We made corresponding changes to Figs. 2 and S2 and Table S1.

To clarify why the data of 254 nm cross-section of hydroperoxyenals in Table S1 is used, we also added the following note to Table S1:

“***5: value of a proxy, methylhydroperoxide, is used as the proxy used in Wolfe et al. (2012), E-2-hexanal, does not contain a hydroperoxy group and hence has little absorption at 254 nm.**”

However, we argue that the absorption of hydroperoxy groups may be more due to themselves than to their interactions with adjacent functional groups. It is unlikely that as dramatic an absorption enhancement could occur between a carbonyl group and a hydroperoxy group as between a carbonyl group and a hydroxyl group. The charge transfer from hydroxyl to carbonyl should take place between the former’s HOMO (highest occupied molecular orbital), n-orbital (non-bonding), and the latter’s possible positive hole, i.e., the orbital from which an electron of the carbonyl is excited by a photon. These two orbitals should be of close energy level so that their interaction for charge transfer can be significant (Carey and Sundberg, 2007). However, the HOMO of a hydroperoxy group is an anti-bonding π*-orbital, whose energy is much higher than that of non-bonding n-orbital of a hydroxyl group. As a consequence, a significant reorganization of their geometric configuration might be required for the interaction between the donor and acceptor orbitals to be maximized (Turro et al., 2009). This requirement might suppress charge transfer between carbonyl and hydroperoxy.

For larger and more functionalized species, see response to R1.1.1.

- R1.1.3) The choices for SOA components (Table S6) are non-obvious. I understand that due to the lack of data, surrogate compounds need to be used. But as described above, SOA molecules will mostly have more than 1-2 functional groups, and therefore may absorb light much more strongly that any of the species listed. There may well also be intermolecular interactions that affect absorption further. The values given should thus be treated as strict lower limits, not averages. In fact, recent measurements find the cross section of a-pinene+O3 SOA to be about 3e-19 cm2 (Wong et al., JPCA 119,

4309−4316, 2015), ~1 order of magnitude higher than any of the (non-aromatic) surrogates used in this study.

We agree that real SOA samples have higher absorption cross-section than the non-aromatic surrogates used in the ACPD manuscript, according to Wong et al. (2015), as well as the references suggested by Referee #2 (see R2.7). We have included these data into Table S7 (Table S6 in the ACPD paper) and Fig. 8.

Indeed, there may also be condensed-phase intermolecular interactions affecting SOA absorption, similar to intramolecular charge transfer in the gas phase discussed above. However, these intermolecular interactions may also lead to low photolysis quantum yields, for the same reason discussed above (Phillips and Smith, 2014, 2015). Moreover, the condensed phase may provide more efficient pathways facilitating the relaxation of excited states than the gas phase, because of fast interactions with the surrounding molecules (Turro et al., 2009). In summary, SOA absorption can be significantly enhanced, but its photolysis rate may not, because of low quantum yields resulting from efficient relaxation.

In addition, we have modified the paragraph in P23563/L6 to read:

"**Recently, photolysis in the UV range has been found to be a potentially significant sink of some types SOA in the troposphere** (Updyke et al., 2012; Lambe et al., 2013; Liu et al., 2013, 2015; Hodzic et al., 2015; Wong et al., 2015; Romonosky et al., 2016)**. It is necessary to also investigate SOA photolysis in OFRs, as photons used in OFRs are highly energetic and non-tropospheric. UV extinction due to aerosol optical scattering and in-particle absorption under OFR conditions is generally negligible (Hodzic et al., 2015). For simplicity, we estimate photodegradation ratios of various SOA component surrogates as well as several SOA samples whose absorptivity was measured in previous studies** (Updyke et al., 2012; Lambe et al., 2013; Liu et al., 2013; Romonosky et al., 2016) **(Fig. 8) under the assumption of unity quantum yield to obtain upper limits of photodegradation ratios, and also under the assumption of lower (0.1 and 0.01) quantum yields.**"

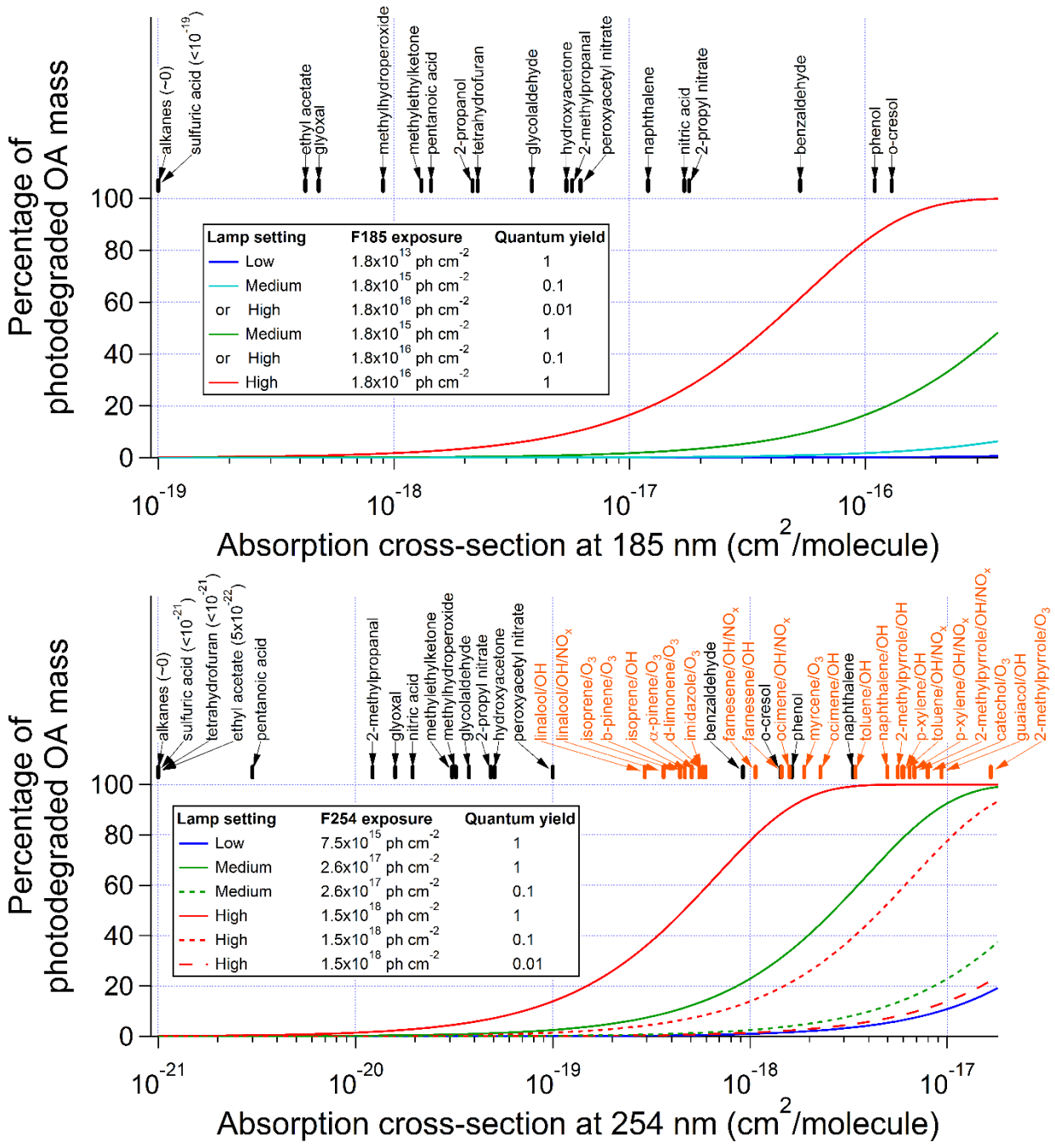

Figure 2. Percentage of SOA photodegradation at (upper panel) 185 and (lower panel) 254 nm at different UV levels as a function of absorption cross-section under the assumptions of quantum yields of 1, 0.1, and 0.01. Absorption cross-sections of some SOA component surrogates (black tag) and SOA samples (orange tag; calculated from data in Lambe et al. (2013) and Romonosky et al. (2015a)) are also shown.

We have also modified the following text in P23564/L13 to read:

"**Wong et al. (2015) conducted α-pinene-derived SOA photolysis experiments in a chamber under UVB irradiation (down to 284 nm). They observed at 85% RH ~30% SOA photolyzed after >30 min irradiation and a photolysis quantum yield of ~1 during the first 10 min. However, in OFRs such a high SOA photodegradation percentage would not occur, since Wong et al. (2015)'s experiments had a high photon flux (~4x10^{15} photons cm^{-2} s^{-1}) and a long irradiation time, and hence a photon flux exposure that is ~5 times that at the highest lamp setting in the OFRs modeled in our work. According to the measurements of Wong et al. (2015), a photolysis fraction of ~6% would be expected for this type of SOA in our OFRs under the highest UV flux, with lower percentages at lower UV settings. In addition, the approximate unity quantum yield observed in Wong et al. (2015) may be due to (hydro)peroxides in α-pinene-derived SOA, since peroxides have high photolysis quantum yields (Goldstein et al., 2007; Epstein et al., 2012), while other functional groups (i.e., mainly hydroxyl and carbonyl) in oxygenated species in SOA are unlikely to have for reasons discussed below.**

Note that a simple addition of absorptivities of different functional groups may not explain SOA absorptivity (Phillips and Smith, 2015). According to the absorption data of SOA samples from Lambe et al. (2013) and Romonosky et al. (2015a), real SOA absorbs ~1–3 orders of magnitude more than non-aromatic component surrogate species shown in Fig. 8 at 254 nm. As discussed for multifunctional oxidation intermediates (with carbonyls and hydroxyls), SOA absorption enhancement may be largely due to transitions of charge transfer complexes formed between carbonyls and hydroxyls in multifunctional oxygenated SOA components (Phillips and Smith, 2014, 2015). These complexes between carbonyls and hydroxyls also have continua of states likely leading to ultrafast relaxation and hence low photolysis quantum yields. Charge transfer transitions have been extensively shown in measurements (Alif et al., 1991; Gao and Zepp, 1998; Johannessen and Miller, 2001; O'Sullivan et al., 2005; Zhang et al., 2006; Osburn et al., 2009; Sharpless and Blough, 2014) to have very low quantum yields in the condensed phase. Sharpless and Blough (2014) compiled quantum yields of various products of humic-like matter photolysis down to 280 nm. No quantum yields except those of the product $^1O_2$, which is generally unimportant for OFRs (see Section 3.1.6), are higher than 0.01. If the photolysis quantum yields of the SOA samples in Fig. 8 at 254 nm are no more than 0.01, no SOA samples will be photolyzed by 20% even at the highest OFR lamp setting, and photolysis of most SOA samples at 254 nm will be minor or negligible in OFRs. Thus, to our current knowledge, lack of solid information on quantum yields of SOA components with multiple carbonyls and hydroxyls at 254 nm prevents a clear assessment of SOA photolysis in OFRs at the medium and high UV. On the other hand, direct measurements are desirable for this issue and caution should still be exercised for OFR experiments at relatively high UV.

SOA photolysis at 185 nm may be lower compared to that at 254 nm. SOA absorptivity data at 185 nm are not available. According to SOA mass-specific absorption cross-section (MAC) data between 250 and 300 nm in Romonosky et al. (2015a), there is a linear relationship between the logarithm of MAC and wavelength for most SOA samples: MAC

increases by a factor of ~3 per 50 nm decrease in wavelength. We thus extrapolate this relationship to 185 nm, where MAC is estimated to be ~3.5 times higher than that at 254 nm. However, the UV flux at 185 nm in our OFR is ~100 times lower than at 254 nm.

Based on the discussion above, the SOA photodegradation ratio of ~30% in Wong et al. (2015)'s non-OFR setup may be explained. α-pinene-derived SOA has ~20–50% weight fraction of peroxides (Docherty et al., 2005; Epstein et al., 2014), which may undergo photolysis in SOA to convert into carbonyls (and hydroxyls) (Epstein et al., 2014). We speculate that after the formation of carbonyls from peroxides, SOA materials cannot proceed significantly further with photolysis as discussed for charge transfer between carbonyl and hydroxyl above. In the experiments of Wong et al. (2015), as well as Epstein et al. (2014), effective photolysis rate constants/quantum yields decreased as SOA photolysis proceeded. Photolysis rates were substantially reduced after a ~30% mass loss due to photolysis in Wong et al. (2015)'s experiments. This mass loss ratio is consistent with the mass percentage of peroxides in α-pinene-derived SOA. Again, we note that, according to the extrapolation from Wong et al. (2015)'s results, the mass loss percentage expected in our OFR under the highest UV flux is ~6% for α-pinene-derived SOA. This value is much lower than that shown in Fig. 8 under the assumption of unity quantum yield (~40%) because of a substantially decreasing quantum yield in the real photolysis experiments. Therefore, in OFRs, even if (hydro)peroxides in SOA may be photolyzed in appreciable amounts, SOA mass is unlikely to be largely destroyed by photons in OFRs, as (hydro)peroxides may convert into carbonyls and hydroxyls, which may substantially lower subsequent photolysis quantum yields.

According to the discussion above, measurements of quantum yields and/or products of SOA photolysis are highly desirable, especially for the photolysis of SOA containing dominantly carbonyl and hydroxyl groups, as (hydro)peroxides, which are likely to form in OFRs, may convert into hydroxyls and carbonyls. With more data on quantum yields of SOA photolysis, a clearer strategy for including or excluding SOA photolysis in OFRs can be made.

Even though SOA photolysis can be significant in OFRs, it only proceeds to a much lesser extent compared to ambient SOA photolysis. We calculate the numbers of e-fold decay of SOA photolysis in OFR254-70 and the troposphere according to the effective ambient photolysis lifetime of SOA from Romonosky et al. (2015a). Under the condition of 70% RH (H_2O = 1.4%) and OHR_{ext} = 25 s^{-1} (typical of ambient conditions), SOA samples are estimated to undergo ~0.01–0.5 e-fold photolysis timescales (i.e., ~1–35% OA photolyzed) in OFR254-70 at an equivalent photochemical age of 1 week under the upper limit assumption of unity quantum yields (Table S8). However, in the atmosphere, those samples may proceed with 10^2–10^4 e-fold decays of photolysis (i.e., virtually complete destruction) at the same photochemical age, if ambient SOA photolysis quantum yields are assumed to be those of H_2O_2 (unity below 400 nm). Even if the quantum yield of acetone (non-zero below 320 nm, see Romonosky et al., 2015a) is taken as a surrogate for SOA, most types of SOA would still be completely or nearly completely photolyzed

under ambient conditions. These results demonstrate that ambient SOA photolysis is likely to be much more important than in OFRs. On the other hand, they also highlight the need for studies of ambient SOA photolysis quantum yields and photolytic aging, as ambient SOA is unlikely to be completely destroyed by photons within only 1 week. Either their quantum yields are much lower than used in this study, or the photolabile groups are destroyed and leave behind others that are not (or less) photolabile during photolytic aging.”

Table S8. Number of e-fold decays of photolysis and percentage of photolyzed OA of several SOA samples at an equivalent photochemical age of 1 week under atmospheric conditions in Romonosky et al. (2015a) and in OFR254-70 at 70% relative humidity (water vapor mixing ratio of 1.4%) and 25 s^{-1} initial OHR_{ext}. Absorption cross-sections at 254 nm and effective ambient photolysis lifetimes of SOA samples are taken from or calculated according to Romonosky et al. (2015a). Ambient photolysis data are obtained assuming quantum yields of SOA samples to be those of H_2O_2 or acetone.

SOA type	Cross-section at 254 nm (cm^2)	Effective ambient photolysis lifetime (min)		Number of e-fold decays due to photolysis			Percentage of photolyzed OA at equivalent photochemical age of 1 week		
		Using QY of H_2O_2	Using QY of acetone	OFR254-70	Ambient using QY of H_2O_2	Ambient using QY of acetone	OFR254-70	Ambient using QY of H_2O_2	Ambient using QY of acetone
2-methylpyrrole/O_3	1.66E-17	1	85	0.461	10080	119	36.9	100	100
guaiacol/OH	9.34E-18	1.7	190	0.259	5929	53	22.8	100	100
catechol/O_3	7.97E-18	3	260	0.221	3360	39	19.8	100	100
2-methylpyrrole/OH/NO_x	6.82E-18	1	130	0.189	10080	78	17.2	100	100
p-xylene/OH/NO_x	6.46E-18	2.5	280	0.179	4032	36	16.4	100	100
p-xylene/OH	5.99E-18	5.5	430	0.166	1833	23	15.3	100	100
toluene/OH/NO_x	5.93E-18	1.3	190	0.164	7754	53	15.2	100	100
2-methylpyrrole/OH	5.61E-18	2.6	260	0.155	3877	39	14.4	100	100
naphthalene/OH	4.98E-18	0.62	64	0.138	16258	158	12.9	100	100
toluene/OH	3.42E-18	6.2	590	0.095	1626	17	9.1	100	100
ocimene/OH	2.27E-18	25	1700	0.063	403	5.9	6.1	100	99.7
myrcene/O_3	1.88E-18	58	3800	0.052	174	2.7	5.1	100	93.0
ocimene/OH/NO_x	1.59E-18	25	1800	0.044	403	5.6	4.3	100	99.6
farnesene/OH	1.44E-18	53	3500	0.040	190	2.9	3.9	100	94.4
farnesene/OH/NO_x	1.07E-18	47	3400	0.030	214	3.0	2.9	100	94.8
d-limonene/O_3	5.95E-19	230	7200	0.016	44	1.4	1.6	100	75.3
imidazole/O_3	5.76E-19	95	4800	0.016	106	2.1	1.6	100	87.8
α-pinene/O_3	5.54E-19	85	4800	0.015	119	2.1	1.5	100	87.8
isoprene/OH	5.07E-19	410	7600	0.014	25	1.3	1.4	100	73.5
b-pinene/O_3	4.68E-19	90	4000	0.013	112	2.5	1.3	100	92.0

isoprene/O_3	4.42E-19	88	5400	0.012	115	1.9	1.2	100	84.5
linalool/OH/NO_x	3.65E-19	100	7700	0.010	101	1.3	1.0	100	73.0
linalool/OH	2.92E-19	160	11000	0.008	63	0.9	0.8	100	60.0

We have accordingly modified the conclusion section in P23567/L22 to read:

"**We assessed the relative significance of the VOC consumption by non-OH reactants to that by OH in OFRs and the troposphere. The only non-tropospheric reaction that can play a major role under OFR conditions is photolysis, especially at 254 nm. The relative importance of photolysis is largest under riskier OFR conditions where OH is low due to low H_2O and/or high OHR_{ext}. Due to lack of quantum yield data, we estimated upper limits of the relative importance of photolysis for the few most susceptible oxidation intermediates, which are comparable to those from aromatic precursors. Reactions of O atoms are not competitive and are actually of lower relative importance (vs. OH) in OFRs than in the troposphere. VOC ozonolysis is much less important than in the troposphere under typical OFR conditions and of similar importance under riskier OFR conditions. Photolysis of SOA in OFRs could be significant at medium and high UV, but only if corresponding quantum yields are high. If SOA photolysis quantum yields are of the order of 0.01 or lower, as measured for many humic-like substances (Sharpless and Blough, 2014), SOA photolysis in OFRs may be minor or negligible under most conditions. Although the reaction fates may be different, numbers of e-fold decays of photolysis for a given OH_{exp} are at least an order-of-magnitude lower in the OFRs compared to the troposphere.**"

We have also added the following paragraph to the conclusion section at P23568/L21:

"**The need for systematic measurements of photolysis quantum yields, for both VOC and SOA, and both at actinic wavelengths and at 185 and 254 nm, was highlighted in this study. When quantum yield data become available, photolysis of oxidation precursors, oxidation intermediates, and SOA in OFRs can be much better quantified, its relative importance compared to OH oxidation, ambient photolysis etc. can be better evaluated, and experimental planning might then be able to be less conservative and have more freedom to avoid non-tropospheric photolysis and realize specific experimental objective(s).**"

To make the abstract consistent with the modifications above, we have also modified the text in P23545/L18 to read:

"**Photolysis at non-tropospheric wavelengths (185 and 254 nm) may play a significant (>20%) role in the degradation of some aromatics, as well as some oxidation intermediates, under riskier reactor conditions, if the quantum yields are high. Under riskier conditions, some biogenics can have substantial destructions by O_3, similarly to the troposphere. Working under low O_2 (volume mixing ratio of 0.002) with the OFR185 mode allows OH to completely dominate over O_3 reactions even for the biogenic species most reactive with O_3.**"

We have also modified the text in P23545/L26 to read:

"**Photolysis of SOA samples is estimated to be significant (>20%) under the upper limit assumption of unity quantum yield at medium ($1x10^{13}$ and $1.5x10^{15}$ photons cm^{-2} s^{-1} at 185 and 254 nm, respectively) or higher UV flux settings. The need for quantum yield measurements of both VOC and SOA photolysis is highlighted in this study.**"

R1.2) The possible fates of the later-generation, multifunctional species therefore need to be examined in more detail in this work. Of course these molecules are highly diverse, and chemical/optical data on them is very sparse. One option would be to extend the quantum chemical calculations to a range of such species, but that would probably be a major project in itself. Instead I would recommend a sensitivity study. If species absorb 254nm or 185nm light at 10x or 100x the cross sections used here, to what extent would photolysis compete with OH? If OH reaction continues to dominate, then the strong conclusions throughout the paper about the importance of OH chemistry still hold; if not, the possibility of photolysis of highly functionalized species needs to be discussed explicitly. (This would suggest an important area of future research, with measurements needed both at these low wavelengths and within the standard actinic window.)

See response to R1.1. Extensively conjugated unsaturated carbonyls formed in aromatic oxidation, β-diketones formed in oxidation of aliphatic moiety, and the extreme case for multifunctional species can be regarded as reasonable upper limits of photolysis relative importance. We thus did not conduct the sensitivity study by simply multiplying cross-sections by 10 or 100 as the Referee suggested.

R1.3) Abstract: an interesting result of this paper is that the model results suggest that under some cases, OH oxidation (relative to other oxidation channels) can actually be more important in the OFR than in the troposphere. This is alluded to in the mention of biogenic species reacting with O3, but should probably be said more explicitly in the abstract.

We agree with this comment and have modified the abstract above to clarify this point (see response to R1.1.3).

R.1.4) 23548 line 9: This sentence mentions peroxy-radical photolysis, which has been suggested to be a non-tropospheric reaction path within OFRs. But this is not explored anywhere in the manuscript. Either it needs to be included, or its exclusion from this paper needs to be stated.

We only cover the chemistry of stable species in OFR in this paper and plan to address OFR peroxy radical chemistry in a future paper. Thus, we modify the sentence to P23548/L9 to read:

"**Klems et al. (2015) concluded that photons at 254nm from Hg-lamp emission played an important role in their OFR experiment, especially for downstream chemistry.**"

And we have modified the text in P23548/L12 to read:

"**In this paper, we apply the model in Peng et al. (2015) to systematically investigate whether significant non-tropospheric or non-OH chemistry occurs in OFRs, and what experimental conditions make it more important. Considering the enormous complexity of organic radical (particularly organic peroxy) chemistry, we only examine the non-OH fate of stable species in the present work. The fate of organic radicals should be the subject of future studies.**"

R1.5) 23549/20-21: This section makes reference to the study of non-plug flow conditions in the cited Peng et al. paper. However, I didn't see any such discussion in that paper. Maybe I'm just missing it? Or did the authors use the wrong reference? (Or are they referring to an version that isn't publicly available?)

We apologize for this confusion. We made the statement on P23549/L20-21 based on the additional work for the revision of Peng et al. (2015b). We were hoping that the responses to the referees' comments to Peng et al. (2015b) would be posted much earlier. However, those responses were extensive and their review by coauthors led to their posting after Referee #1's comments to this ACPD paper. Please see these responses at http://www.atmos-meas-tech-discuss.net/8/C3671/2015/amtd-8-C3671-2015-supplement.pdf. The final version of Peng et al. (2015b) has been published in AMT and indeed contains an extensive study of the impact of non-plug-flow conditions in OFRs.

R1.6) Figs 1-2 (and S1-S2): The x-axes in these plots, which are not discussed at all in the manuscript, are quite unusual, and probably should be changed. "Exposure" is best defined as "concentration times time". The x axis is given in units of cm/s; assuming the OH exposure is in the standard units (molecules-s/cm3), this would mean the authors are expressing "photon exposure" in molecule/cm2, which is very hard to interpret, particularly in terms of an "exposure". The most intuitive unit to use for photon exposure is photon density times time; this would make the x axis unitless, as is the case for Figs 3-5.

The unit of x-axes in Figs. 1 and 2 (cm s^{-1}) can be explained. F185 (F254) exposure is the product of 185 (254) nm photon flux (in photons cm^{-2} s^{-1}) and time (in s), whose unit is photons cm^{-2}, while OH_{exp} is in molecules cm^{-3} s^{-1}. Therefore, F185 (F254) exposure/OH exposure has a unit of cm s^{-1}.

Photon density can be obtained as photon flux divided by the speed of light. For instance, a photon flux of $3x10^{13}$ photons cm^{-2} s^{-1} corresponds to a photon density of $3x10^{13}$ photons cm^{-2} s^{-1} / ($3x10^{8}$ m s^{-1}) = $1x10^{3}$ photons cm^{-3}. However, photon flux is commonly used for kinetic studies involving light. It is very unusual in our experience to use photon density instead. Therefore, we keep the x-axis unit of Figs. 1 and 2 as it is, and clarify this unit by adding the following text to their caption:

"**F185 (F254) exposure (in photons cm^{-2}) is the product of 185 (254) nm photon flux (in photons cm^{-2} s^{-1}) and time (in s). F185 (F254) exposure / OH exposure is thus in cm s^{-1}.**"

R1.7) Figs 2-5: This is a very complicated figure. The laboratory-study parameters might be easier to understand if they were presented as horizontal lines (ranges) rather than two markers with differently-placed labels.

We have worked a lot on these figures and made many different versions, e.g., an alternative version that we experimented with can be seen in Supp. Info. If we present the laboratory-study ranges as horizontal lines, those lines greatly clutter the plots as the space for showing these ranges in Figs. 2–5 is already limited. We thus prefer to keep the format of these figures as it is, except that the horizontal lines (ranges) for OFR are replaced by fractional occurrence distribution of exposure ratios to make them more informative and define "riskier" ("pathological" conditions are now called "riskier" conditions in the revised manuscript) conditions etc. more clearly (see revised Fig. 2 above as an example).

We have replaced the paragraph in P23552/L8 by the following text with new and clearer definitions of the input condition categories to read:

"**In these figures, the relationships of all non-OH reactive species to OH are similar for certain common conditions. We define three types of conditions to help guide experimental design and evaluation in terms of the relative importance of non-OH reactants. Under "riskier conditions" of high/very high OHR_{ext} (≥100 s^{-1} in OFR185 and >200 s^{-1} in OFR254 (-7 to -70)) and/or low H_2O (<0.1%), non-OH reactions can be significant depending on the species. Conversely, under "safer conditions" with relatively low OHR_{ext} (<30 s^{-1} in OFR185 and <50 s^{-1} in OFR254), *and* high H_2O (>0.8% in OFR185 and >0.5% in OFR254), and moderate or higher UV (>1x10^{12} photons cm^{-2} s^{-1} at 185 nm) in OFR185, reaction with OH is dominant (Figs. 1–5 and S1–5). We denote all other conditions as "transition conditions." High H_2O and zero/low OHR_{ext} lead to strong OH production and no/weak OH suppression, respectively. Thus, OH is more abundant and dominates species consumption under those conditions. In the case of low H_2O and high OHR_{ext}, OH is generally lower because of less production and more suppression. These conditions increase the relative contribution of non-OH species. UV light intensity is generally less influential on non-OH VOC fate than H_2O and OHR_{ext}, although OH production is nearly proportional to UV (Peng et al., 2015), because the non-OH reactive species also scale (nearly) proportional to UV. As a result, UV generally has smaller effects on exposure ratios between OH and the non-OH reactants. However, under a UV near the lower bound of the explored range in this study (<1x10^{12} photons cm^{-2} s^{-1} at 185 nm) in OFR185, OH production is so small that the effect of OHR_{ext} on OH suppression can be amplified and hence some exposure ratios may be affected. In OFR254 OH is more resilient to suppression even at low UV because of the OH-recycling by initially injected O_3 (Peng et al., 2015). Note that we call these conditions "riskier" and "safer" mainly in terms of non-tropospheric VOC fate, but not of VOC fate by all non-OH reactants, as some of the non-OH reactant studied in this work may also play a role under some tropospheric conditions (see Sections 3.1.4 and 3.1.5). In addition to the common features above, individual non-OH reactants have their own features as well as**

a few exceptions to the above mentioned general observations, which we will detail below."

We have also made minor modifications throughout the manuscript in accordance with this definition change.

R1.8) 23564/21: "Generation" is a confusing word here, since it usually refers to the number of reactions in a chemical mechanism required to form a specific compound. The more standard term for describing the time to an e-fold of decay is "characteristic lifetime" (e.g., Smith et al., ACP 9, 3209–3222, 2009).

We replace "generation" by "e-fold decay" throughout the ACPD manuscript whenever needed.

R1.9) 23557/section 3.1.5: It should also be noted that ozonolysis can play a major role in the oxidation of dihydrofurans, which can be formed from any number of saturated species, including anthropogenic species. This is described in multiple papers by Ziemann and coworkers; as noted in those papers, OH-only chemistry is not fully representative of the atmospheric conditions in that case, since ozonolysis (or reaction with NO3) will dominate the fate of those compounds. This could have substantial implications for SOA formation within the OFR.

We agree with the comment about dihydrofurans that their ozonolysis can play a major role, and thus add a curve, a marker, and data for 4,5-dihydro-2-methylfuran (representative species of dihydrofurans) to Fig. 5, Fig. S5, and Table S3, respectively. We also add the following text to P23558/L23:

"**However, unsaturated oxidation intermediates may have larger contributions from O_3 because of C=C bonds. In particular, dihydrofurans, possible intermediates of saturated hydrocarbon oxidation (Ziemann and Atkinson, 2012; Aimanant and Ziemann, 2013), may be predominantly oxidized by O_3 in the troposphere. In OFR254, they can still have significant contributions from O_3 even outside the low-H_2O and/or high-OHR_{ext} conditions.**"

R1.10) 23558/28 (and elsewhere): Focusing on OH-only chemistry under conditions where OH is not the relevant atmospheric oxidant (such as in the dihydrofuran example above) does not seem to be a very important area of research. It's unclear to me then why so much text is devoted to discussing how to carry out such experiments.

We underline that it is not possible to replicate the atmosphere in any reactor/chamber. Different experimenters may be interested in different regimes of reactions, and thus will try to isolate those regimes in reactors/chambers by various methods, even though those experiments will not reflect the real atmosphere in a perfectly comprehensive manner. For instance, in chambers OH scavengers are often used to study O_3 reactions to simplify the chemistry under study, or excess NO is added to suppress O_3 and NO_3, to isolate OH chemistry. In P23558–23559, we

present some guidelines to control the relative importance of OH vs. O_3 oxidation in the reactor. These guidelines will serve to guide experimenters to design experiments that fulfill *their own* objectives.

Therefore, we think that this text is meaningful and keep it. However, for clarity, we have modified the text in P23558/L26 to read:

"**An experimentalist may be interested in obtaining an O_{3exp}/OH_{exp} in an OFR close to ambient values, which requires lower H_2O and higher OHR_{ext} conditions, although care should be taken to avoid other non-tropospheric reactions under those conditions. On the other hand, one may want to study OH-dominated chemistry and thus want to avoid significant ozonolysis of VOCs to reduce the complexity of VOC fate. This is analogous to the addition of excess NO to suppress O_3 in some chamber experiments.**"

R1.11) 23560/8: This paragraph neglects what may be the most interesting/important aspect of HO2 chemistry, the formation of HO2-carbonyl adducts (to form hydroxyhydroperoxy radicals). Under the very high HO2 concentrations of the OFR, these may then form hydroxyhydroperoxides, probably to a higher extent than would happen in the troposphere. This channel should be explored here.

In this paper, we focus on the fate of stable species in OFRs only, as there are many other issues that concern the fate of peroxy radicals in OFRs, as also discussed in response to comment R1.4. We plan to explore those issues in a separate publication. Nevertheless, carbonyl compounds can be stable species. We thus briefly discuss their fate by reaction with HO_2 and modify the text to P23560/L9 to read:

"**Typically, the rate constants of reactions of HO_2 with alkenes are smaller than 10^{-20} cm^3 $molecule^{-1}$ s^{-1} at room temperature, and those with almost all saturated VOCs (except aldehydes and ketones) are even smaller (Tsang, 1991; Baulch et al., 1992, 2005). Therefore, we briefly discuss reactions of HO_2 with aldehydes and ketones, and neglect those with all other VOCs in this study. Ketones react with HO_2 at rate constants on the order of 10^{-16} cm^3 $molecule^{-1}$ s^{-1} or lower (Gierczak and Ravishankara, 2000; Cours et al., 2007). Therefore, only at low H_2O, low UV and high OHR_{ext}, the reaction of acetone with HO_2 may compete with that with OH. The same is likely true for the reactions of acetaldehyde and larger aldehydes with HO_2, as their rate constants are likely to be around or less than $1x10^{-14}$ cm^3 $molecule^{-1}$ s^{-1} (da Silva and Bozzelli, 2009). Formaldehyde is the only stable carbonyl compound that may react with HO_2 (rate constant: $7.9x10^{-14}$ cm^3 $molecule^{-1}$ s^{-1}; Ammann et al., 2015) at a rate competing with that with OH under conditions that are not low-H_2O, low-UV, and high-OHR_{ext}. Note that the reaction of formaldehyde with HO_2 is also significant in the atmosphere (Pitts and Finlayson, 1975; Gäb et al., 1985). However, its product, hydroxymethylperoxy radical, dominantly undergoes decomposition via thermal reaction and photolysis (Kumar and Francisco, 2015), compared to the hydroxymethylhydroperoxide formation pathway via a further reaction with HO_2 (Ziemann and Atkinson, 2012). Even if hydroxymethylhydroperoxide is**

produced in appreciable amounts, in the high-OH environment of OFRs, this species can be easily predicted to convert into formic acid (Francisco and Eisfeld, 2009) and eventually CO_2. All these products have very few interactions with other VOCs, and hence should not significantly perturb the reaction system of OFRs."

R1.12) Table S6: Presumably these are intended to be "surrogate" SOA components, not "possible" ones, since most are far too volatile to be in the condensed phase.

This is indeed the case. We have replaced "possible" in P23563/L11 and the caption of Table S6 in the ACPD paper by "surrogate".

Anonymous Referee #2

Peng et al. conduct a modeling study to examine the importance of UV photolysis as well as O_3, $O(^1D)$, and $O(^3P)$ reactions relative to OH reactions in oxidation flow reactors (OFRs). Overall, this manuscript addresses important issues regarding the application of oxidation flow reactors to examine OH oxidation chemistry in targeted laboratory and field studies. The authors examine a wide range of operating conditions in flow reactors and identify a subset of "optimal" and "pathological" conditions. Before the manuscript can be considered for publication in ACP, significant rewriting/reorganization is required to more clearly present and discuss the implications of the modeling work. Specific comments and suggestions are listed below.

R2.1) F185, F254, $O(^1D)$ exposure, and $O(^3P)$ exposure are all correlated with OH exposure to some extent, yet the modeling work in this manuscript suggests it is possible to vary $F185/OH_{exp}$, $F254/OH_{exp}$, $O(^1D)_{exp}/OH_{exp}$, and $O(^3P)_{exp}/OH_{exp}$ over orders of magnitude range by varying the water vapor mixing ratio, photon flux, and external OH reactivity. To provide useful context/introduction to Figures 1-5, I suggest parameterizing these ratios as a function of input OFR conditions, because in its current form the manuscript mostly uses qualitative statements relating high $F185/OH_{exp}$, $F254/OH_{exp}$, $O(^1D)_{exp}/OH_{exp}$, and $O(^3P)_{exp}/OH_{exp}$ values to "pathological conditions".

For example, plotting (i) $F185/OH_{exp}$ (ii) $F254/OH_{exp}$ (iii) $O(^1D)_{exp}/OH_{exp}$ (iv) $O(^3P)_{exp}/OH_{exp}$ versus $OHR_{ext}/[H_2O]$ – or a similar combination of input parameters that incorporate correlation of $F185/OH_{exp}$ with OHR_{ext} and anti-correlation with H_2O – over appropriate range of OHR_{ext} and $[H_2O]$. Individual traces could be shown corresponding to "L", "M", "H" photon fluxes displayed in Table 1 for "OFR185, "OFR254-7" and "OFR254-70" as appropriate. These figures could allow for quantitative comparison of, for example: $[H_2O]$ = 2.3% at OHR_{ext} = 1000 s^{-1} versus $[H_2O]$ = 0.07% at OHR_{ext} = 0 s^{-1} , as well as other intermediate conditions that are for the most part not considered in the manuscript. Presumably these plots can be derived from the model simulation data that has already been obtained, and perhaps consolidated into a single figure with a few subpanels.

We agree that a parameterization of those exposures would be very practical for future studies, and thank the reviewer for the suggestion. Thus we have derived estimation equations for $O(^1D)_{exp}$, $O(^3P)_{exp}$, and O_{3exp} in both OFR185 and OFR254. $F185_{exp}$ and $F254_{exp}$ can be regarded as input experimental conditions. Therefore, all exposure ratios of these species can now be obtained. To document the details of these estimation equations, we have added a section in Supp. Info. to read:

"**S3. Estimation equations of non-OH reactant exposures**

In order that one may practically estimate exposure ratios between non-OH reactants and OH under any condition for OFR operation, we provide the estimation equations of $O(^3P)$, $O(^1D)$, and O_3 exposures obtained by fitting the modeling results (Table S9). The equations for OFR254 are fitted from the results of the same runs as in Peng et al. (2015b), while those for OFR185 from the modeling data under conditions spanning the

same H_2O, UV, and OHR_{ext} ranges as for OFR254, but without the initial O_3 ($O_{3,in}$) dimension. Exposures estimated from these equations compare very well with the modeled exposures (Fig. S6). Scatter plots between a few exposures are also shown in Fig. S6.

For OFR254, UV at 254 nm can be estimated by collectively considering and solving Eqs. 11 and 12 in Peng et al. (2015b), if rO_3 (i.e., ratio between O_3 at the reactor entrance and exit) is known, and vice versa. For OFR185, one of UV at 185 nm and O_{3exp} (or average O_3) can be obtained if the other is known according to Eq. S1 below. UV at 254 nm in OFR185 can be calculated by Eq. S1 in Li et al. (2015), and then photon flux exposures can be easily estimated.

The ratios of F185 and F254 exposures to OH exposure are the most important parameter in this work that determine the relative contribution of non-tropospheric VOC photolysis. Therefore, we also provide equations for directly estimating these parameters from measurable surrogates of UV (i.e., O_{3exp} in OFR185 and rO_3 in OFR254) (Table S9 and Fig. S6).

Table S9. Estimation equations of $O(^3P)$, $O(^1D)$, and O_3 exposures and ratios of $F254_{exp}$ to OH_{exp} for both OFR185 and OFR254, and ratio of $F185_{exp}$ to OH_{exp} for OFR185. UV in the equations for OFR185 and OFR254 are the photon fluxes at 185 and 254 nm, respectively. Numbers of fitted datapoints and average absolute value of the relative deviations (AAVRD) of the estimates by the equations from the fitted datapoints are also shown. rO_3 is the ratio between O_3 at the reactor exit and entrance. For OFR254, one of rO_3 and UV can be obtained by collectively considering and solving Eqs. 11 and 12 in Peng et al. (2015b) if the other is known. OH, O_3, $O(^1D)$, and $O(^3P)$ exposures are in molecules cm^{-3} s, $F185_{exp}$ and $F254_{exp}$ in photons cm^{-2}, OHR_{ext} in s^{-1}, UV in photons cm^{-2} s^{-1}, $O_{3,in}$ in ppb, and H_2O and rO_3 unitless.

OFR type	Eq. No.	Estimation equation	Number of fitted data-points	AAVRD (%)
OFR185	S1	$\log O_{3exp} = 3.1825 + 0.98741 \log UV + 40.352 H_2O - 3.8184 H_2O \cdot \log UV$	28800	6
	S2	$\log O(^3P)_{exp} = 313.61 - 558.66 \log(\log O_{3exp}) - 171.59 H_2O + 254.33 (\log(\log O_{3exp}))^2 + 147.27 H_2O \cdot \log(\log O_{3exp})$		6
	S3	$\log O(^1D)_{exp} = 90.595 - 208.28 \log(\log O_{3exp}) - 155.9 H_2O + 114.15 (\log(\log O_{3exp}))^2 + 134.4 H_2O \cdot \log(\log O_{3exp})$		4

	S4	$\log(F185_{exp}/OH_{exp}) = -2.7477 - 0.79645 \log H_2O + 0.25018 \log O_{3exp} + 3.8051 \log OHR_{ext} - 0.22685 \log OHR_{ext} \cdot \log O_{3exp} + 0.0086381 (\log OHR_{ext})^2 \cdot \log O_{3exp}$		14
	S5	$\log(F254_{exp}/OH_{exp}) = 3.325 - 0.8268 \log H_2O + 3.7467 \log OHR_{ext} - 0.22294 \log OHR_{ext} \cdot \log O_{3exp} + 0.0086345 (\log OHR_{ext})^2 \cdot \log O_{3exp}$		14
OFR254	S6	$\log O_{3exp} = 15.559 + \log O_{3,in} + 0.42073 \log rO_3$	316800	1
	S7	$\log O(^3P)_{exp} = 7.6621 + 0.16135 \log(-\log rO_3) - 1.1342 \log H_2O + 0.59182 \log O_{3,in} - 0.17007 \log H_2O \cdot \log(-\log rO_3) - 0.3797 (\log(-\log rO_3))^2 + 0.099902 \log OHR_{ext}$		5
	S8	$\log O(^1D)_{exp} = 3.7371 + 0.1608 \log(-\log rO_3) - 1.1344 \log H_2O + 0.59179 \log O_{3,in} - 0.17019 \log H_2O \cdot \log(-\log rO_3) - 0.37983 (\log(-\log rO_3))^2 + 0.099941 \log OHR_{ext}$		5
	S9	$\log(F254_{exp}/OH_{exp}) = 2.8045 - 0.888519 \log H_2O - 0.015648 \log(-\log rO_3) - 0.2607 \log OHR_{ext} - 0.1641 (\log(-\log rO_3))^2 + (OHR_{ext}/O_{3,in})^{0.25142}$		14

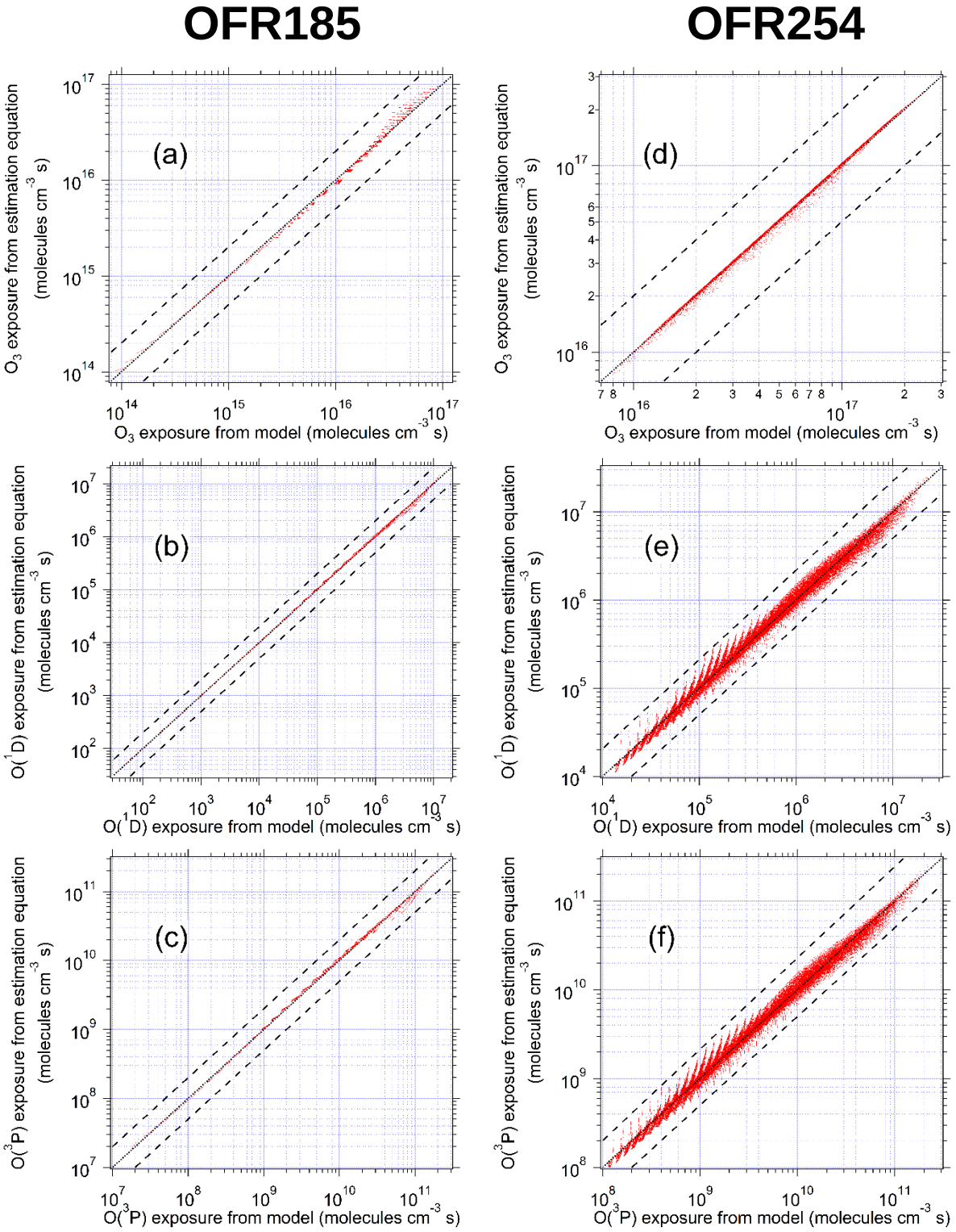
OFR185
OFR254
(a)
(b)
(c)
(d)
(e)
(f)
O3 exposure from estimation equation (molecules cm-3 s)
O3 exposure from model (molecules cm-3 s)
O(1D) exposure from estimation equation (molecules cm-3 s)
O(1D) exposure from model (molecules cm-3 s)
O(3P) exposure from estimation equation (molecules cm-3 s)
O(3P) exposure from model (molecules cm-3 s)

OFR185

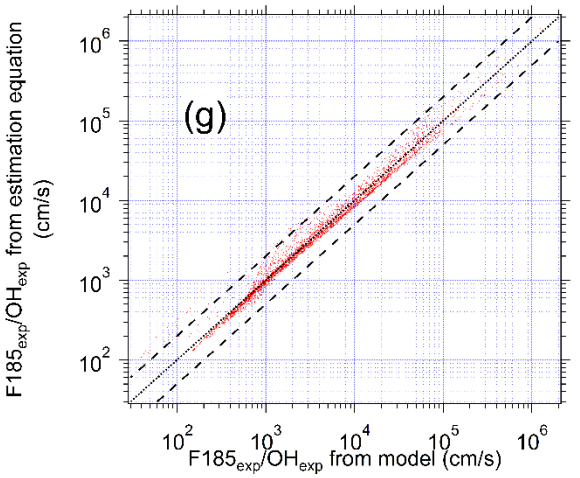

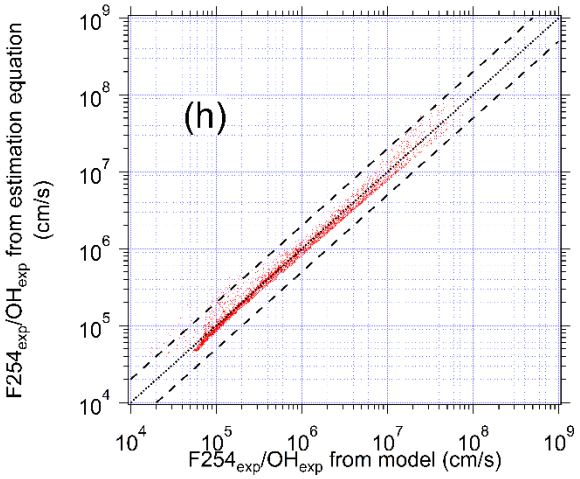

OFR254

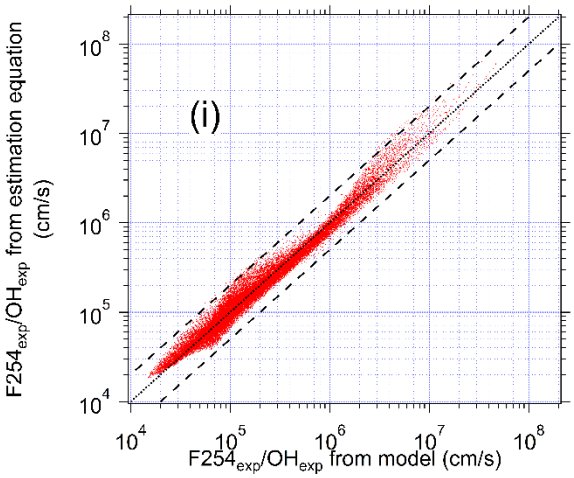

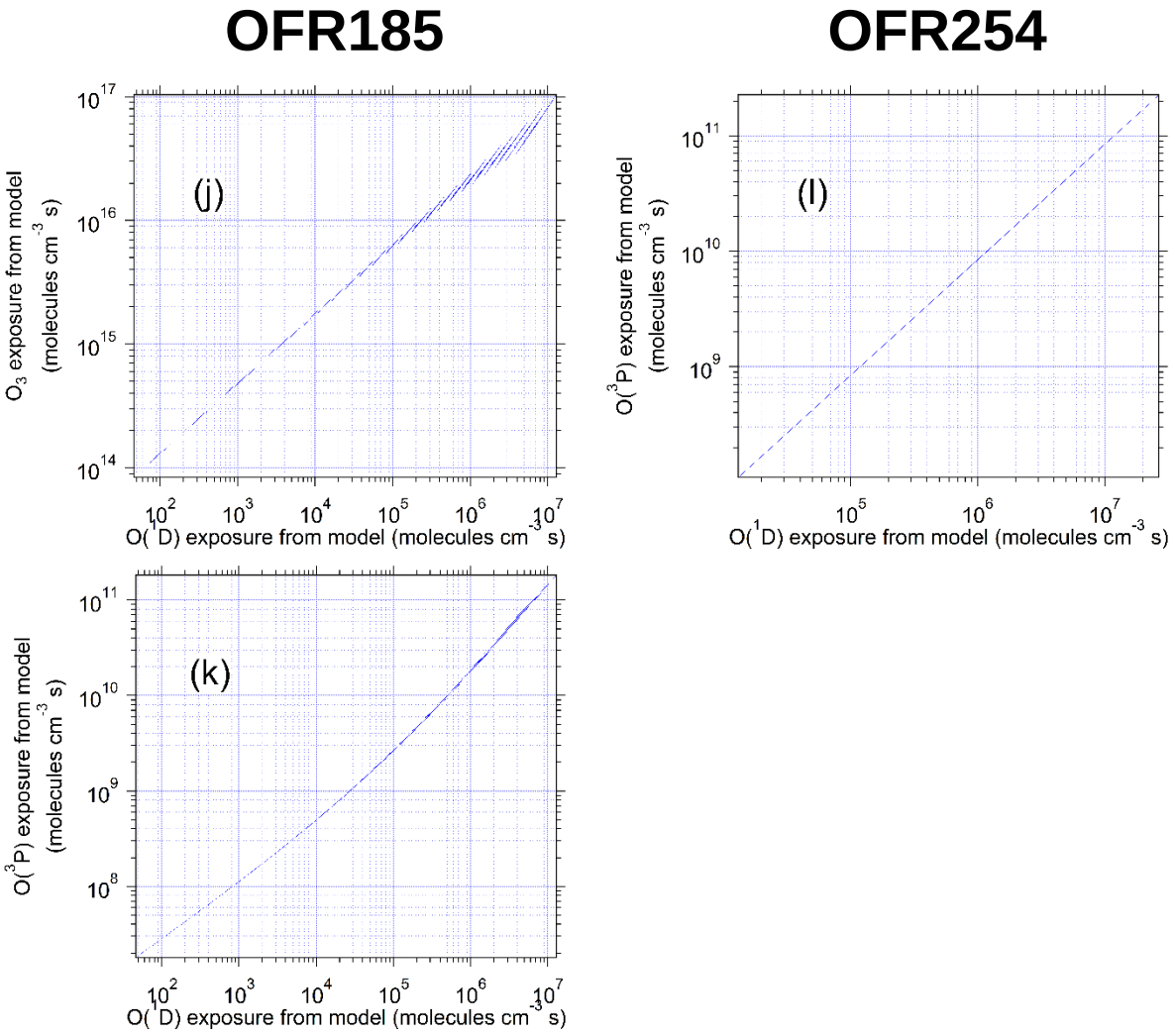

Figure S6. O_3, $O(^1D)$, and $O(^3P)$ exposures and ratios of F185 and F254 exposures to OH exposure from estimation equations vs. those from the model for (a–c, g, h) OFR185 and (d–f, i) OFR254. 1:1 (dotted), 1:2, and 2:1 (dashed) lines are shown in (a–i) to facilitate comparison. Scatter plots between modeled exposures for (j, k) OFR185 and (l) OFR254 are also shown.

We have also added the following paragraph to P23556/L21 to read:

"**OFR experiments can be simply conducted under safer conditions to avoid non-tropospheric VOC fate, while riskier conditions can lead to significant non-tropospheric VOC fate, depending on the species under study. The conditions in between, i.e., "transition" conditions, are explicitly discussed above. However, one may want to be able to more quantitatively estimate the relative importance of non-OH reactants under different conditions so that a more detailed experimental planning becomes possible that simultaneously ensures insignificant non-tropospheric VOC fate and specific experimental goals. For this purpose, we provide a series of estimation equations for**

non-OH reactant exposures (Section S3, Table S9, and Fig. S6, as well as Excel file). With these equations, the relative contribution of non-OH reactants under all conditions explored in this study can be easily estimated. In OFR studies where a different OFR design is adopted and/or chemistry beyond the approximations in our model is involved, a new model may need to be established, which can be done in similar manner as Peng et al. (2015), to obtain the relative importance of non-OH VOC fate and then perform experimental design."

Regarding the consolidation of figures, see responses to R1.7 and R2.2.

R2.2) Figures 1-5 are too difficult to read and interpret. There is too much data shown here – 28 compounds in Figure 1, 29 compounds in Figure 2, 9 compounds in Figure 3, 32 compounds in Figure 4, and 25 compounds in Figure 5 – making the figures overwhelming to the point of not being useful, especially with the histograms and insets that are also displayed in the figures.

See response to R1.7. Also note that all curves for all the compounds all have the same shape and only differ in their X-axis offset. To further facilitate reading, all species in the legend are sorted by the fractional importance of their non-OH fate, and several species categories of particular interest (e.g., aromatics and ketones in Fig. 2) are denoted with markers. Thus, although that Figs. 1–5 are complex, we think that this level of complexity is needed to serve as a useful reference for future studies.

R2.3) The "fractional importance of X" (X = F185, F254, $O(^1D)$, $O(^3P)$, O_3) curves are derived from the literature rate constants and absorption cross sections that are summarized in Tables S1 and S2. Since they only serve as qualitative reference points to interpret the modeling results, it would be sufficient to show them only in Figures S1-S5 and reference as needed in the text, which could be cut back a bit. This might also make Figures 1-5 compact enough to consolidate into two figures, perhaps one with two subpanels ($F185/OH_{exp}$ and $F254/OH_{exp}$), and the other with three subpanels ($O(^1D)_{exp}/OH_{exp}$, $O(^3P)_{exp}/OH_{exp}$, O_{3exp}/OH_{exp}).

See responses to R1.7 and R2.2. Figures 1–5 were designed as they are in order that readers can straightforwardly evaluate various non-OH destruction pathways of specific (categories of) compounds under different conditions in OFRs, and easily relate them to field, source, and laboratory studies, which are key goals of this paper. We believe that curves and insets in Figs. 1–5 carry necessary information and cannot be substantially reduced or simplified without major loss of information.

R2.4) It is not clear how to quantitatively interpret the CalNex, SOAS and BEACHON histograms because they are shrunk to a minimal size to make room for the X/(X + OH) curves. If they have a labeled ordinate, it is not clear to me what it is. Also, even though it is stated in the figure captions that "all curves, markers, and histograms share the same abscissa" (not the same ordinate) the natural tendency is to look at Figure 1, for example, and assume that $j_{185}/(j_{185} + k_{OH}[OH]) > 20\%$ for the field studies and $j_{185}/(j_{185} + k_{OH}[OH]) \sim 75\%$ for the source studies.

We apologize for omitting the Y-axis for these histograms, and we realize how this could be confusing. The relevant ordinate for these histograms is the fractional occurrence of a given condition (X_{exp}/OH_{exp}) in each field study. We have added these axes in the revised version of the figures.

We have also added explanations and modified the text in the relevant figure captions for clarity, e.g., in the caption of Fig. 1:

"**The lower inset shows histograms of model-estimated F185/OH exposures for three field studies where OFR185 was used to process ambient air. Their ordinate is the fractional occurrence of a given condition (X_{exp}/OH_{exp}). All histograms are normalized to be of identical total area (i.e., total probability of 1). The upper inset (black and blue markers) shows similar information for source studies of biomass smoke (FLAME-3; Ortega et al., 2013) and an urban tunnel (Tkacik et al., 2014). All curves, markers, and histograms in this figure share the same abscissa.**"

R2.5) I would like to see more discussion of the characteristic features of the histograms displayed in Figures 1-5 and what causes them differ from one campaign to the next. For example, in Figure 1, there appears to be two distinct clusters of $F185/OH_{exp}$ in the SOAS campaign, whereas there is a wider band of $F185/OH_{exp}$ in CalNex. Then, in Figure 2, the SOAS dataset has a wider range of $F254/OH_{exp}$ than the CalNex dataset. What specific ambient or OFR conditions yield these results?

These histograms are model outputs, which have a complex dependence on ambient temperature, OHR_{ext}, and H_2O, as well as on the UV lamp settings used for each campaign etc. Differences in these histograms for different campaigns, is both due to ambient variations (temperature, OHR_{ext}, and H_2O) and experimental setup (UV settings). We have added a mention of this to P23550/L20:

"**Note that the outputs for field studies, i.e., histograms, have a complex dependence on ambient temperature, H_2O, and OHR_{ext}, as well as UV steps used. The specific histogram shapes for different field campaigns are influenced by both ambient and experimental parameters.**"

Exploring this issue in the revised paper would require quite a bit more space and would appear to be of very narrow interest. We thus refrain from doing so in the revised manuscript. We can provide further details upon request.

R2.6) The results shown in Figure 6 would be more useful if displayed in a table format with columns: Species, Ambient photolysis %, OFR185 photolysis %, OFR254-70 photolysis %. Figure 6 is too busy/cluttered with all of the tags, and it is impossible to decipher the OFR photolysis percentages below the 1:100 and 1:1000 lines.

We have added the requested table to Supp. Info. (Table S5). However we prefer to keep the information in graphical form in the main paper, which is much superior for communication purposes to a table format, in our experience. We have relocated some of the tags to reduce clutter and make the figure easier to read. The new table and figure are reproduced below.

Table S5. Absorption cross-sections at 185 and 254 nm for several atmospheric oxidation intermediates from Keller-Rudek et al. (2015), ambient photolysis rate constants from Hodzic et al. (2015), and photolysis percentages in OFR185 and OFR254-70 (under the condition of 70% relative humidity and 25 s^{-1} initial OHR_{ext}) and in the troposphere at an OH exposure equivalent to a photochemical age of 1 week (assuming an ambient OH concentration of $1.5x10^6$ molecules cm^{-3}). "N/A" in the table stands for "not available".

Species	Cross-sections (cm^2)		Ambient photolysis rate constant (s^{-1})	Photolysis percentage		
	185 nm	254 nm		OFR185	OFR254-70	Ambient
acrolein	2.82E-17	7.00E-22	1.39E-06	4.1	0.002	57
methacrolein	6.77E-18	1.78E-21	1.34E-05	1.0	0.005	100
acetone	2.91E-18	3.01E-20	3.82E-07	1.1	0.083	21
biacetyl	1.46E-18	3.71E-20	2.29E-04	1.0	0.103	100
pyruvic acid	N/A	1.61E-20	1.03E-04	N/A	0.045	100
methyl vinyl ketone	N/A	2.41E-21	4.72E-06	N/A	0.007	94
methylglyoxal	N/A	2.76E-20	7.79E-05	N/A	0.076	100
hydroxyacetone	5.40E-18	5.07E-20	1.51E-06	1.9	0.140	60
2,4-dimethyl-3-pentanone	N/A	1.66E-20	8.30E-06	N/A	0.046	99
2-methylpropanal	5.71E-18	1.22E-20	3.80E-05	1.1	0.034	100
4-methyl-2-pentanone	N/A	2.75E-20	5.48E-06	N/A	0.076	96
5-methyl-2-hexanone	N/A	2.39E-20	4.34E-06	N/A	0.066	93
2-propyl nitrate	1.79E-17	4.86E-20	1.93E-06	3.7	0.135	69
crotonaldehyde	1.05E-17	2.80E-21	9.87E-06	1.6	0.008	100
acetaldehyde	7.83E-20	1.57E-20	3.51E-06	0.4	0.044	88
3-pentanone	N/A	3.00E-20	3.07E-06	N/A	0.083	84
methyl ethyl ketone	1.31E-18	3.09E-20	2.98E-06	0.9	0.086	83
propanal	1.42E-17	1.75E-20	1.30E-05	2.5	0.048	100
n-butanal	7.99E-18	1.45E-20	1.14E-05	1.5	0.040	100
n-pentanal	N/A	1.43E-20	1.63E-06	N/A	0.040	63
n-hexanal	N/A	1.14E-20	1.18E-05	N/A	0.032	100
1-butyl nitrate	1.81E-17	4.60E-20	1.71E-06	3.6	0.127	64
1-propyl nitrate	1.81E-17	4.40E-20	1.84E-06	3.6	0.122	67
ethyl nitrate	1.71E-17	4.10E-20	1.16E-06	3.4	0.114	50
methyl nitrate	2.10E-17	3.34E-20	7.27E-07	3.8	0.093	36
methylhydroperoxide	9.00E-19	3.23E-20	4.25E-06	0.9	0.089	92
glyoxal	4.80E-19	1.59E-20	4.72E-04	0.4	0.044	100
peroxyacetyl nitrate	6.20E-18	1.00E-19	6.24E-07	3.1	0.277	31
glycolaldehyde	3.85E-18	3.76E-20	6.82E-06	1.4	0.104	98
hydroxymethyl hydroperoxide	N/A	2.88E-20	3.90E-06	N/A	0.080	91

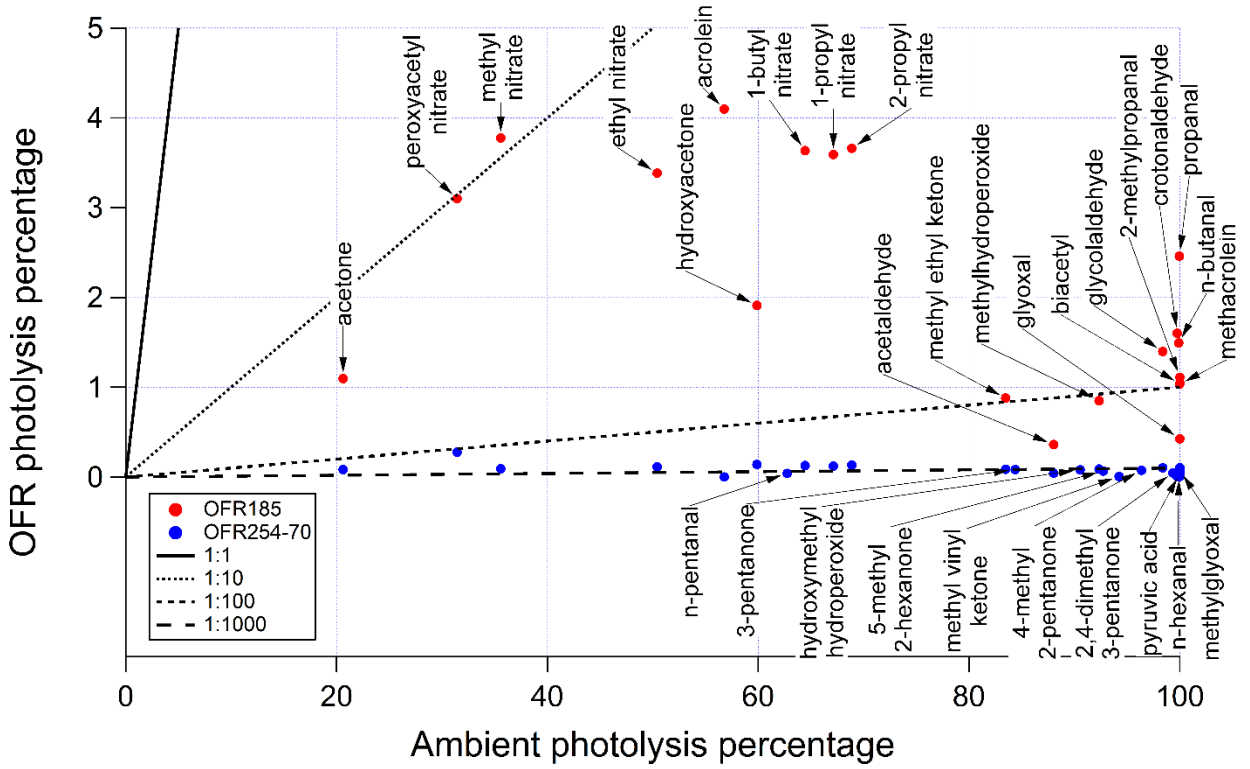

Figure 6. Ambient photolysis fractions of secondary species in a week (calculated from photolysis rates reported in Hodzic et al. (2015)) vs. photolysis fractions of those species in OFR185 and OFR254-70 when reaching the same photochemical age (ambient OH concentration of 1.5×10^6 molecules cm^{-3} assumed) under conditions of 70% relative humidity (water vapor mixing ratio of 1.4%) and 25 s^{-1} initial OHR_{ext}. If the points of a certain species for both OFR185 and OFR254-70 are available, the species name is tagged on the OFR185 point (downward arrow), otherwise on the OFR254-70 point (upward arrow). The 1:1, 1:10, 1:100, and 1:1000 lines are also shown for comparison.

R2.7) P23653 and Figure 8: "We use surrogate gas-phase species for the different functional groups as the cross sections of SOA-relevant species at these wavelengths are not available." There are at least two literature studies reporting SOA absorption cross-sections down to λ = 300 nm (Updyke et al., 2012; Lambe et al. 2013; both of which report absorption Angstrom exponents that can be used to extrapolate down to λ = 254 nm), at least one study reporting SOA absorption cross sections down to λ = 250 nm (Romonosky et al., 2015), and at least two literature studies that report SOA absorption cross sections down to λ = 220 nm (Liu et al., 2013; Liu et al., 2015):

- Updyke et al., 2012: SOA generated from OH oxidation of naphthalene and cedar leaf oil
- Lambe et al., 2013: SOA generated from OH oxidation of α-pinene, tricyclo[5.2.1.$0^{2,6}$]decane, naphthalene, and guaiacol
- Romonosky et al., 2015: SOA generated from ozonolysis and OH oxidation of isoprene and α-pinene, and OH oxidation of m-xylene. There are 25 total SOA systems with reported absorption cross sections down to approx. λ = 280 nm).

- Liu et al., 2013: SOA generated from ozonolysis of α-pinene, limonene and catechol
- Liu et al., 2015: SOA generated from OH oxidation of toluene and m-xylene

All of these studies should be referenced in the Section 3.2 text, and a representative subset of the data should be incorporated into Figure 8.

See a detailed response to this issue in response to comment R1.1.3.

R2.8) Figure 8 and related discussion: aside from sulfuric acid, glyoxal, and nitric acid, virtually all of the individual compounds shown in this plot are either already presented on similar axes in Fig. 1, 2, S1 and S2, and/or are too volatile to participate in SOA formation processes. Thus, they are not relevant surrogate compounds for SOA. While it is true that λ = 185 nm absorption cross sections are available for these compounds but not for SOA, the authors have already shown that the trends at λ = 185 nm and λ = 254 nm relative to OH_{exp} are similar. In this figure and related discussion, I suggest only showing relative photolysis rates at 254 nm for the SOA systems outlined in Comment #7, then if needed briefly mention in the text that the 185 nm results are expected to be similar.

See response to comment R1.1.3.

R2.9) Section 3.2: To supplement Figure 7, where the effects of (1) increasing RH from 3% to 60% in a laboratory SOA experiment and (2) diluting sample in two source measurements are shown, I would like to see an example of how humidifying an ambient sample to [H2O] = 2.3% prior to introduction to the OFR influences the $F185/OH_{exp}$ and/or $F254/OH_{exp}$ histograms of one of the field studies shown in Figures 1-5. While the field measurements are generally not subject to "pathological conditions" as defined by the authors, this analysis would quantitatively demonstrate the efficacy of minimizing non-OH chemistry in OFRs using one of the suggested improvements in experiment design.

We can add an example in the paper to show the effect of humidifying an ambient sample to H_2O = 2.3% on X_{exp}/OH_{exp}. However, this cannot be done as suggested by the Referee, since the saturated water vapor mixing ratio during the night was often lower than 2.3% in these field campaigns, while ambient H_2O during the day was sometimes higher than 2.3%. Even if the humidification is always done to near water vapor saturation, its effect still depends on relative humidity prior to humidification, temperature, and pressure, which differ for all datapoints of ambient measurements. As a result, this effect can only be quantitatively assessed under specific conditions. Therefore, we take the average condition of the BEACHON-RoMBAS study as the reference, whose temperature, pressure, OHR_{ext}, relative humidity etc. are fixed (Table S4). Then the quantitative comparison of the reference condition with the humidified condition (H_2O = 2.3%) becomes possible.

We add the data corresponding to the humidified condition to Table S4 and the text in P23565/L21 to read:

"**Humidifying the average condition of the BEACHON-RoMBAS** (Palm et al., 2016) **campaign from H_2O = 1.6% (RH = 63%) to H_2O = 2.3% (RH = 92%) leads to significant (from ~20% for 185 nm photon flux to a factor of ~3 for $O(^3P)$) decreases in all exposure ratios between non-OH reactants and OH (Table S4).**"

R2.10) Water vapor concentrations are discussed in terms of both mixing ratio and relative humidity. It would be preferable to choose one or the other and stick with that throughout the manuscript.

We change all "relative humidity" or "RH" to "water vapor mixing ratio" or "H_2O" in the manuscript, except when specific relative humidity values mentioned in the discussion related to previous OFR studies. In those cases we add the corresponding water vapor mixing ratios in parentheses for clarity, e.g., in P23565/L19 to read:

"**For example, increasing RH from 3% to 60% (H_2O from ~0.06% to ~1.2%) lowers the percentage of non-tropospheric consumption of p-xylene in Kang et al. (2011)'s mixture experiment from ~20% to 1.5%.**"

R2.11) P23545, L17: Quantify "low RH" and "high OHR_{ext}".

We have given a clearer definition of these conditions above (see response to R1.7), and modify the text in P23545/L16 to read:

"**We define "riskier OFR conditions" as those with either low H_2O (<0.1%) or high OHR_{ext} (≥100 s^{-1} in OFR185 and >200 s^{-1} in OFR254). We strongly suggest avoiding such conditions as the importance of non-OH reactants can be substantial for the most sensitive species, although depending on the species present OH may still dominate under some riskier conditions.**"

R2.12) P23545, L21: Quantify "low O_2".

We modify the text in P23545/L16 to read:

"**Working under low O_2 (volume mixing ratio of 0.002) with the OFR185 mode allows OH to completely dominate over O_3 reactions even for the biogenic species most reactive with O_3.**"

R2.13) P23545, L26-28: "*SOA photolysis is shown to be insignificant for most functional groups, except for nitrates and especially aromatics, which may be photolyzed at high UV flux settings.*" Quantify "insignificant", "high UV flux", and the extent of photolysis that is deemed significant at the high UV flux.

We have modified this sentence above (see response to R1.1.3). In the revised sentence, "significant", "high UV flux" etc. have been quantified.

R2.14) P23545-6, L28-2: "*The results allow improved OFR operation and experimental design, as well as guidance for the design of future reactors.*" Briefly summarize the suggested improvements, which include (1) maximizing [H2O] (2) minimizing OHR_{ext} through sample dilution and (3) operating OFR254 at [O_3] ~ 70 ppm rather than ~7 ppm. Also, while there is extensive discussion of how to improve OFR operation and experiment design, I did not notice any discussion in the manuscript about "guidance for the design of future reactors" – either delete this text or add specific suggestions for how to improve future reactor design.

We already stated in P23545/L23 that "*Non-tropospheric VOC photolysis may have been a problem in some laboratory and source studies, but can be avoided or lessened in future studies by diluting source emissions and working at lower precursor concentrations in lab studies, and by humidification.*" Significant non-tropospheric VOC photolysis should be avoided, which can be done by increasing H_2O and/or lowering OHR_{ext}. It is not always desirable to avoid all non-OH VOC fates, as some actually also occur in the atmosphere, and rather this aspect should be part of the experimental design (see responses to R1.3, R1.9, and R1.10). Although increasing H_2O and/or lowering OHR_{ext} may achieve frequent goals/conditions, we did not and should not recommend specific approaches for *all purposes*.

For clarity, we modify the sentence quoted by the Referee in P23545/28 to read:

"**The results of this study allow improved OFR operation and experimental design, and also inform the design of future reactors.**"

R2.15) P23548, L5: "…whose intensity can be rapidly computer-controlled." This seems like extraneous detail to include - consider deleting.

The fact that UV lamp setting can be rapidly computer-controlled is not an extraneous detail but an important and relevant one. It highlights the convenience of conducting UV-controlled OFR experiments and the possibility of rapidly scanning UV lamp settings during an experiment. In particular, the latter has unique applications to OFR experiments in field studies. In these experiments, OFRs enable the exploration of a very large range of photochemical age during a short period when ambient conditions usually do not significantly change. Therefore, we keep this sentence as it is.

To clarify this point, we add the following text to P23549/L17:

"**Rapid computer-controlled UV lamp setting allows rapidly scanning UV lamp settings during an experiment, and has unique applications to OFR experiments in field studies** (Hu et al., 2015; Ortega et al., 2015; Palm et al., 2016)**. In these experiments, OFRs enable the exploration of a very large range of photochemical age during a short period (~2 hr) when ambient conditions often do not significantly change.**"

R2.16) P23549, L21: subscript "exp" in "OHexp".

We thank the Referee for pointing out this typo and have corrected it.

R2.17) P23550, L16: suggested revision: “estimate ~~some~~ **parameters that are not specified or measured** (e.g. UV) as needed”.

We have revised this sentence as suggested by the Referee.

R2.18) P23551, L3: “Photolysis of SOA, **a pathway ignored in previous OFR studies**, is also investigated.” SOA photolysis is considered in Lambe et al. (2013), which uses an OFR. Photolysis of α-pinene SOA generated in a flow cell is characterized by Epstein et al. (2014), and photolysis of several SOA types generated in a flow cell were characterized by Romonosky et al. (2015).

We have removed the text bolded by the Referee. The sentence in P23551/L3 now reads:

“**Photolysis of SOA is also investigated.”**

R2.19) P23552, L24: Elsewhere in the manuscript, the “low” water vapor mixing ratio is represented as 0.07% rather than 0.0007.

We have changed “0.0007” here to “0.07%” to maintain consistency.

R2.20) P23558, L26: Replace “experimenter” with “experimentalist”.

We have made this change as suggested by the Referee.

R2.21) P23565, L7: Replace “faithfully” with “accurately”.

We have made this change as suggested by the Referee.

References (for responses to both reviewers)

Aimanant, S. and Ziemann, P. J.: Chemical Mechanisms of Aging of Aerosol Formed from the Reaction of n-Pentadecane with OH Radicals in the Presence of NOx, Aerosol Sci. Technol., 47(9), 979–990, doi:10.1080/02786826.2013.804621, 2013.

Alif, A., Pilichowski, J. and Boule, P.: photochemistry and environment XIII phototransformation of 2-nitrophenol in aqueous solution, J. Photochem. Photobiol. A Chem., 59, 209–219, doi:10.1016/1010-6030(91)87009-K, 1991.

Ammann, M., Cox, R. A., Crowley, J. N., Jenkin, M. E., Mellouki, A., Rossi, M. J., Troe, J., Wallington, T. J., Cox, B., Atkinson, R., Baulch, D. L. and Kerr, J. A.: IUPAC Task Group on Atmospheric Chemical Kinetic Data Evaluation, [online] Available from: http://iupac.pole-ether.fr/#, 2015.

Atkinson, R. and Arey, J.: Atmospheric degradation of volatile organic compounds., Chem. Rev., 103(12), 4605–38, doi:10.1021/cr0206420, 2003.

Baulch, D. L., Bowman, C. T., Cobos, C. J., Cox, R. A., Just, T., Kerr, J. A., Pilling, M. J., Stocker, D., Troe, J., Tsang, W., Walker, R. W. and Warnatz, J.: Evaluated kinetic data for combustion modeling: Supplement II, J. Phys. Chem. Ref. Data, 34(3), 757–1397, doi:10.1063/1.1748524, 2005.

Baulch, D. L., Cobos, C. J., Cox, R. A., Esser, C., Frank, P., Just, T., Kerr, J. A., Pilling, M. J., Troe, J., Walker, R. W. and Warnatz, J.: Evaluated Kinetic Data for Combustion Modelling, J. Phys. Chem. Ref. Data, 21(3), 411, doi:10.1063/1.555908, 1992.

Bouzidi, H., Aslan, L., El Dib, G., Coddeville, P., Fittschen, C. and Tomas, A.: Investigation of the Gas-Phase Photolysis and Temperature-Dependent OH Reaction Kinetics of 4-Hydroxy-2-butanone, Environ. Sci. Technol., 49(20), 12178–12186, doi:10.1021/acs.est.5b02721, 2015.

Bouzidi, H., Laversin, H., Tomas, a., Coddeville, P., Fittschen, C., El Dib, G., Roth, E. and Chakir, a.: Reactivity of 3-hydroxy-3-methyl-2-butanone: Photolysis and OH reaction kinetics, Atmos. Environ., 98(3), 540–548, doi:10.1016/j.atmosenv.2014.09.033, 2014.

Burdett, J. L. and Rogers, M. T.: Keto-Enol Tautomerism in β-Dicarbonyls Studied by Nuclear Magnetic Resonance Spectroscopy. 1 I. Proton Chemical Shifts and Equilibrium Constants of Pure Compounds, J. Am. Chem. Soc., 86(11), 2105–2109, doi:10.1021/ja01065a003, 1964.

Calvert, J. G., Atkinson, R., Becker, K. H., Kamens, R. M., Seinfeld, J. H., Wallington, T. H. and Yarwood, G.: The Mechanisms of Atmospheric Oxidation of the Aromatic Hydrocarbons, Oxford University Press, USA. [online] Available from: https://books.google.com/books?id=P0basaLrxDMC, 2002.

Carey, F. A. and Sundberg, R. J.: Advanced Organic Chemistry. Part A: Structure and Mechanisms, 5th ed., Springer US, Boston, MA., 2007.

Cours, T., Canneaux, S. and Bohr, F.: Features of the potential energy surface for the reaction of HO2 radical with acetone, Int. J. Quantum Chem., 107(6), 1344–1354, doi:10.1002/qua.21269, 2007.

Docherty, K. S., Wu, W., Lim, Y. Bin and Ziemann, P. J.: Contributions of Organic Peroxides to Secondary Aerosol Formed from Reactions of Monoterpenes with O3, Environ. Sci. Technol., 39(11), 4049–4059, doi:10.1021/es050228s, 2005.

Epstein, S. A., Blair, S. L. and Nizkorodov, S. A.: Direct Photolysis of α-Pinene Ozonolysis Secondary Organic Aerosol: Effect on Particle Mass and Peroxide Content, Environ. Sci.

Technol., 48(19), 11251–8, doi:10.1021/es502350u, 2014.

Epstein, S. A., Shemesh, D., Tran, V. T., Nizkorodov, S. A. and Gerber, R. B.: Absorption Spectra and Photolysis of Methyl Peroxide in Liquid and Frozen Water, J. Phys. Chem. A, 116(24), 6068–6077, doi:10.1021/jp211304v, 2012.

Evans, R. C., Douglas, P. and Burrow, H. D., Eds.: Applied Photochemistry, Springer Netherlands, Dordrecht., 2013.

Foster, R.: Organic Charge-Transfer Complexes, Academic Press, New York., 1969.

Francisco, J. S. and Eisfeld, W.: Atmospheric Oxidation Mechanism of Hydroxymethyl Hydroperoxide †, J. Phys. Chem. A, 113(26), 7593–7600, doi:10.1021/jp901735z, 2009.

Gäb, S., Hellpointner, E., Turner, W. V. and Koŕte, F.: Hydroxymethyl hydroperoxide and bis(hydroxymethyl) peroxide from gas-phase ozonolysis of naturally occurring alkenes, Nature, 316(6028), 535–536, doi:10.1038/316535a0, 1985.

Gao, H. and Zepp, R. G.: Factors Influencing Photoreactions of Dissolved Organic Matter in a Coastal River of the Southeastern United States, Environ. Sci. Technol., 32(19), 2940–2946, doi:10.1021/es9803660, 1998.

Gierczak, T. and Ravishankara, A. R.: Does the HO2 radical react with ketones?, Int. J. Chem. Kinet., 32(9), 573–580, doi:10.1002/1097-4601(2000)32:9<573::AID-KIN7>3.0.CO;2-V, 2000.

Goldstein, S., Aschengrau, D., Diamant, Y. and Rabani, J.: Photolysis of Aqueous H 2 O 2 : Quantum Yield and Applications for Polychromatic UV Actinometry in Photoreactors, Environ. Sci. Technol., 41(21), 7486–7490, doi:10.1021/es071379t, 2007.

Hodzic, A., Madronich, S., Kasibhatla, P. S., Tyndall, G., Aumont, B., Jimenez, J. L., Lee-Taylor, J. and Orlando, J.: Organic photolysis reactions in tropospheric aerosols: effect on secondary organic aerosol formation and lifetime, Atmos. Chem. Phys., 15(16), 9253–9269, doi:10.5194/acp-15-9253-2015, 2015.

Hu, W. W., Campuzano-Jost, P., Palm, B. B., Day, D. A., Ortega, A. M., Hayes, P. L., Krechmer, J. E., Chen, Q., Kuwata, M., Liu, Y. J., de Sá, S. S., McKinney, K., Martin, S. T., Hu, M., Budisulistiorini, S. H., Riva, M., Surratt, J. D., St. Clair, J. M., Isaacman-Van Wertz, G., Yee, L. D., Goldstein, A. H., Carbone, S., Brito, J., Artaxo, P., de Gouw, J. A., Koss, A., Wisthaler, A., Mikoviny, T., Karl, T., Kaser, L., Jud, W., Hansel, A., Docherty, K. S., Alexander, M. L., Robinson, N. H., Coe, H., Allan, J. D., Canagaratna, M. R., Paulot, F. and Jimenez, J. L.: Characterization of a real-time tracer for isoprene epoxydiols-derived secondary organic aerosol (IEPOX-SOA) from aerosol mass spectrometer measurements, Atmos. Chem. Phys., 15(20), 11807–11833, doi:10.5194/acp-15-11807-2015, 2015.

Johannessen, S. C. and Miller, W. L.: Quantum yield for the photochemical production of dissolved inorganic carbon in seawater, Mar. Chem., 76(4), 271–283, doi:10.1016/S0304-4203(01)00067-6, 2001.

Kang, E., Toohey, D. W. and Brune, W. H.: Dependence of SOA oxidation on organic aerosol mass concentration and OH exposure: experimental PAM chamber studies, Atmos. Chem. Phys., 11(4), 1837–1852, doi:10.5194/acp-11-1837-2011, 2011.

Keller-Rudek, H., Moortgat, G. K., Sander, R. and Sörensen, R.: The MPI-Mainz UV/VIS Spectral Atlas of Gaseous Molecules of Atmospheric Interest, [online] Available from: www.uv-vis-spectral-atlas-mainz.org, 2015.

Klems, J. P., Lippa, K. a and McGivern, W. S.: Quantitative Evidence for Organic Peroxy

Radical Photochemistry at 254 nm, J. Phys. Chem. A, 119(2), 344–351, doi:10.1021/jp509165x, 2015.

Kumar, M. and Francisco, J. S.: Red-Light-Induced Decomposition of an Organic Peroxy Radical: A New Source of the HO 2 Radical, Angew. Chemie Int. Ed., doi:10.1002/anie.201509311, 2015.

Kwok, E. and Atkinson, R.: Estimation of hydroxyl radical reaction rate constants for gas-phase organic compounds using a structure-reactivity relationship: An update, Atmos. Environ., 29(14), 1685–1695, doi:10.1016/1352-2310(95)00069-B, 1995.

Lambe, A. T., Cappa, C. D., Massoli, P., Onasch, T. B., Forestieri, S. D., Martin, A. T., Cummings, M. J., Croasdale, D. R., Brune, W. H., Worsnop, D. R. and Davidovits, P.: Relationship between Oxidation Level and Optical Properties of Secondary Organic Aerosol, Environ. Sci. Technol., 47(12), 6349–6357, doi:10.1021/es401043j, 2013.

Lambe, A. T., Onasch, T. B., Massoli, P., Croasdale, D. R., Wright, J. P., Ahern, A. T., Williams, L. R., Worsnop, D. R., Brune, W. H. and Davidovits, P.: Laboratory studies of the chemical composition and cloud condensation nuclei (CCN) activity of secondary organic aerosol (SOA) and oxidized primary organic aerosol (OPOA), Atmos. Chem. Phys., 11(17), 8913–8928, doi:10.5194/acp-11-8913-2011, 2011.

Laue, T. and Plagens, A.: Named Organic Reactions, 2nd ed., John Wiley & Sons, Chichester, England, New York. [online] Available from: http://www.wiley.com/WileyCDA/WileyTitle/productCd-047001041X.html, 2005.

Li, R., Palm, B. B., Ortega, A. M., Hu, W., Peng, Z., Day, D. A., Knote, C., Brune, W. H., de Gouw, J. and Jimenez, J. L.: Modeling the radical chemistry in an Oxidation Flow Reactor (OFR): radical formation and recycling, sensitivities, and OH exposure estimation equation, J. Phys. Chem. A, 119(19), 4418–4432, doi:10.1021/jp509534k, 2015.

Liu, P. F., Abdelmalki, N., Hung, H.-M., Wang, Y., Brune, W. H. and Martin, S. T.: Ultraviolet and visible complex refractive indices of secondary organic material produced by photooxidation of the aromatic compounds toluene and m-Xylene, Atmos. Chem. Phys., 15(3), 1435–1446, doi:10.5194/acp-15-1435-2015, 2015.

Liu, P., Zhang, Y. and Martin, S. T.: Complex refractive indices of thin films of secondary organic materials by spectroscopic ellipsometry from 220 to 1200 nm, Environ. Sci. Technol., 47, 13594–13601, doi:10.1021/es403411e, 2013.

Messaadia, L., El Dib, G., Ferhati, A. and Chakir, A.: UV–visible spectra and gas-phase rate coefficients for the reaction of 2,3-pentanedione and 2,4-pentanedione with OH radicals, Chem. Phys. Lett., 626, 73–79, doi:10.1016/j.cplett.2015.02.032, 2015.

O'Sullivan, D. W., Neale, P. J., Coffin, R. B., Boyd, T. J. and Osburn, C. L.: Photochemical production of hydrogen peroxide and methylhydroperoxide in coastal waters, Mar. Chem., 97(1-2), 14–33, doi:10.1016/j.marchem.2005.04.003, 2005.

Ortega, A. M., Day, D. A., Cubison, M. J., Brune, W. H., Bon, D., de Gouw, J. A. and Jimenez, J. L.: Secondary organic aerosol formation and primary organic aerosol oxidation from biomass-burning smoke in a flow reactor during FLAME-3, Atmos. Chem. Phys., 13(22), 11551–11571, doi:10.5194/acp-13-11551-2013, 2013.

Ortega, A. M., Hayes, P. L., Peng, Z., Palm, B. B., Hu, W., Day, D. A., Li, R., Cubison, M. J., Brune, W. H., Graus, M., Warneke, C., Gilman, J. B., Kuster, W. C., de Gouw, J. A. and Jimenez, J. L.: Real-time measurements of secondary organic aerosol formation and aging from

ambient air in an oxidation flow reactor in the Los Angeles area, Atmos. Chem. Phys. Discuss., 15(15), 21907–21958, doi:10.5194/acpd-15-21907-2015, 2015.

Osburn, C. L., Retamal, L. and Vincent, W. F.: Photoreactivity of chromophoric dissolved organic matter transported by the Mackenzie River to the Beaufort Sea, Mar. Chem., 115(1-2), 10–20, doi:10.1016/j.marchem.2009.05.003, 2009.

Palm, B. B., Campuzano-Jost, P., Ortega, A. M., Day, D. A., Kaser, L., Jud, W., Karl, T., Hansel, A., Hunter, J. F., Cross, E. S., Kroll, J. H., Peng, Z., Brune, W. H. and Jimenez, J. L.: In situ secondary organic aerosol formation from ambient pine forest air using an oxidation flow reactor, Atmos. Chem. Phys., 16(5), 2943–2970, doi:10.5194/acp-16-2943-2016, 2016.

Peng, Z., Day, D. A., Stark, H., Li, R., Lee-Taylor, J., Palm, B. B., Brune, W. H. and Jimenez, J. L.: HOx radical chemistry in oxidation flow reactors with low-pressure mercury lamps systematically examined by modeling, Atmos. Meas. Tech., 8(11), 4863–4890, doi:10.5194/amt-8-4863-2015, 2015.

Phillips, S. M. and Smith, G. D.: Light Absorption by Charge Transfer Complexes in Brown Carbon Aerosols, Environ. Sci. Technol. Lett., 1(10), 382–386, doi:10.1021/ez500263j, 2014.

Phillips, S. M. and Smith, G. D.: Further Evidence for Charge Transfer Complexes in Brown Carbon Aerosols from Excitation–Emission Matrix Fluorescence Spectroscopy, J. Phys. Chem. A, 119(19), 4545–4551, doi:10.1021/jp510709e, 2015.

Pitts, J. N. and Finlayson, B. J.: Mechanismen der photochemischen Luftverschmutzung, Angew. Chemie, 87(1), 18–33, doi:10.1002/ange.19750870103, 1975.

Pretsch, E., Bühlmann, P. and Badertscher, M.: Structure Determination of Organic Compounds, Springer Berlin Heidelberg, Berlin, Heidelberg., 2009.

Romonosky, D. E., Ali, N. N., Saiduddin, M. N., Wu, M., Lee, H. J. (Julie), Aiona, P. K. and Nizkorodov, S. A.: Effective absorption cross sections and photolysis rates of anthropogenic and biogenic secondary organic aerosols, Atmos. Environ., 130, 172–179, doi:10.1016/j.atmosenv.2015.10.019, 2016.

Sharpless, C. M. and Blough, N. V: The importance of charge-transfer interactions in determining chromophoric dissolved organic matter (CDOM) optical and photochemical properties, Environ. Sci. Process. Impacts, 16(4), 654, doi:10.1039/c3em00573a, 2014.

da Silva, G. and Bozzelli, J. W.: Role of the α-hydroxyethylperoxy radical in the reactions of acetaldehyde and vinyl alcohol with HO2, Chem. Phys. Lett., 483(1-3), 25–29, doi:10.1016/j.cplett.2009.10.045, 2009.

Strollo, C. M. and Ziemann, P. J.: Products and mechanism of secondary organic aerosol formation from the reaction of 3-methylfuran with OH radicals in the presence of NOx, Atmos. Environ., 77, 534–543, doi:10.1016/j.atmosenv.2013.05.033, 2013.

Tkacik, D. S., Lambe, A. T., Jathar, S., Li, X., Presto, A. A., Zhao, Y., Blake, D., Meinardi, S., Jayne, J. T., Croteau, P. L. and Robinson, A. L.: Secondary Organic Aerosol Formation from in-Use Motor Vehicle Emissions Using a Potential Aerosol Mass Reactor, Environ. Sci. Technol., 48(19), 11235–11242, doi:10.1021/es502239v, 2014.

Tsang, W.: Chemical kinetic data base for combustion chemistry part V. Propene, J. Phys. Chem. Ref. data, 20(2), 221–274, doi:10.1063/1.555880, 1991.

Turro, N. J., Ramamurthy, V. and Scaiano, J. C.: Principles of Molecular Photochemistry: An Introduction, University Science Books, Sausalito, CA, USA. [online] Available from:

http://www.uscibooks.com/turro2.htm, 2009.

Updyke, K. M., Nguyen, T. B. and Nizkorodov, S. a.: Formation of brown carbon via reactions of ammonia with secondary organic aerosols from biogenic and anthropogenic precursors, Atmos. Environ., 63, 22–31, doi:10.1016/j.atmosenv.2012.09.012, 2012.

Wolfe, G. M., Crounse, J. D., Parrish, J. D., St. Clair, J. M., Beaver, M. R., Paulot, F., Yoon, T. P., Wennberg, P. O. and Keutsch, F. N.: Photolysis, OH reactivity and ozone reactivity of a proxy for isoprene-derived hydroperoxyenals (HPALDs), Phys. Chem. Chem. Phys., 14(20), 7276, doi:10.1039/c2cp40388a, 2012.

Wong, J. P. S., Zhou, S. and Abbatt, J. P. D.: Changes in Secondary Organic Aerosol Composition and Mass due to Photolysis: Relative Humidity Dependence, J. Phys. Chem. A, 119(19), 4309–4316, doi:10.1021/jp506898c, 2015.

Zhang, Y., Xie, H. and Chen, G.: Factors Affecting the Efficiency of Carbon Monoxide Photoproduction in the St. Lawrence Estuarine System (Canada), Environ. Sci. Technol., 40(24), 7771–7777, doi:10.1021/es0615268, 2006.

Ziemann, P. and Atkinson, R.: Kinetics, products, and mechanisms of secondary organic aerosol formation, Chem. Soc. Rev., 41(19), 6582, doi:10.1039/c2cs35122f, 2012.

Non-OH chemistry in oxidation flow reactors for the study of atmospheric chemistry systematically examined by modeling

Z. Peng[1,2], D.A. Day[1,2], A.M. Ortega[1,3,*], B.B. Palm[1,2], W.W. Hu[1,2], H. Stark[1,2,5], R. Li[1,3,4,**], K. Tsigaridis[6], W.H. Brune[7], and J.L. Jimenez[1,2]

[1] Cooperative Institute for Research in Environmental Sciences, University of Colorado, Boulder, CO 80309, USA
[2] Department of Chemistry and Biochemistry, University of Colorado, Boulder, CO 80309, USA
[3] Department of Atmospheric and Oceanic Sciences, University of Colorado, Boulder, CO 80309, USA
[4] Chemical Sciences Division, Earth System Research Laboratory, National Oceanic and Atmospheric Administration, Boulder, CO 80305, USA
[5] Aerodyne Research, Inc., Billerica, MA 01821, USA
[6] Center for Climate Systems Research, Columbia University, and NASA Goddard Institute for Space Studies, New York, NY 10025, USA
[7] Department of Meteorology, Pennsylvania State University, University Park, PA 16802, USA
[*] now at: Chemical and Environmental Engineering, University of Arizona, Tucson, AZ 85721, USA
[**] now at: Markes International, Inc., Cincinnati, OH 45242, USA
Correspondence to: J.L. Jimenez (jose.jimenez@colorado.edu)

Abstract. Oxidation flow reactors (OFRs) using low-pressure Hg lamp emission at 185 and 254 nm produce OH radicals efficiently and are widely used in atmospheric chemistry and other fields. However, knowledge of detailed OFR chemistry is limited, allowing speculation in the literature about whether some non-OH reactants, including several not relevant for tropospheric chemistry, may play an important role in these OFRs. These non-OH reactants are UV radiation, $O(^1D)$, $O(^3P)$, and O_3. In this study, we investigate the relative importance of other reactants to OH for the fate of reactant species in OFR under a wide range of conditions via box modeling. The relative importance of non-OH species is less sensitive to UV light intensity than to water vapor mixing ratio (H_2O) and external OH reactivity (OHR_{ext}), as both non-OH reactants and OH scale roughly proportionally to UV intensity. We show that for field studies in forested regions and also the urban area of Los Angeles, reactants of atmospheric interest are predominantly consumed by OH. We find that $O(^1D)$, $O(^3P)$, and O_3 have relative contributions to VOC consumption that are similar or lower than in the troposphere. The impact of O atoms can be neglected under most conditions in both OFR and troposphere. We define "riskier OFR conditions" as those with either low H_2O (<0.1%) or high OHR_{ext} (≥100 s^{-1} in OFR185 and >200 s^{-1} in OFR254). We strongly suggest avoiding such conditions as the importance of non-OH reactants can be substantial for the most sensitive species, although depending on the species present OH may still dominate under some riskier conditions. Photolysis at non-tropospheric wavelengths (185 and 254 nm) may play a significant (>20%) role in the degradation of some aromatics, as well as some oxidation intermediates, under riskier reactor conditions, if the quantum yields are high. Under riskier conditions, some biogenics can have substantial destructions by O_3, similarly to the troposphere. Working under low O_2 (volume mixing ratio of 0.002) with the OFR185 mode allows OH to completely dominate over O_3 reactions even for the biogenic species most reactive with O_3. Non-tropospheric VOC photolysis may have been a problem in some laboratory and source studies, but can be avoided or lessened in future studies by diluting source emissions and working at lower precursor concentrations in laboratory studies, and by humidification. Photolysis of SOA samples is estimated to be significant (>20%) under the upper limit assumption of unity quantum yield at medium ($1x10^{13}$ and $1.5x10^{15}$ photons cm^{-2} s^{-1} at 185 and 254 nm, respectively) or higher UV flux settings. The need for quantum yield measurements of both VOC and SOA photolysis is highlighted in this study. The results of this study allow improved OFR operation and experimental design, and also inform the design of future reactors.

Formatted: Justified, Line spacing: Exactly 16 pt, No widow/orphan control
Deleted: relative humidity (RH
Deleted: proportional
Deleted: Under "pathological
Deleted: of
Deleted: RH and/
Deleted: ,
Deleted: is enhanced because
Deleted: is suppressed. Some biogenics can have substantial destructions by O_3, and photolysis
Formatted: Font color: Text 1
Deleted: also
Formatted: Font color: Text 1
Formatted: Font color: Text 1
Deleted: under pathological conditions.
Formatted: Font color: Text 1
Formatted: Font color: Text 1
Formatted: Font: 9 pt, Font color: Text 1
Deleted: lab
Formatted: Font color: Text 1
Deleted: photolysis
Formatted: Font color: Text 1
Deleted: shown
Formatted: Font color: Text 1
Deleted: insignificant for most functional groups, except for nitrates
Formatted: Font color: Text 1
Deleted: especially aromatics, which may be photolyzed at high
Formatted: Font color: Text 1
Deleted: Our work further establishes the OFR's usefulness as a tool to
Formatted: Font color: Text 1
Deleted: atmospheric chemistry and enables better experiment design and interpretation, as well as
Formatted: Font color: Text 1
Formatted: Font color: Text 1
Deleted: reactor design.¶

1 Introduction

For decades, environmental chambers have been employed to study atmospheric chemical processes, particularly, volatile organic compound (VOC) oxidation processes in the atmosphere (Cocker et al., 2001; Carter et al., 2005; Presto et al., 2005; Wang et al., 2011; Platt et al., 2013), without the interference of some transport processes (e.g., advection and wet deposition). These oxidation processes are the key to secondary organic aerosol (SOA) formation (Odum et al., 1996; Hoffmann et al., 1997; Hallquist et al., 2009), and air pollutant removal (Levy II, 1971). Atmospheric simulation chambers usually have volumes on the order of several m^3, and use light sources longer than 300 nm (e.g., sunlight or UV blacklights) to generate oxidants (mainly OH). These settings leads to OH concentrations (10^6–10^8 molecules cm^{-3}) that are not much higher than the typical ambient values (10^6–10^7 molecules cm^{-3}; Mao et al., 2009). Relatively low OH concentrations require long residence/simulation times (generally hours) and limit the ability of those setups to reach very high photochemical ages that are atmospherically-relevant (George et al., 2007; Kang et al., 2007; Carlton et al., 2009; Seakins, 2010; Wang et al., 2011). Residence times are ultimately limited due to losses of gases and particles to Teflon walls with timescales of tens of minutes to several hours (Cocker et al., 2001; Matsunaga and Ziemann, 2010; Zhang et al., 2014) as well as by the limited volume of the bag relative to the sampling instrumentation (Nguyen et al., 2014). Besides, large sizes and support systems (e.g. clean air generators) make it difficult to use large chambers in field or source studies.

Oxidation flow reactors (OFR) are an alternative that offers some advantages over environmental chambers, especially for rapid changes of experimental conditions, and/or for field experiments. They generally have a smaller size (on the order of 10 L), and typically use low-pressure Hg lamps as light sources for producing OH in large amounts via O_3 and/or H_2O photolysis. These design choices lead to good portability, short experimental timescales, ability to reach long photochemical ages, and potentially reduced wall losses.

Due to these advantages, OFRs have been employed in many recent field and laboratory studies in atmospheric chemistry, particularly in SOA-related research (George et al., 2007; Kang et al., 2007, 2011; Smith et al., 2009; Massoli et al., 2010; Cubison et al., 2011; Lambe et al., 2011a, 2011b, 2012, 2013; Bahreini et al., 2012; Saukko et al., 2012; Wang et al., 2012; Ortega et al., 2013; Li et al., 2013). OFRs are also used in related applied fields, such as scrubbing of pollution from air (Johnson et al., 2014). In contrast to their popularity, the chemistry occurring in OFRs is still incompletely characterized, although the formation and interconversion reactions of most oxidants in OFRs have been well characterized (Sander et al., 2011; Ammann et al., 2015). To our knowledge, there are only three studies of OFR radical oxidation chemistry up to date: Ono et al. (2014) focused on the dependence of O_3 destruction on H_2O concentration. We have recently made progress on the characterization of HO_x radical chemistry in OFRs (Li et al., 2015; Peng et al., 2015). We have developed a kinetic model for OFRs, which provides predictions in good agreement with laboratory experiments. This model has also shown that OH exposure (OH_{exp}, i.e., OH concentration integrated over the reactor residence time) increases with H_2O concentration and UV intensity, and decreases with external OH reactivity [$OHR_{ext}=\sum k_i c_i$, i.e.,

the sum of the products of concentrations of externally introduced OH-consuming species (c_i) and rate constants of their reactions with OH (k_i)]. The OH_{exp} decrease due to OHR_{ext} was defined as "OH suppression," and can reach two orders-of-magnitude in some cases (Li et al., 2015; Peng et al., 2015). We also showed that relative uncertainties of the outputs of our box model (e.g., OH_{exp}) due to uncertain kinetic parameters are typically only 20% (Peng et al., 2015). However, none of these studies directly address the fate of VOCs (including oxygenated VOCs), simply regarded as external OH reactants in the prior studies.

The primary reason for the use of the OFRs studied here is for the study of reactions of species or mixtures of atmospheric relevance with the OH radical. However, other highly reactive species are also present at very elevated concentrations, including the radicals $O(^1D)$ and $O(^3P)$, 185 and 254 nm photons, and O_3. If a substantial fraction of the species of interest reacted with those non-OH reactants, then the chemistry in the OFR would deviate from the OH radical chemistry intended to investigate. The absence of systematic research on VOC fate in OFRs leaves room for some speculation that non-OH or non-tropospheric chemistry can play a major role in OFRs: for example, Johnson et al. (2014) suggested that $O(^1D)$ and $O(^3P)$ significantly consumed VOCs. Klems et al. (2015) concluded that photons at 254nm from Hg-lamp emission played an important role in their OFR experiment, especially for downstream chemistry. Lack of clarity about these types of questions and of clear guidelines about how to apply OFRs to avoid such problems have limited the application of OFRs for years. In this paper, we apply the model in Peng et al. (2015) to systematically investigate whether significant non-tropospheric or non-OH chemistry occurs in OFRs, and what experimental conditions make it more important. Considering the enormous complexity of organic radical (particularly organic peroxy) chemistry, we only examine the non-OH fate of stable species in the present work. The fate of organic radicals should be the subject of future studies. The results allow improved OFR operation and experimental design, as well as guidance for the design of future reactors.

Deleted: concluded that photons at 254 nm from Hg-lamp emission played an important role in their OFR experiment, especially for downstream peroxy radical chemistry. Lack of clarity about these types of questions and of clear guidelines about how to apply OFRs to avoid such problems have limited the application of OFRs for years. In this paper, we apply the model in Peng et al. (2015) to systematically investigate whether significant non-tropospheric or non-OH chemistry occurs in OFRs, and what experimental conditions make it more important. The results allow improved OFR operation and experimental design, as well as guidance for the design of future reactors.¶
Methods¶

2 Methods

The OFR and the model used here have been described in detail elsewhere (Kang et al., 2007; Li et al., 2015; Peng et al., 2015). Here, we only present a brief introduction for each.

2.1 Potential Aerosol Mass flow reactor

Kang et al. (2007) first introduced the Potential Aerosol Mass (PAM) flow reactor. Although there were earlier versions of the PAM reactor, the version of cylindrical geometry with a volume of ~13 L has been widely used and is currently in use in many SOA research groups (Massoli et al., 2010; Cubison et al., 2011; Kang et al., 2011; Lambe et al., 2011a, 2011b, 2012, 2013; Bahreini et al., 2012; Saukko et al., 2012; Wang et al., 2012; Li et al., 2013; Ortega et al., 2013). The reactor is made of aluminum or of glass and aluminum, and equipped with 1–4 low-pressure Hg lamps (model no. 82-9304-03, BHK Inc.) located inside the flow tube. The Hg lamps produce UV emissions at 185 and 254 nm, whose intensity can be rapidly computer-controlled. The operation mode using both 185 and 254 nm emissions is called "OFR185". In this mode, photons at 185 nm dissociate H_2O and O_2 molecules to produce OH+H and

155 $O(^3P)$, respectively. Recombination of $O(^3P)$ with O_2 forms O_3. UV light at 254 nm then photolyzes O_3 to
156 produce $O(^1D)$, which reacts with H_2O and produces additional OH. OFR can also be operated in another
157 mode where photons at 185 nm are filtered by quartz sleeves around the lamps. In this case, only 254
158 nm UV light is active to generate OH ("OFR254" mode), and injection of externally generated O_3 into
159 the reactor is required for OH production. The amount of injected O_3 plays a critical role in the OFR
160 chemistry (Peng et al., 2015). For this reason this amount (X ppm) is also included in OFR operation
161 mode notation in the form of OFR254-X. For example, OFR254-70 and OFR254-7 denote experiments
162 with 70 and 7 ppm O_3 injected, respectively. We use the PAM as the basic OFR design. Other designs
163 will be specified below if needed. Rapid computer-controlled UV lamp setting allows rapidly scanning
164 UV lamp settings during an experiment, and has unique applications to OFR experiments in field studies
165 (Hu et al., 2015; Ortega et al., 2015; Palm et al., 2016). In these experiments, OFRs enable the
166 exploration of a very large range of photochemical age during a short period (~2 hr) when ambient
167 conditions often do not significantly change.

168 **2.2 Model description**

169 We use the same model as in Peng et al. (2015), a standard chemical-kinetic model under plug-
170 flow conditions. The effect of non-plug flow residence time distributions (RTD) was also investigated in
171 that study. Non-plug-flow models result in similar OH_{exp} than plug-flow in most cases, except under
172 specific conditions with very high UV, H2O, and OHR_{ext} (Peng et al., 2015). Therefore, plug-flow OH_{exp} is
173 used in this study, as a proxy of OH_{exp} estimated from OHR_{ext} decay and to avoid the much increased
174 computational expense for complex RTDs. All O_x and HO_x reactions available in the JPL Chemical Kinetic
175 Data Evaluation (Sander et al., 2011) are taken into account. Reactions of some external OH reactants
176 (externally introduced reactants destructing OH), such as SO_2, CO and NO_x, are also included. SO_2 is used
177 as a proxy of other external OH reactants (e.g., VOCs). We believe that this is a realistic approximation
178 in terms of OHR_{ext} decay vs. OH_{exp} for many precursors, as discussed in Peng et al. (2015).

179 When studying the OFR, we assume a residence time of 180 s, and use typical temperature (295
180 K) and atmospheric pressure (835 mbar) in Boulder, CO, USA. H_2O mixing ratio (abbr. H_2O hereafter)
181 ranges from 0.07 to 2.3% (equivalent to relative humidity (RH) of 3–92%). According to Li et al. (2015),
182 UV photon fluxes (abbr. UV hereafter) at 185 and 254 nm are estimated to be in the ranges $1.0x10^{11}$–
183 $1.0x10^{14}$ and $4.2x10^{13}$–$8.5x10^{15}$ photons cm^{-2} s^{-1}, respectively. Four levels of OHR_{ext}, 0, 10, 100, and 1000
184 s^{-1} covering the range of most field and laboratory studies are investigated. In the explored parameter
185 space, the same 3-character labels as in Peng et al. (2015) are used to denote typical cases (Table 1). For
186 OFR254, we study OFR254-70 and OFR254-7, representing OFR254 experiments with high (Palm et al.,
187 2016) and low O_3 (Kang et al., 2011; Liu et al., 2015), respectively. To model literature OFR studies, we
188 adopt corresponding parameters (reactor volume, H_2O, residence time, etc.), and estimate parameters
189 that are specified or measured (e.g., UV) as needed. In particular, for some field studies, where long
190 time-series of experimental data [42 d in BEACHON-RoMBAS (Palm et al., 2016), 42 d in SOAS (Hu et al.,
191 2015), and 15 d in CalNex-LA (Ortega et al., 2015)] were recorded, we model all valid datapoints and
192 present outputs in the form of histograms. Note that the outputs for field studies, i.e., histograms, have

Deleted: some

a complex dependence on ambient temperature, H_2O, and OHR_{ext}, as well as UV steps used. The specific histogram shapes for different field campaigns are influenced by both ambient and experimental parameters.

3 Results and Discussions

In the following sections we explore the relative importance of five non-OH pathways (photons at 185 and 254 nm, $O(^1D)$, $O(^3P)$, and O_3) vs. the OH reaction for species of atmospheric interest, including a variety of typical biogenic and anthropogenic VOCs and a few important inorganic species (e.g., SO_2 and NO_2). Because of the huge complexity of VOC oxidation mechanisms, only consumption/oxidation of specific VOCs is investigated. In such an investigation, a large amount of kinetic data is required. We collected the required data (Tables S1–S3) according to the principles in Section S1. Photolysis of SOA is also investigated.

3.1 Fractional loss of VOCs to non-OH reactants

As shown in Peng et al. (2015), OH_{exp} in OFRs depends on various physical conditions, e.g., H_2O and OHR_{ext}. However, the non-OH reactants are much less dependent on these parameters. H_2O and external OH reactants only contribute less than 1% to absorption at 185 and 254 nm. Therefore, they have almost no impact on effective UV. O_3 can absorb a fraction of the 254 nm radiation, but the optical depth due to 70 ppm O_3 in the reactor is ~0.11, and thus the attenuation of 254 nm photons by O_3 absorption is a minor effect. The dominant fates of $O(^1D)$ and $O(^3P)$ are the quenching by air and the recombination with O_2, respectively, with which no reactions involving H_2O or external OH reactants can compete. Thus the concentrations of $O(^1D)$ and $O(^3P)$ in the reactor depend on UV intensity and H_2O, but not on OHR_{ext}. Since OH can be strongly modulated by OHR_{ext}, changing input conditions may result in very different relative importance of OH to other reactive species. To fully evaluate this issue, it is necessary to explore a very wide range of conditions as in Peng et al. (2015).

3.1.1 Common features of all the non-OH reactants

Figs. 1–5 show the relative consumption of several species vs. ratio of exposures to individual non-OH species (X) to OH exposure (X_{exp}/OH_{exp}) for 185 and 254 nm photons, $O(^1D)$, $O(^3P)$, and O_3, respectively. Fig. S1-S5 present the same information in an alternative format that may be useful to evaluate the fate of species not included in our study. They show ratios of rate constants of species with OH to those with non-OH species (X), mathematically equivalent to the X_{exp}/OH_{exp} where corresponding X/(OH+X) is 50%. X/(OH+X) denotes the fractional importance of X in the sum of the contribution of OH and X to VOC. If a VOC has a higher ratio of rate constant with OH to that with a non-OH reactant (X) than with another reactant (Y), the relative contribution of X, X/(OH+X), should be smaller than that of Y. In these figures, we also show the X_{exp}/OH_{exp} range for OFR254-70, OFR254-7, and OFR185, under different conditions, including key laboratory and field studies, and identify the X_{exp}/OH_{exp} ranges where non-OH contribution to species fate is significant. A dissociation quantum yield of unity is assumed for the photolysis reactions, which results in upper limits for the relative importance of those pathways.

In these figures, the relationships of all non-OH reactive species to OH are similar for certain common conditions. We define three types of conditions to help guide experimental design and

Deleted: those

Deleted: , a pathway ignored in previous OFR studies,

Deleted: Under "pathological conditions" of high/very high OHR_{ext} (≥100 s^{-1}) and/or low RH (3%), non-OH reactions can be significant depending on the species. Conversely, under low OHR_{ext} and high RH, reaction with OH is dominant (Figs. S1–5). High H_2O and zero/low OHR_{ext} lead to strong OH production and no/weak OH suppression, respectively. Thus, OH is more abundant and dominates species consumption under those conditions. In the case of low H_2O and high OHR_{ext}, OH is generally lower because of less production and more suppression. These conditions increase the relative contribution of non-OH species. UV light intensity is generally less influential on non-OH VOC fate than H_2O and OHR_{ext}, although OH production is nearly proportional to UV (Peng et al., 2015), because the non-OH reactive species also scale (nearly) proportional to UV. As a result, UV only has minor effects on exposure ratios between OH and the non-OH reactants. In addition to the common features above, individual non-OH reactants have their own features as well as a few exceptions to the abovementioned

evaluation in terms of the relative importance of non-OH reactants. Under "riskier conditions" of high/very high OHR_{ext} (≥100 s^{-1} in OFR185 and >200 s^{-1} in OFR254 (-7 to -70)) and/or low H_2O (<0.1%), non-OH reactions can be significant depending on the species. Conversely, under "safer conditions" with relatively low OHR_{ext} (<30 s^{-1} in OFR185 and <50 s^{-1} in OFR254), *and* high H_2O (>0.8% in OFR185 and >0.5% in OFR254), and moderate or higher UV (>1x10^{12} photons cm^{-2} s^{-1} at 185 nm) in OFR185, reaction with OH is dominant (Figs. 1–5 and S1–5). We denote all other conditions as "transition conditions." High H_2O and zero/low OHR_{ext} lead to strong OH production and no/weak OH suppression, respectively. Thus, OH is more abundant and dominates species consumption under those conditions. In the case of low H_2O and high OHR_{ext}, OH is generally lower because of less production and more suppression. These conditions increase the relative contribution of non-OH species. UV light intensity is generally less influential on non-OH VOC fate than H_2O and OHR_{ext}, although OH production is nearly proportional to UV (Peng et al., 2015), because the non-OH reactive species also scale (nearly) proportional to UV. As a result, UV generally has smaller effects on exposure ratios between OH and the non-OH reactants. However, under a UV near the lower bound of the explored range in this study (<1x10^{12} photons cm^{-2} s^{-1} at 185 nm) in OFR185, OH production is so small that the effect of OHR_{ext} on OH suppression can be amplified and hence some exposure ratios may be affected. In OFR254 OH is more resilient to suppression even at low UV because of the OH-recycling by initially injected O_3 (Peng et al., 2015). Note that we call these conditions "riskier" and "safer" mainly in terms of non-tropospheric VOC fate, but not of VOC fate by all non-OH reactants, as some of the non-OH reactant studied in this work may also play a role under some tropospheric conditions (see Sections 3.1.4 and 3.1.5). In addition to the common features above, individual non-OH reactants have their own features as well as a few exceptions to the above mentioned general observations, which we will detail below.

3.1.2 Reactions with OH vs. photolysis at 185 nm

Under riskier reactor conditions, photolysis at 185 nm of several aromatic compounds, such as toluene, benzene, and p-xylene, are estimated to be significant and even dominant vs. the OH reactions (Fig. 1). This results from their aromatic ring, which is not only highly efficient as a chromophore, but also relatively resistant to OH attack.

It is not common to perform field studies for SOA at H_2O as low as 0.1% or OHR_{ext}≥100 s^{-1} (Table 1). According to $F185_{exp}/OH_{exp}$ calculated from the field studies where OFR185 was deployed, i.e., BEACHON-RoMBAS (Palm et al., 2016), SOAS (Hu et al., 2015), and CalNex-LA (Ortega et al., 2015) all these studies are generally under safer conditions (infrequent low H_2O mixing ratio and ambient OH reactivity estimated to be ~15–25 s^{-1}). For instance, none of these field studies fell into the conditions where the fractional importance of photolysis at 185 nm was significant for aromatic species. However, in some source studies using OFRs, e.g. when sampling biomass burning smoke (FLAME-3; Ortega et al. 2013) or air in a traffic tunnel (Tkacik et al., 2014), OHR_{ext} can be very high reaching values of several 100 s^{-1} (Table S4). Especially on the smoke study, photolysis of aromatics may have played a role. However, it has long been known that excited aromatic molecules may undergo various deactivation pathways (e.g., vibronic coupling, intersystem crossing, and collisional quenching) without molecular

Deleted: At a low H_2O volume mixing ratio of 0.0007 (RH=3% at 22 °C) and OHR_{ext}≥100 s^{-1}

Deleted: RH

Deleted: 3

Deleted: BEACHON-RoMBAS (Palm et al., 2015), SOAS (Hu et al., 2015), and CalNex-LA (Ortega et al., 2015) (ambient OH reactivity estimated to be ~15–25 s^{-1}), by our model

fragmentation (Beddard et al., 1974; Nakashima, 1982; Nakashima and Yoshihara, 1983; Fang and Phillips, 2002), preventing unity quantum yields. Therefore, the photolysis of aromatics at 185 nm in the abovementioned source studies may not be as significant as estimated in Fig. 1.

Under riskier conditions, some organic peroxy nitrates and nitrates (e.g., peroxyacetyl nitrate and 2-propyl nitrate in Fig. 1) have an estimated contribution from photolysis at 185 nm to their fate that is comparable to or even larger than that of reaction with OH. Nevertheless, this does not mean that we need to make extra efforts to avoid the photolysis of organic nitrates and peroxy nitrates at 185 nm. Although they have cross-sections at 185 nm ~10–100 times smaller than those of aromatics, these organic compounds react remarkably slowly with OH (~2 order of magnitude slower than reactions of aromatics with OH), so photolysis appears substantial with respect to reaction with OH, but really two slow rates are being compared. Thus, absolute photolyzed amounts of these species are not substantial. For example, only ~10% of peroxyacyl nitrate is photolyzed by 185 nm photons at the highest OFR185 lamp setting. Even if photolysis of nitrates and peroxy nitrates by low-pressure Hg lamp emission proceeds to a significant extent, it may still not be a problem, as it generally leads to the same products as their ambient photolysis (Renlund and Trott, 1984; Roberts and Fajer, 1989). Nitrate and peroxy nitrate photolysis is actually much more important in the atmosphere than in OFRs for the same photochemical age (see below and Fig. 6).

SO_2 has been used in some studies to calibrate OH_{exp} (Lambe et al., 2015; Li et al., 2015). It does undergo significant photolysis at 185 nm under riskier conditions. However, this photolysis does not lead to an overestimation of OH_{exp}, since the S-bearing product of SO_2 photolysis at 185 nm, SO, converts back to SO_2 very rapidly through its reaction with O_2.

Oxidation intermediates may also photolyze at 185 nm. However, their photolysis is unlikely to be significant when OFR is operated under safer conditions. To clarify this issue, a detailed discussion about the photolysis of oxidation intermediates at 254 nm is required as a premise. We thus discuss oxidation intermediate photolysis at both 185 and 254 nm in Section 3.1.3.

3.1.3 Reactions with OH vs. photolysis at 254 nm

The photon flux in the reactor at 254 nm is 80–250 times larger than at 185 nm (Li et al., 2015). Although absorption cross sections of all molecules investigated in this study are significantly lower at 254 than 185 nm, the higher photon flux compensates, at least partially, for this effect, so that in OFR185 photolysis of many species at 254 nm is of similar relative importance as photolysis at 185 nm, with potentially important effects at low H_2O and/or high OHR_{ext} (Figs. 2 and S2). As for 185 nm, 254 nm photolysis is a concern mainly for aromatic compounds, because of the high light absorptivity and low OH reactivity of aromatic rings as previously discussed. Again, note that this concern may be less serious than shown in Fig. 2 because of possible lower quantum yields. Photolysis of organic nitrates and peroxy nitrates at 254 nm also appears to be important relative to reactions with OH, and is still not a concern for the same reasons as photolysis at 185 nm. SO_2 can absorb efficiently at 254 nm, but it is still not a problem for SO_2-based OH_{exp} calibration, since photons at 254 nm are not sufficiently energetic to dissociate SO_2 molecules.

Deleted: pathological

Deleted: (low RH and/or high OHR_{ext}),

Deleted: a

Deleted: nitrates

Deleted: . However

Deleted: nitrates

Deleted: emissions

Deleted: pathological

Deleted: one of

Deleted: products

Deleted: much

Deleted: approximately

High UV generally appears to be more problematic than low UV in OFR254 (Fig. S2). This is in contrast to the trend of OFR185. In OFR254, O_3 is the only primary OH source, and a substantial fraction of O_3 can be photolyzed at the highest lamp settings, leading to a substantial reduction of OH production (compared with proportional scaling with UV). OFR254-70 appears to be less prone to riskier conditions than OFR254-7, since higher O_3 favors HO_2-to-OH recycling, making OH more resilient to suppression (Peng et al., 2015).

Under highly risky conditions (H_2O<0.1% and OHR_{ext}≥100 s^{-1} for OFR185, and H_2O<0.1% and OHR_{ext}>200 s^{-1} for OFR254), some saturated carbonyl compounds (e.g., pyruvic acid, methyl ethyl ketone and hydroxyacetone) have significant photolysis at 254 nm relative to reactions with OH. This significant relative contribution of photolysis also results from remarkably slow reactions of saturated carbonyl compounds with OH. Although secondary species without C=C double bond, e.g., saturated carbonyls, hydroperoxides, and nitrates, can be photolyzed in OFRs at low H_2O and/or high OHR_{ext}, their photolysis only proceeds to a ~10–1000 times smaller extent than ambient photolysis at the same photochemical age (Fig. 6).

Unsaturated carbonyls may have much higher absorption cross-sections if their C=C bonds are conjugated with carbonyls. However, according to our following analysis, conjugated unsaturated carbonyl compounds do not often cause problems of non-tropospheric photolysis at 254 nm. Carbonyls have π–π* and n–π* transitions. The former corresponds to high cross-section (typically >10^{-18} cm^2) and typically occurs around or below 200 nm. The latter is forbidden, and thus has weak absorption (cross-section on the order of 10^{-19} cm^2 or lower), and typically occurs around or above 300 nm (Turro et al., 2009). Conjugation usually does not substantially enhance the absorption of n–π* transition but it does for π–π* transitions (Turro et al., 2009). As a result, through conjugation, the only reason why cross-sections of carbonyls at 254 nm may be elevated above 10^{-18} cm^2 is the red-shift of the maximum absorption wavelength of their π–π* transitions due to conjugation. According to Woodward's rules (Pretsch et al., 2009) and available cross-section data of α,β-unsaturated carbonyls in Keller-Rudek et al. (2015), a conjugation of at least 3–4 double bonds is required for the excitation at 254 nm to dominantly correspond to π–π* transition. Conjugated oxidation intermediates containing at least 3–4 double bonds including C=C bond(s) are virtually impossible to form from aliphatic hydrocarbon oxidation in OFRs. Nevertheless, such intermediates may form via ring-opening pathways of aromatic oxidation (Calvert et al., 2002; Atkinson and Arey, 2003; Strollo and Ziemann, 2013). E,E-2,4-hexadienedial may be regarded as an example of this type of intermediates. Even under assumption of a unity quantum yield, its fraction of photolysis at 254 nm is not much higher than that of aromatic precursors (Fig. 2). Therefore, 254 nm photolysis of conjugated intermediates should not be problematic as long as safer experimental conditions are adopted.

To our knowledge, the only exception that has strong absorption at 254 nm due to conjugation with <2 double bonds are β-diketones, which may be formed in aliphatic hydrocarbon oxidation, particularly that of long-chain alkanes (Ziemann and Atkinson, 2012). The peculiarity of β-diketones is that their enol form may have a highly conjugated ring structure due to very strong resonance (Scheme

Deleted: pathological

Deleted: ,

Deleted: ketones

Deleted: Significant

Deleted: ketones

Deleted: RH

S1), and hence cross-sections on the order of 10^{-17} cm^2 at 254 nm (Messaadia et al., 2015). However, even under the assumption of unity quantum yield, the fractional contribution of 254 nm photolysis of acetylacetone (representative of β-diketones) is only slightly larger than for aromatic VOCs (Fig. 2), since its enol form also contains a C=C bond leading to very high reactivity toward OH. Furthermore, we argue that the actual probability that a concrete structural change (in number and type of functional groups, O/C ratio, average C oxidation state etc.) of β-diketones resulting from photoexcitation at 254 nm may be low. As their excitation at 254 nm corresponds to π–π* transition, their rigid ring structure likely hinders cyclic structural change at the 1st singlet excited state ($S_1(\pi,\pi^*)$) while the biradical structure of the 1st triplet state ($T_1(\pi,\pi^*)$) may favor H-shift between two O atoms, which ends up with the same/similar structure than prior to the H-shift (Scheme S1). Also, the excitation of β-diketones at 254 nm may also lead to charge transfer complex formation via direct excitation and/or radiationless transition from a local excited state (Phillips and Smith, 2015), which is likely to result in low quantum yields, as discussed in detail below.

In addition to conjugated species, Phillips and Smith (2014, 2015) reported a new type of highly absorbing species that may be formed from VOC oxidation. Although their studies were conducted in the condensed phase, it is likely that the main conclusions of these studies are generally transferable to the gas-phase conditions, since no long-range interactions, which do not exist in normal gases, were involved in these studies. Phillips and Smith (2014, 2015) investigated the photoabsorption enhancement of multifunctional oxygenated species in SOA and found that the high absorptivity of these species can largely be explained by transitions toward the electronic states of charge transfer complex formed between hydroxyl groups (donor) and neighboring carbonyl groups (acceptor). They also pointed out that charge transfer complexes of this kind have a continuum of states whose energy levels range from that of local excited states (radiative transition wavelength <300 nm) to very low levels (radiative transition wavelength >600 nm). The latter are insufficient to cause common photochemical reactions. Relaxation through a continuum of states is usually ultrafast according to Fermi's golden rule (Turro et al., 2009), likely leading to low quantum yields of chemical reactions. The low quantum yields may be seen even from species with only one hydroxyl and one carbonyl: the photolysis of 3-hydroxy-3-methyl-2-butanone and 4-hydroxy-2-butanone at wavelengths down to 270 nm has quantum yields around only 0.1 (Bouzidi et al., 2014, 2015). Although measurements of photolysis quantum yield for multifunctional species are challenging and rare, it is reasonable to expect even lower quantum yields for larger and/or highly substituted (by hydroxyl and carbonyl) species, since larger species have more degrees of freedom for relaxation of excited molecules, and more and/or larger complex sites generally lead to more efficient relaxation through a continuum of states, in accordance with common photophysical sense (Sharpless and Blough, 2014). Therefore, even though species with a number of hydroxyls and carbonyls are formed in VOC oxidation and can absorb >1 order of magnitude more efficiently at 254 nm than mono- and difunctional species, they may still have low effective photolysis rates because of low quantum yields.

For this type of species, we estimate an upper limit of the fractional importance of their photolysis

at 254 nm. Molar absorption coefficients of charge transfer transitions of organic molecules are usually ~10^3–$1x10^4$ L mol^{-1} cm^{-1}, i.e., cross-sections of ~$3.9x10^{-18}$–$3.9x10^{-17}$ cm^2 (Foster, 1969). Based on that, it is reasonable to estimate an upper limit of absorption cross-sections of charge transfer transitions of $5x10^{-17}$ cm^2. On the other hand, photolysis quantum yields of multifunctional species are unlikely to be larger than that of species with only one carbonyl and one hydroxyl, i.e., ~0.1 (see discussion above). We thus take 0.1 as an upper limit of photolysis quantum yields. Besides, $6x10^{-12}$ cm^3 $molecule^{-1}$ s^{-1} can be a conservative estimate of rate constants of multifunctional oxygenated species with OH, as it is roughly an average value for ketones (Atkinson and Arey, 2003), and the enhancement of H-abstraction by hydroxyl groups (Kwok and Atkinson, 1995; Ziemann and Atkinson, 2012) and the fast abstraction of aldehydic H atoms (Atkinson and Arey, 2003) are completely neglected. With the three estimates combined, the estimated maximum fractional contribution from photolysis at 254 nm to the fate of multifunctional species (Fig. 2) is close to that of E,E-2,4-hexadienedial and acetylacetone.

The problem of photolysis of oxidation intermediates at 185 nm is unlikely to be worse than at 254 nm. According to available UV spectra of carbonyl compounds in Keller-Rudek et al. (2015), 185 nm is almost always located within the π–π* transition band, whose maximum cross-section is on the order of 10^{-17} cm^2. Even if all types of radiative transitions at normal radiation intensity are considered, an approximate upper limit of absorption cross-sections is ~10^{-16} cm^2 (Evans et al., 2013). However, UV intensity at 185 nm in the OFR185 mode is ~100 times lower than that at 254 nm (Li et al., 2015). The photolysis rate of oxidation intermediates at 185 nm should thus be generally smaller than at 254 nm.

Therefore, in summary, photolysis of oxidation intermediates are, to our knowledge, conservatively estimated to be of limited importance relative to their reactions with OH, as long as the experimental conditions are in the safer range. Although studies on photolysis quantum yields of oxidation intermediates are very sparse, we reason, based on the existing studies on this topic and common photophysical and photochemical rules, that the photolysis quantum yields of these species may be lower than the values assumed in this study (e.g., 1 for E,E-2,4-hexadienedial and acetylacetone and 0.1 for multifunctional species). As a result, actual rates and relative importance of photolysis might be significantly smaller than the upper limits estimated in our study.

As discussed for photolysis at 185 nm, in all ambient OFR field studies (BEACHON-RoMBAS, SOAS, and CalNex-LA), reactions with OH dominate over photolysis at 254 nm (Fig. 2). The fractional consumption of several anthropogenic aromatic VOCs, such as benzene and naphthalene, in the urban CalNex-LA campaign by 254 nm photolysis is estimated as a few percent under most conditions and at most ~15%. At the BEACHON-RoMBAS and SOAS forested sites, photolysis at 254 nm should be a negligible contributor to the fate of biogenic VOCs such as isoprene and monoterpenes.

Some laboratory and source studies may have had an appreciable contribution to aromatic species fate from 254 nm at low H_2O and/or high OHR_{ext}. $F254_{exp}/OH_{exp}$ in the biomass smoke and urban tunnel source studies (source OHR_{ext} up to ~300 s^{-1}; Ortega et al., 2013; Tkacik et al., 2014) and the Kang et al. (2011) laboratory study (H_2O down to ~0.1%) can be as high as 10^6–10^7 cm/s. In this range, photolysis of a few aromatic VOCs (e.g., benzene and naphthalene) at 254 nm could account for ~20–80% of their

Deleted: RH and/or high OHR_{ext}. $F254_{exp}/OH_{exp}$ in the biomass smoke and urban tunnel source studies (source OHR_{ext} up to ~300 s^{-1}; Ortega et al., 2013; Tkacik et al., 2014) and the

Deleted: RH

Deleted: 3

destruction.

Note that photolysis of oxidation intermediates also needs to be taken into account. If multifunctional species, β-diketones, and extensively conjugated species are photolyzed as shown in Fig. 2, these photolyses would be significant in some previous source and laboratory studies examined here, as they were conducted at relatively low H_2O and/or high OHR_{ext}. To our knowledge, none of these studies reported a significant photolysis of oxidation intermediates. Klems et al. (2015) attributed large amounts of fragmentation products detected in their OFR experiments with dodecanoic acid to photolysis of peroxy radicals. However, these products may also be at least partially accounted for by photolysis of carbonyls leading to carbon-chain cleavage via Norrish reactions (Laue and Plagens, 2005). The OFR used by Klems et al. (2015) has a different design from the PAM, which is regarded as the base design in this study. Their reactor employs a light source stronger than the PAM's highest lamp setting, with UV at 254 nm estimated to be ~$3x10^{16}$ photons cm^{-2} s^{-1} (~4 times the value at the highest lamp setting of the PAM OFR) based on the lamp power and the reactor geometry. Such high UV may even result in significant photolysis of saturated carbonyl intermediates, which are very likely formed in the oxidation of long-chain alkane-like dodecanoic acid.

3.1.4 Reactions with OH vs. reactions with $O(^1D)$ and $O(^3P)$

The results for these two radicals are shown in Figs. 3–4. The potential impact of $O(^1D)$ is smaller than for 185 and 254 nm photons, due to the low concentration of $O(^1D)$ in the reactor. Only for methane may reaction with $O(^1D)$ be significant, because the reaction of methane with $O(^1D)$ is close to the collision rate, while CH_4 is the most resistant VOC to H-abstraction by OH. This could be important if CH_4 was used for OH_{exp} calibration under riskier reactor conditions, or if the fate of CH_4 is important to the experiment for other reasons. Other VOCs react more slowly with $O(^1D)$ and much faster with OH. As a result, reactions of VOCs (other than CH_4) with $O(^1D)$ in all laboratory, field, and source studies previously discussed are almost always negligible. We also note that the ratio of $O(^1D)_{exp}/OH_{exp}$ in the OFR is actually much lower than in the troposphere (Monks, 2005), except under some riskier conditions. It is believed that the contribution of $O(^1D)$ to VOC destruction in the atmosphere should be negligible (Calvert et al., 2002), and their relative importance is even lower under most OFR conditions.

Reactions with $O(^3P)$ are small or negligible contributors to VOC consumption except under extreme riskier conditions. Unless at low H_2O (<0.1%) and very high external OH reactivity (~1000 s^{-1}), VOC consumption by $O(^3P)$ cannot be larger than 10% of that by OH (Figs. 4 and S4). This results from both very low concentrations of $O(^3P)$ and relatively low reactivity compared to that of OH. Among the species that we examine, biogenic VOC consumption may have some contribution from $O(^3P)$ under the abovementioned riskier conditions, due to the higher reactivity of double bonds in these species with $O(^3P)$. For example α-pinene in the mixture experiments in Kang et al. (2011) may have had a ~5% contribution from $O(^3P)$. Similarly to $O(^1D)$, $O(^3P)_{exp}/OH_{exp}$ in the troposphere (Calvert et al., 2002) is higher than in the OFR except for riskier conditions. Thus the relative importance of both $O(^1D)$ and $O(^3P)$ to OFR chemistry is typically lower than in the troposphere.

3.1.5 Reactions with OH vs. reactions with O_3

Deleted: Note that in field and source studies, where the composition of VOCs is highly complex, the presence of common aromatic species such as benzene and naphthalene is likely. In contrast, in laboratory studies, the identity of the VOC is usually well controlled. Only the precursor and its oxidation intermediates, usually oxygenated species (e.g., ketones, aldehydes, and alcohols), need to be considered. Therefore, one may conduct laboratory experiments with OFRs under conditions that would be pathological for some field or source studies, if photolysis of the specific studied species and corresponding intermediates at 254 nm is not significant in its destruction. For example this is the case for the experiments with α-pinene in Kang et al. (2011), and those with isoprene in Lambe et al. (2011b). In all these experiments, the fractional photolytic consumption of the precursors by 254 nm photons is less than 1%. The fractional consumption of oxygenated intermediates is also just a few percent, even if we assume that all intermediates have as high a relative photolytic impact as methyl ethyl ketone. Lambe et al. injected isoprene at OHR_{ext} as high as 792 s^{-1} into their OFR (Table S4) which is expected to substantially reduce the OH concentration (Peng et al., 2015), but the relative impact of isoprene photolysis at 254 nm is still negligible thanks to the very rapid reaction of isoprene with OH.¶
However, Klems et al. (2015)'s experiment with dodecanoic acid may have had a significant fractional impact from photolysis at 254 nm, although photolysis of the precursor is negligible compared to its reaction with OH.

Formatted: Font color: Text 1

Formatted: Font color: Text 1

Formatted: Font color: Text 1

Formatted: Font color: Text 1

Formatted: Font color: Text 1

Formatted: Font color: Text 1

Formatted: Font color: Text 1

Deleted: Photolysis of carbonyls often lead to carbon-chain cleavage via Norrish reaction (Laue and Plagens, 2005), which may account for some of large amounts of fragmentation products observed in the Klems et al. (2015) experiments.

Deleted: pathological

Deleted: pathological

Deleted: atoms

Deleted: pathological

Deleted: (

Deleted: pathological

Deleted: O atoms

Reaction with O_3 is a major, even dominant pathway of the consumption of many biogenic VOCs in the troposphere. However, it is of interest to quantify the relative importance of OH vs. O_3 across OFR experiments (Figs. 5 and S5). This allows comparison with the relative importance in the troposphere, as well as potentially designing experiments where the relative influence of O_3 is minimized or adjusted as desired.

A large amount of O_3 is injected into OFR254, and O_3 concentration in that type of reactor does not change much with UV flux (negligibly under most conditions and up to a factor of ~2 at high H_2O and UV, Peng et al. 2015). Since OH_{exp} is proportional to UV flux, as UV decreases, OH_{exp} is lowered and the fractional species destruction by O_3 increases. In OFR185, O_3 production is almost linearly dependent on UV, while a significant portion of OH production has a quadratic relationship with UV. Thus OH increases faster with increasing UV than O_3. Therefore, lower UV in OFR185 also leads to a higher relative importance of O_3 for VOC consumption.

The distribution of O_{3exp}/OH_{exp} expected for the troposphere was obtained from the GISS ModelE2 climate model (Schmidt et al., 2014) and is estimated as the ratio of the simulated daily mean concentration of O_3 and OH on a horizontal grid of 2 degrees in latitude and 2.5 degrees in longitude for the year 2000. Interestingly, the simulated relative importance of O_3 to OH in the troposphere is higher than when OFRs are operated under safer conditions, and similar to OFRs when they are operated under riskier conditions (Figs. 5 and S5). In those cases, a number of biogenic VOCs can be significantly consumed by O_3. In particular, some monoterpenes (e.g., α-terpinene) and sesquiterpenes (e.g., β-caryophyllene) have a fractional reaction with O_3 close to 100% in the troposphere. In contrast to biogenics, reactions with O_3 do not play any role in the consumption of most anthropogenic VOCs, e.g., benzene, toluene, and alkanes. Besides, ozonolysis of saturated oxidation intermediates (e.g. carbonyls and alcohols) is minor or negligible in both OFRs and the atmosphere, since they react with OH at ~10^{-13}–10^{-11} cm^3 $molecule^{-1}$ s^{-1} while their ozonolysis rate constants are <10^{-20} cm^3 $molecule^{-1}$ s^{-1} (Atkinson and Arey, 2003). However, unsaturated oxidation intermediates may have larger contributions from O_3 because of C=C bonds. In particular, dihydrofurans, possible intermediates of saturated hydrocarbon oxidation (Ziemann and Atkinson, 2012; Aimanant and Ziemann, 2013), may be predominantly oxidized by O_3 in the troposphere. In OFR254, they can still have significant contributions from O_3 even outside the low-H_2O and/or high-OHR_{ext} conditions.

An experimentalist may be interested in obtaining an O_{3exp}/OH_{exp} in an OFR close to ambient values, which requires lower H_2O and higher OHR_{ext} conditions, although care should be taken to avoid other non-tropospheric reactions under those conditions. On the other hand, one may want to study OH-dominated chemistry and thus want to avoid significant ozonolysis of VOCs to reduce the complexity of VOC fate. This is analogous to the addition of excess NO to suppress O_3 in some chamber experiments. In this case the OFRs should be operated under opposite conditions, i.e., high H_2O, high UV, and low OHR_{ext}. This strategy enhancing OH_{exp} is effective for most VOCs, except those with the highest k_{O3}/k_{OH} ratios, e.g., α-terpinene and β-caryophyllene. To further decrease the importance of reactions of VOC with O_3, it is necessary to lower the O_3 concentration. For OFR254, one can inject less O_3 into the reactor

Deleted: normal

Deleted: pathological

Deleted: It has to be noted though that the values used

Deleted: the model are daily means, which underestimates the amount

Formatted: Font: 9 pt, Font color: Text 1

Formatted: Font color: Text 1

Deleted: OH in the atmosphere during daytime by roughly a factor

Formatted: Font color: Text 1

Deleted: 2.

Formatted: Font color: Text 1

Deleted: experimenter

Deleted: the

Deleted: low RH

Deleted: high

Deleted: .

Formatted: Font color: Text 1

Deleted: wants

Formatted: Font color: Text 1

Deleted: .

Formatted: Font: 9 pt, Font color: Text 1

Deleted: that

Formatted: Font: Not Italic

Formatted: Font: Not Italic

and increase the UV lamp setting. The comparison between OFR254-70 and OFR254-7 in Fig. S5 demonstrates this approach. For OFR185, we propose another strategy, i.e., lowering O_2 concentration in the reactor. This decreases O_3 production but affects OH production to a much lesser extent, thanks to the major OH production by H_2O photolysis. We simulate the OFR185 cases with 2‰ O_2 and observe that VOC ozonolysis can be excluded at high H_2O and high UV (Fig. S5).

Among the literature OFR studies, the field studies employing OFRs in urban and forested areas all operated under O_{3exp}/OH_{exp} values 100 times lower than in the atmosphere. In these field studies reaction of almost all VOCs with O_3 can be neglected, except for the most reactive biogenics with O_3, e.g., α-terpinene and β-caryophyllene. The source study in an urban tunnel of Tkacik et al. (2014) operated under similar conditions. Some laboratory studies using OFR254 (Kang et al., 2011; Lambe et al., 2011b) as well as the biomass smoke source study (Ortega et al., 2013) operated at O_{3exp}/OH_{exp} close to tropospheric values, because the injected O_3 plays a key role for OFR254 studies and the biomass smoke experiments were conducted at high OHR_{ext}. Nevertheless, only α-pinene and β-pinene, both biogenics, are significantly consumed by O_3. Another OFR254 study, Klems et al. (2015), had O_{3exp}/OH_{exp} significant lower than tropospheric values, since the initial O_3 in their experiment was only 2 ppm, and the UV light in their experiment was stronger than our lamps' highest setting and further reduced effective O_3.

3.1.6 Reactions with $^1O_2$ and HO_2

Singlet oxygen, $^1O_2$, can be produced in various ways in OFRs (Calvert et al., 2002; Ono et al., 2014) and react with alkenes at appreciable rate constants (~10^{-17}–10^{-14} cm^3 $molecule^{-1}$ s^{-1}; Huie and Herron, 1973; Eisenberg et al., 1986). We estimate $^1O_2$ concentration by the expression proposed by Ono et al. (2014). Only at the lowest H_2O, the highest lamp setting, and the highest OHR_{ext} in this study (Table 1), may the most reactive alkene (endo-cyclic conjugated dienes, e.g., cyclopentadiene, α-terpinene, and α-phellandrene) have >10% contribution from $^1O_2$ to their fate. For all other species and under all other conditions, reactions of VOCs with $^1O_2$ are negligible. Thus, this reactant is not discussed further in the present work.

HO_2 is a major radical in the OFR chemistry. However, it is much less reactive than OH toward VOCs. Typically, the rate constants of reactions of HO_2 with alkenes are smaller than 10^{-20} cm^3 $molecule^{-1}$ s^{-1} at room temperature, and those with almost all saturated VOCs (except aldehydes and ketones) are even smaller (Tsang, 1991; Baulch et al., 1992, 2005). Therefore, we briefly discuss reactions of HO_2 with aldehydes and ketones, and neglect those with all other VOCs in this study. Ketones react with HO_2 at rate constants on the order of 10^{-16} cm^3 $molecule^{-1}$ s^{-1} or lower (Gierczak and Ravishankara, 2000; Cours et al., 2007). Therefore, only at low H_2O, low UV and high OHR_{ext}, the reaction of acetone with HO_2 may compete with that with OH. The same is likely true for the reactions of acetaldehyde and larger aldehydes with HO_2, as their rate constants are likely to be around or less than $1x10^{-14}$ cm^3 $molecule^{-1}$ s^{-1} (da Silva and Bozzelli, 2009). Formaldehyde is the only stable carbonyl compound that may react with HO_2 (rate constant: $7.9x10^{-14}$ cm^3 $molecule^{-1}$ s^{-1}; Ammann et al., 2015) at a rate competing with that with OH under conditions that are not low-H_2O, low-UV, and high-OHR_{ext}. Note that the reaction of

Deleted: 5

Deleted: RH

Deleted: HO_2 is a major radical in the OFR chemistry. However, it is much less reactive than OH toward VOCs. Typically, the rate constants of reactions of HO_2 with alkenes are smaller than 10^{-20} cm^3 $molecule^{-1}$ s^{-1} at room temperature, and those with saturated VOCs are even smaller (Tsang, 1991; Baulch et al., 1992, 2005). Therefore, all reactions of HO_2 with VOCs can be simply neglected in this study.¶

formaldehyde with HO_2 is also significant in the atmosphere (Pitts and Finlayson, 1975; Gäb et al., 1985). However, its product, hydroxymethylperoxy radical, dominantly undergoes decomposition via thermal reaction and photolysis (Kumar and Francisco, 2015), compared to the hydroxymethylhydroperoxide formation pathway via a further reaction with HO_2 (Ziemann and Atkinson, 2012). Even if hydroxymethylhydroperoxide is produced in appreciable amounts, in the high-OH environment of OFRs, this species can be easily predicted to convert into formic acid (Francisco and Eisfeld, 2009) and eventually CO_2. All these products have very few interactions with other VOCs, and hence should not significantly perturb the reaction system of OFRs.

3.1.7 Overall contribution of non-OH reactants to gas-phase chemistry

In this section we summarize the combined effect of all non-OH reactants to VOC consumption. However, we can no longer use X_{exp}/OH_{exp} to express total non-OH VOC consumption as for individual reactants. Total non-OH VOC consumption is thus discussed case by case.

In the explored range of conditions (i.e., H_2O, UV, OHR_{ext}, and initial O_3 for OFR254), there are obviously conditions where all non-OH fates of VOCs are negligible. Most simply, the highest H_2O and UV in this study and a very small non-zero OHR_{ext} result in a VOC consumption nearly 100% by OH, regardless of the VOC type (Table S6). Lowering UV can make non-OH contribution even smaller for OFR185, but not for OFR254. This difference occurs because OH production is reduced while O_3 roughly remains at the same level in OFR254, leading to enhanced relative contribution from O_3 to the fate of biogenics. At the lowest non-zero UV in Li et al. (2015)'s PAM reactor ($7.9x10^{11}$ photons cm^{-2} s^{-1} at 185 nm; $2.0x10^{14}$ photons cm^{-2} s^{-1} at 254 nm), the fractional destructions of α-pinene (representative of biogenic VOCs) by O_3 are 21% and 4.2% in OFR254-70 and OFR254-7, respectively. Other OFR designs may reach lower UV, e.g., the "low UV" case defined in this study ($1.0x10^{11}$ photons cm^{-2} s^{-1} at 185 nm; $4.2x10^{13}$ photons cm^{-2} s^{-1} at 254 nm). At these UV levels, the fate of α-pinene by O_3 further increases to 44% and 13% in OFR254-70 and OFR254-7, respectively.

On the other hand, non-OH reactants can dominate VOC fate under opposite conditions that lead to low OH production and strong OH suppression. At the lowest H_2O and UV and the highest OHR_{ext} in this study, >95% of α-pinene and ~80% of toluene are consumed by non-OH reactants in OFR185. In OFR254, almost all α-pinene has non-OH fate while non-OH fate of toluene is still minor or negligible. If OFRs are operated at the low UV setting from Li et al. (2015)'s PAM, ~8 times higher the lowest UV in this study, the situation hardly changes, as a very large OH suppression persists. Nevertheless, if UV is increased to the highest level, non-OH fate of α-pinene is lowered to ~60–70% and that of toluene in OFR185 decreases to 24%. When H_2O is at the highest level, non-OH fate is systematically lower than at low H_2O in all types of OFRs. In particular, Case HHV has non-OH fates of α-pinene only up to ~10% and negligible non-OH fates of toluene, despite very high OHR_{ext}.

We also summarize VOC fate for key laboratory, source, and field studies examined in the present work in Fig. 7. For each case, the fate of one or a few typical VOCs is investigated. In laboratory studies, Kang et al. (2011) performed experiments with a mixture of α-pinene, m-xylene, and p-xylene, and one of Lambe et al. (2011b)'s experiments used biogenics (α-pinene and isoprene, respectively) as

Deleted: RH

Deleted: RH

Deleted: S5

Deleted: RH

Deleted: RH

Deleted: RH

precursors. In both cases, O_3 plays a role in the fate of biogenics when H_2O is low (Kang et al.), or OHR_{ext} is high and UV is low (Lambe et al.), as shown in Fig. 7. The fate of isoprene by O_3 is less significant despite the very high OHR_{ext}, because isoprene, compared to α-pinene, is more reactive with OH and less reactive with O_3. Besides, $O(^3P)$ contributes up to a few percent to the fate of biogenics. In the literature experiments performed at a higher H_2O (Kang et al.) or a higher UV (Lambe et al.), non-OH fate of both VOCs significantly decreases because of increases in OH_{exp}. About 20% of p-xylene in Kang et al.'s mixture experiment at very low H_2O may be destroyed by 254 nm photons, under the assumption of unity quantum yield. Other laboratory study cases with aromatics have lower non-OH fates because of higher H_2O. n-decane in one of Lambe et al.'s experiments and dodecanoic acid in Klems et al. (2015)'s study are consumed ~100% by OH, as these alkane(-like) species neither react rapidly with O_3, nor absorb UV efficiently. However, as previously discussed, some carbonyl compounds may be formed and significantly photolyzed at 254 nm in Klems et al.'s experiments, although the huge complexity of intermediates and limited knowledge of reaction mechanisms prevents a quantitative assessment of the fate of carbonyl intermediates by photons at 254 nm.

Source and field studies usually have highly complex precursors. For the urban tunnel study (Tkacik et al., 2014) and the CalNex-LA study in the Los Angeles basin (Ortega et al., 2015), we choose toluene as a representative of aromatic species, as these are major anthropogenic VOCs and SOA precursors in urban environment (Dzepina et al., 2009; Borbon et al., 2013; Hayes et al., 2015; Jathar et al., 2015). Although alkanes are also major anthropogenic VOCs, their non-OH fate is not quantitatively assessed for the same reason as discussed for dodecanoic acid in Klems et al. (2015)'s experiment. For the smoke aging study, FLAME-3 (Ortega et al., 2013), we select benzene and α-pinene, which are important VOCs in biomass burning emissions (Warneke et al., 2011). For the BEACHON-RoMBAS and SOAS studies at forested sites, α-pinene and isoprene are chosen, respectively, as they are major emitted biogenic VOCs at those corresponding sites. Both the urban tunnel and FLAME-3 studies have aromatic precursors significantly photolyzed at 185 and 254 nm (assuming quantum yield = 1) under the conditions of high source concentrations (Fig. 7). The toluene fate by UV in the tunnel study is less substantial than that of benzene in FLAME-3, since NO_x, the largest fraction of external OH reactant in the tunnel study, is converted into HNO_3 very rapidly (Li et al., 2015) and does not further suppress OH. In the cases of lower OHR_{ext} (e.g., the tunnel experiments with low source concentration and CalNex), toluene is dominantly consumed by OH. It also holds for biogenic VOCs that non-OH fate decreases with decreasing OHR_{ext} due to less OH suppression. The non-OH fate of α-pinene in FLAME-3, dominated by reaction with O_3, is larger than 20%, while the non-OH fates of α-pinene in BEACHON-RoMBAS and of isoprene in SOAS are both negligible, since OHR_{ext} in the former study is >10 times higher than in the latter two studies.

3.2 SOA photolysis

Recently, photolysis in the UV range has been found to be a potentially significant sink of some types SOA in the troposphere (Updyke et al., 2012; Lambe et al., 2013; Liu et al., 2013, 2015; Hodzic et al., 2015; Wong et al., 2015; Romonosky et al., 2016). It is necessary to also investigate SOA photolysis in OFRs, as photons used in OFRs are highly energetic and non-tropospheric. UV extinction due to

Deleted: RH

Deleted: both

Deleted: RH

Deleted: However, the contribution of $O(^3P)$ to isoprene fate almost remains the same, since both OH and $O(^3P)$ increase with UV.

Deleted: RH

Deleted: .

Deleted: RH

Deleted: Recently, photolysis has been found to be a potentially significant sink of some types SOA in the troposphere (Wong et al., 2014; Hodzic et al., 2015). It is necessary to also investigate SOA photolysis in OFRs, as photons used in OFRs are highly energetic and non-tropospheric. UV extinction due to aerosol optical scattering and in-particle absorption is generally negligible (Hodzic et al., 2015). For simplicity, we estimate photodegradation ratios of various possible SOA components (Fig. 8) under the assumption of unity quantum yield. Therefore, the estimates are actually the upper limits of photodegradation ratios. We use surrogate gas-phase species for the different functional groups as the cross sections of SOA-relevant species at these wavelengths are not available, as done in other studies (Hodzic et al., 2015).¶

aerosol optical scattering and in-particle absorption under OFR conditions is generally negligible (Hodzic et al., 2015). For simplicity, we estimate photodegradation ratios of various SOA component surrogates as well as several SOA samples whose absorptivity was measured in previous studies (Updyke et al., 2012; Lambe et al., 2013; Liu et al., 2013; Romonosky et al., 2016) (Fig. 8) under the assumption of unity quantum yield to obtain upper limits of photodegradation ratios, and also under the assumption of lower (0.1 and 0.01) quantum yields.

Most SOA functional groups are oxygenated (e.g., peroxides, carbonyls, carboxylic acids, alcohols). The absorption cross sections of most of these functional groups are too low at 185 and 254 nm given the OFR residence time and UV light intensity, leading to a small contribution of photolysis to SOA degradation (Fig. 8). For example, glycolaldehyde has a negligible fractional contribution of photolysis except at the highest lamp setting, when only ~5% of this species photolyzes at each wavelength. Species (e.g., isoprene) with conjugated double bonds as efficient chromophores will not be present in SOA because of their high reactivity with OH and O_3. Nitrate groups may have a ~30% contribution from photolysis at the highest UV settings, and a negligible contribution at intermediate or low UV settings.

Aromatic rings are more resistant to OH attack and usually strongly absorb UV light. Under our assumptions, the photolysis of some aromatic SOA components (e.g., o-cresol at 185 nm and naphthalene at 254 nm) is already important at medium UV flux. At the highest lamp setting, most aromatics in SOA would be destroyed if the quantum yields are indeed near unity. However, as previously discussed, photolysis quantum yields of aromatics may be significantly lower than 1. This is more probable in the condensed phase (Damschen et al., 1978; Baker et al., 2015) than in the gas phase, as quenching processes in the condensed-phase matrix are usually much more efficient than through gas-phase molecular collisions. It has recently been reported that photolysis quantum yields of aromatics in SOA were low under UVB irradiation (Romonosky et al., 2015). Although the range and relevance of the species investigated in that study are limited, it is reasonable to assume low quantum yield for aromatic photolysis in SOA at 185 and 254 nm.

Wong et al. (2015) conducted α-pinene-derived SOA photolysis experiments in a chamber under UVB irradiation (down to 284 nm). They observed at 85% RH ~30% SOA photolyzed after >30 min irradiation and a photolysis quantum yield of ~1 during the first 10 min. However, in OFRs such a high SOA photodegradation percentage would not occur, since Wong et al. (2015)'s experiments had a high photon flux (~4×10^{15} photons cm^{-2} s^{-1}) and a long irradiation time, and hence a photon flux exposure that is ~5 times that at the highest lamp setting in the OFRs modeled in our work. According to the measurements of Wong et al. (2015), a photolysis fraction of ~6% would be expected for this type of SOA in our OFRs under the highest UV flux, with lower percentages at lower UV settings. In addition, the approximate unity quantum yield observed in Wong et al. (2015) may be due to (hydro)peroxides in α-pinene-derived SOA, since peroxides have high photolysis quantum yields (Goldstein et al., 2007; Epstein et al., 2012), while other functional groups (i.e., mainly hydroxyl and carbonyl) in oxygenated species in SOA are unlikely to have for reasons discussed below.

Note that a simple addition of absorptivities of different functional groups may not explain SOA

absorptivity (Phillips and Smith, 2015). According to the absorption data of SOA samples from Lambe et al. (2013) and Romonosky et al. (2015a), real SOA absorbs ~1–3 orders of magnitude more than non-aromatic component surrogate species shown in Fig. 8 at 254 nm. As discussed for multifunctional oxidation intermediates (with carbonyls and hydroxyls), SOA absorption enhancement may be largely due to transitions of charge transfer complexes formed between carbonyls and hydroxyls in multifunctional oxygenated SOA components (Phillips and Smith, 2014, 2015). These complexes between carbonyls and hydroxyls also have continua of states likely leading to ultrafast relaxation and hence low photolysis quantum yields. Charge transfer transitions have been extensively shown in measurements (Alif et al., 1991; Gao and Zepp, 1998; Johannessen and Miller, 2001; O'Sullivan et al., 2005; Zhang et al., 2006; Osburn et al., 2009; Sharpless and Blough, 2014) to have very low quantum yields in the condensed phase. Sharpless and Blough (2014) compiled quantum yields of various products of humic-like matter photolysis down to 280 nm. No quantum yields except those of the product $^1O_2$, which is generally unimportant for OFRs (see Section 3.1.6), are higher than 0.01. If the photolysis quantum yields of the SOA samples in Fig. 8 at 254 nm are no more than 0.01, no SOA samples will be photolyzed by 20% even at the highest OFR lamp setting, and photolysis of most SOA samples at 254 nm will be minor or negligible in OFRs. Thus, to our current knowledge, lack of solid information on quantum yields of SOA components with multiple carbonyls and hydroxyls at 254 nm prevents a clear assessment of SOA photolysis in OFRs at the medium and high UV. On the other hand, direct measurements are desirable for this issue and caution should still be exercised for OFR experiments at relatively high UV.

SOA photolysis at 185 nm may be lower compared to that at 254 nm. SOA absorptivity data at 185 nm are not available. According to SOA mass-specific absorption cross-section (MAC) data between 250 and 300 nm in Romonosky et al. (2015a), there is a linear relationship between the logarithm of MAC and wavelength for most SOA samples: MAC increases by a factor of ~3 per 50 nm decrease in wavelength. We thus extrapolate this relationship to 185 nm, where MAC is estimated to be ~3.5 times higher than that at 254 nm. However, the UV flux at 185 nm in our OFR is ~100 times lower than at 254 nm.

Based on the discussion above, the SOA photodegradation ratio of ~30% in Wong et al. (2015)'s non-OFR setup may be explained. α-pinene-derived SOA has ~20–50% weight fraction of peroxides (Docherty et al., 2005; Epstein et al., 2014), which may undergo photolysis in SOA to convert into carbonyls (and hydroxyls) (Epstein et al., 2014). We speculate that after the formation of carbonyls from peroxides, SOA materials cannot proceed significantly further with photolysis as discussed for charge transfer between carbonyl and hydroxyl above. In the experiments of Wong et al. (2015), as well as Epstein et al. (2014), effective photolysis rate constants/quantum yields decreased as SOA photolysis proceeded. Photolysis rates were substantially reduced after a ~30% mass loss due to photolysis in Wong et al. (2015)'s experiments. This mass loss ratio is consistent with the mass percentage of peroxides in α-pinene-derived SOA. Again, we note that, according to the extrapolation from Wong et al. (2015)'s results, the mass loss percentage expected in our OFR under the highest UV flux is ~6% for

Deleted: for aromatic SOA systems

Formatted: Font: 9 pt

Deleted: For most SOA components, photolysis is unimportant in OFRs in terms of absolute photolyzed amount. This is also true compared to ambient SOA photolysis. OH_{exp} in OFRs is normally on the order of 10^{11}–10^{13} molecules cm^{-3} s, equivalent to photochemical ages of a day to several months. Case HHH (Table 1) is one of the cases just outside the pathological region, i.e., with the highest photon-to-OH ratio and without problems of non-tropospheric chemistry. OH_{exp} is ~$2x10^{13}$ molecules cm^{-3} s in this case. Hodzic et al. (2015) estimated an average ambient SOA photolysis lifetime of 3.5 days. Therefore, on average, ambient SOA may undergo ~40 generations of photolysis (1 generation of photolysis means that the species concentration decreases by a factor of *e* due to photolysis) in the troposphere before it is as OH-aged in ambient air as in Case HHH in OFRs. Some components in SOA (e.g., glyoxal and 2-methylpropanal) may proceed with more than 500 generations of ambient photolysis before they reach an ambient OH exposure comparable to in an OFR. In contrast, only 5 generations of photolysis at most have occurred on SOA in Case HHH in OFRs (Table S6). Except for species that do not photolyze in the troposphere, the photolysis of all SOA components proceeds to an extent of at least one order of magnitude smaller than that in the troposphere (Table S6). Although the photolysis products may be different at the different wavelengths, this result indicates that the relative importance of SOA photolysis is much lower in OFRs compared to the troposphere. Nevertheless, aromatic photolysis in SOA may lead to different chemistry in OFRs from that in the troposphere, if this type of photolysis really occurs to a significant extent.¶

α-pinene-derived SOA. This value is much lower than that shown in Fig. 8 under the assumption of unity quantum yield (~40%) because of a substantially decreasing quantum yield in the real photolysis experiments. Therefore, in OFRs, even if (hydro)peroxides in SOA may be photolyzed in appreciable amounts, SOA mass is unlikely to be largely destroyed by photons in OFRs, as (hydro)peroxides may convert into carbonyls and hydroxyls, which may substantially lower subsequent photolysis quantum yields.

According to the discussion above, measurements of quantum yields and/or products of SOA photolysis are highly desirable, especially for the photolysis of SOA containing dominantly carbonyl and hydroxyl groups, as (hydro)peroxides, which are likely to form in OFRs, may convert into hydroxyls and carbonyls. With more data on quantum yields of SOA photolysis, a clearer strategy for including or excluding SOA photolysis in OFRs can be made.

Even though SOA photolysis can be significant in OFRs, it only proceeds to a much lesser extent compared to ambient SOA photolysis. We calculate the numbers of e-fold decay of SOA photolysis in OFR254-70 and the troposphere according to the effective ambient photolysis lifetime of SOA from Romonosky et al. (2015a). Under the condition of 70% RH (H_2O = 1.4%) and OHR_{ext} = 25 s^{-1} (typical of ambient conditions), SOA samples are estimated to undergo ~0.01–0.5 e-fold photolysis timescales (i.e., ~1–35% OA photolyzed) in OFR254-70 at an equivalent photochemical age of 1 week under the upper limit assumption of unity quantum yields (Table S8). However, in the atmosphere, those samples may proceed with 10^2–10^4 e-fold decays of photolysis (i.e., virtually complete destruction) at the same photochemical age, if ambient SOA photolysis quantum yields are assumed to be those of H_2O_2 (unity below 400 nm). Even if the quantum yield of acetone (non-zero below 320 nm, see Romonosky et al., 2015a) is taken as a surrogate for SOA, most types of SOA would still be completely or nearly completely photolyzed under ambient conditions. These results demonstrate that ambient SOA photolysis is likely to be much more important than in OFRs. On the other hand, they also highlight the need for studies of ambient SOA photolysis quantum yields and photolytic aging, as ambient SOA is unlikely to be completely destroyed by photons within only 1 week. Either their quantum yields are much lower than used in this study, or the photolabile groups are destroyed and leave behind others that are not (or less) photolabile during photolytic aging.

3.3 Guidelines for OFR experimental design and operation

It is necessary to avoid significant non-tropospheric chemistry in OFRs in order to more accurately simulate tropospheric aging. Only photolysis at 185 and 254 nm are important non-tropospheric pathways in OFRs and reactions with O atoms are generally unimportant. Ozonolysis is also a major VOC sink in the troposphere, and the desirability of including or excluding its effects depends on the goals of each experiment.

In the cases where the exclusion of VOC ozonolysis is desired, there is no dilemma for the experimental design, as the exclusion of both VOC ozonolysis and non-tropospheric VOC consumption requires similar conditions, i.e., safer conditions. As shown above, all examined field studies do not have significant non-tropospheric contribution to VOC fate, while some past laboratory and source studies

Deleted: faithfully

Deleted: high H_2O and low OHR_{ext}, opposite to the "pathological"

do because of low H_2O and/or very high OHR_{ext} in those experiments. It is possible to improve the latter experiments by increasing H_2O and/or lowering OHR_{ext}. In detail, source humidification and dilution can be feasible measures to increase H_2O and decrease OHR_{ext}, respectively. For example, increasing RH from 3% to 60% (H_2O from ~0.06% to ~1.2%) lowers the percentage of non-tropospheric consumption of p-xylene in Kang et al. (2011)'s mixture experiment from ~20% to 1.5%. Humidifying the average condition of the BEACHON-RoMBAS (Palm et al., 2016) campaign from H_2O = 1.6% (RH = 63%) to H_2O = 2.3% (RH = 92%) leads to significant (from ~20% for 185 nm photon flux to a factor of ~3 for $O(^3P)$) decreases in all exposure ratios between non-OH reactants and OH (Table S4). Also, a 5-fold source dilution in FLAME-3 reduces the non-tropospheric fate of benzene from >60% to ~15% (Table S4 and "Improved" cases in Fig. 7). Injecting less precursor is a simple way to keep a reasonably low OHR_{ext} in laboratory studies. The comparison between the cases with high and low concentrations in the urban tunnel study (Tkacik et al., 2014) is a good example (Table S4 and Fig. 7). Note that when taking the measures above to limit non-tropospheric VOC fate, one generally reduces the contribution from all non-OH reactants. Increasing H_2O and source dilution also significantly lower the relative importance of ozonolysis in the fate of α-pinene in Kang et al.'s mixture experiments and the FLAME-3 study (Table S4 and Fig. 7). Although increasing UV may increase OH production, OH reactant destruction, and hence the relative contribution of OH to VOC fate in some cases, one has to be cautious when taking this measure to reduce effective OHR_{ext}, as high UV may cause non-tropospheric photolysis of aromatic SOA components.

In laboratory experiments, running OFRs under safer conditions ensures a minor contribution of non-tropospheric photolysis, based on the current knowledge of oxidation intermediate photolysis (Fig. 2). This also reduces the relative contribution of ozonolysis to VOC fate. However, when more information becomes available about photoysis quantum yields of oxidation intermediates (vs. the upper limits assumed here), there may be additional flexibility to include ozonolysis while excluding non-tropospheric VOC consumption. As the precursor composition is usually relatively simple in laboratory experiments, it is sufficient to ensure the insignificance of non-tropospheric consumption of only the precursor(s) and possible intermediates (usually oxygenated species), rather than for a large variety of VOC precursors and intermediates. For example, in the case of quantum yields significantly lower than used in the present work, we may perform OFR254-70 experiments with a large amount of biogenics at medium H_2O and UV. In this case, a tropospheric O_{3exp}/OH_{exp} ratio can be obtained without major side effects, because the fractional contribution of photolysis of possible intermediates is still minor due to low quantum yields. On the other hand, OFR experiments with some anthropogenic VOCs, such as alkanes, can just be conducted at high H_2O and low OHR_{ext} to avoid the contribution of all non-OH reactants, since ozonolysis of alkanes is negligible even at a tropospheric O_{3exp}/OH_{exp}.

OFR experiments can be simply conducted under safer conditions to avoid non-tropospheric VOC fate, while riskier conditions can lead to significant non-tropospheric VOC fate, depending on the species under study. The conditions in between, i.e., "transition" conditions, are explicitly discussed above. However, one may want to be able to more quantitatively estimate the relative importance of

Deleted: RH
Deleted: RH
Deleted: RH
Formatted: Font: 9 pt, Font color: Text 1
Deleted: (Tkacik et al., 2014)
Deleted: RH
Deleted: usually with
Formatted: Font color: Text 1
Deleted: single VOC or a relatively simple mixture,
Formatted: Font color: Text 1
Formatted: Font color: Text 1
Deleted: is much more
Formatted: Font color: Text 1
Deleted: for experimental design
Formatted: Font color: Text 1
Deleted: , since
Formatted: Font color: Text 1
Deleted: component
Formatted: Font color: Text 1
Deleted: .
Formatted: Font color: Text 1
Formatted: Font color: Text 1
Deleted: OFR
Formatted: Font color: Text 1
Deleted: low
Formatted: Font color: Text 1
Deleted: as long as the experiment is not conducted under extremely pathological conditions.
Formatted: Font color: Text 1
Formatted: Font color: Text 1
Deleted: perfectly
Formatted: Font color: Text 1
Deleted: biogenics and
Formatted: Font color: Text 1
Deleted: (e.g., ketones) at 185 and 254 nm
Formatted: Font color: Text 1
Deleted: or negligible.
Formatted: Font color: Text 1
Formatted: Font color: Text 1
Deleted: and alkylbenzenes
Formatted: Font color: Text 1
Deleted: RH
Formatted: Font color: Text 1
Deleted: and alkylbenzenes
Formatted: Font color: Text 1
Deleted: A challenge of OFR operation is to explore the low OH_{exp} ...

non-OH reactants under different conditions so that a more detailed experimental planning becomes possible that simultaneously ensures insignificant non-tropospheric VOC fate and specific experimental goals. For this purpose, we provide a series of estimation equations for non-OH reactant exposures (Section S3, Table S9, and Fig. S6, as well as Excel file). With these equations, the relative contribution of non-OH reactants under all conditions explored in this study can be easily estimated. In OFR studies where a different OFR design is adopted and/or chemistry beyond the approximations in our model is involved, a new model may need to be established, which can be done in similar manner as Peng et al. (2015), to obtain the relative importance of non-OH VOC fate and then perform experimental design.

4 Conclusions

We used a kinetic model to investigate non-OH contribution (from 185 and 254 nm photons, $O(^1D)$, $O(^3P)$, and O_3) to VOC destruction, as well as to SOA photolysis at 185 and 254 nm in OFRs. We assessed the relative significance of the VOC consumption by non-OH reactants to that by OH in OFRs and the troposphere. The only non-tropospheric reaction that can play a major role under OFR conditions is photolysis, especially at 254 nm. The relative importance of photolysis is largest under riskier OFR conditions where OH is low due to low H_2O and/or high OHR_{ext}. Due to lack of quantum yield data, we estimated upper limits of the relative importance of photolysis for the few most susceptible oxidation intermediates, which are comparable to those from aromatic precursors. Reactions of O atoms are not competitive and are actually of lower relative importance (vs. OH) in OFRs than in the troposphere. VOC ozonolysis is much less important than in the troposphere under typical OFR conditions and of similar importance under riskier OFR conditions. Photolysis of SOA in OFRs could be significant at medium and high UV, but only if corresponding quantum yields are high. If SOA photolysis quantum yields are of the order of 0.01 or lower, as measured for many humic-like substances (Sharpless and Blough, 2014), SOA photolysis in OFRs may be minor or negligible under most conditions. Although the reaction fates may be different, numbers of e-fold decays of photolysis for a given OH_{exp} are at least an order-of-magnitude lower in the OFRs compared to the troposphere.

We examined some past field, laboratory, and source studies using OFRs. In the field studies of aged urban and forest ambient air, non-OH VOC fate was not important because of relatively high H_2O and moderate OHR_{ext}. However, some laboratory and source studies were conducted at low H_2O and/or high OHR_{ext}, and have significant non-tropospheric VOC consumption. Humidification and/or dilution are recommended in these cases to reduce the importance of non-tropospheric reactants. We proposed different approaches to avoid non-OH VOC consumption, as well as strategies to employ insignificant non-tropospheric photolysis and significant tropospheric ozonolysis simultaneously in laboratory experiments. Our work has implications for the interpretation of past OFR studies, and should be useful for designing and conducting future OFR experiments for atmospheric research, as well as in related applied fields.

The need for systematic measurements of photolysis quantum yields, for both VOC and SOA, and both at actinic wavelengths and at 185 and 254 nm, was highlighted in this study. When quantum yield data become available, photolysis of oxidation precursors, oxidation intermediates, and SOA in OFRs

Formatted: Font color: Text 1
Deleted: reactions
Formatted: Font color: Text 1
Deleted: are
Formatted: Font color: Text 1
Formatted: Font color: Text 1
Deleted: 185 and
Formatted: Font color: Text 1
Deleted: Their
Formatted: Font color: Text 1
Deleted: "pathological"
Formatted: Font color: Text 1
Formatted: Font color: Text 1
Formatted: Font color: Text 1
Deleted: RH
Formatted: Font color: Text 1
Formatted: Font color: Text 1, Not Superscript/ Subscript
Formatted: Font color: Text 1
Formatted: Font color: Text 1
Deleted: pathological
Formatted: Font color: Text 1
Deleted: aromatic
Formatted: Font color: Text 1
Deleted: components at 185 and 254 nm
Formatted: Font color: Text 1
Formatted: Font color: Text 1
Formatted: Font color: Text 1
Deleted: were high, for which direct experimental evidence is not available.
Formatted: Font color: Text 1
Formatted: Font color: Text 1
Deleted: rates
Formatted: Font color: Text 1
Deleted: actually
Formatted: Font color: Text 1
Deleted: RH
Deleted: RH

can be much better quantified, its relative importance compared to OH oxidation, ambient photolysis etc. can be better evaluated, and experimental planning might then be able to be less conservative and have more freedom to avoid non-tropospheric photolysis and realize specific experimental objective(s).

Acknowledgements

We thank Veronica Vaida, Paul Ziemann, Andrew Lambe, and the PAM user community for useful discussions. Andrew Lambe and Daniel Tkacik for providing some OFR experimental data, and the reviewers for their useful comments for improving the manuscript. This research was partially supported by CARB 11-305, DOE (BER/ASR) DE-SC0011105, NSF AGS-1243354 & AGS-1360834, and NASA NNX15AT96G. AMO acknowledges fellowships from DOE and CU Graduate School. RL and BBP acknowledge CIRES Fellowships. BBP is grateful for a Fellowship from US EPA STAR (FP-91761701-0). Resources supporting this work were provided by the NASA High-End Computing (HEC) Program through the NASA Center for Climate Simulation (NCCS) at Goddard Space Flight Center.

Deleted: and

Deleted: .

Deleted: and

References

Aimanant, S. and Ziemann, P. J.: Chemical Mechanisms of Aging of Aerosol Formed from the Reaction of n-Pentadecane with OH Radicals in the Presence of NOx, Aerosol Sci. Technol., 47(9), 979–990, doi:10.1080/02786826.2013.804621, 2013.

Alif, A., Pilichowski, J. and Boule, P.: photochemistry and environment XIII phototransformation of 2-nitrophenol in aqueous solution, J. Photochem. Photobiol. A Chem., 59, 209–219, doi:10.1016/1010-6030(91)87009-K, 1991.

Ammann, M., Cox, R. A., Crowley, J. N., Jenkin, M. E., Mellouki, A., Rossi, M. J., Troe, J., Wallington, T. J., Cox, B., Atkinson, R., Baulch, D. L. and Kerr, J. A.: IUPAC Task Group on Atmospheric Chemical Kinetic Data Evaluation, [online] Available from: http://iupac.pole-ether.fr/#, 2015.

Atkinson, R. and Arey, J.: Atmospheric degradation of volatile organic compounds., Chem. Rev., 103(12), 4605–38, doi:10.1021/cr0206420, 2003.

Bahreini, R., Middlebrook, A. M., Brock, C. A., de Gouw, J. A., McKeen, S. A., Williams, L. R., Daumit, K. E., Lambe, A. T., Massoli, P., Canagaratna, M. R., Ahmadov, R., Carrasquillo, A. J., Cross, E. S., Ervens, B., Holloway, J. S., Hunter, J. F., Onasch, T. B., Pollack, I. B., Roberts, J. M., Ryerson, T. B., Warneke, C., Davidovits, P., Worsnop, D. R. and Kroll, J. H.: Mass spectral analysis of organic aerosol formed downwind of the Deepwater Horizon oil spill: field studies and laboratory confirmations., Environ. Sci. Technol., 46(15), 8025–34, doi:10.1021/es301691k, 2012.

Baker, L. a., Horbury, M. D., Greenough, S. E., Coulter, P. M., Karsili, T. N. V., Roberts, G. M., Orr-Ewing, A. J., Ashfold, M. N. R. and Stavros, V. G.: Probing the Ultrafast Energy Dissipation Mechanism of the Sunscreen Oxybenzone after UVA Irradiation, J. Phys. Chem. Lett., 6, 1363–1368, doi:10.1021/acs.jpclett.5b00417, 2015.

Baulch, D. L., Bowman, C. T., Cobos, C. J., Cox, R. A., Just, T., Kerr, J. A., Pilling, M. J., Stocker, D., Troe, J., Tsang, W., Walker, R. W. and Warnatz, J.: Evaluated kinetic data for combustion modeling: Supplement II, J. Phys. Chem. Ref. Data, 34(3), 757–1397, doi:10.1063/1.1748524, 2005.

Baulch, D. L., Cobos, C. J., Cox, R. A., Esser, C., Frank, P., Just, T., Kerr, J. A., Pilling, M. J., Troe, J., Walker, R. W. and Warnatz, J.: Evaluated Kinetic Data for Combustion Modelling, J. Phys. Chem. Ref. Data, 21(3), 411, doi:10.1063/1.555908, 1992.

Beddard, G. S., Fleming, G. R., Gijzeman, O. L. J. and Porter, G.: Vibrational Energy Dependence of Radiationless Conversion in Aromatic Vapours, Proc. R. Soc. A Math. Phys. Eng. Sci., 340(1623), 519–533, doi:10.1098/rspa.1974.0168, 1974.

Borbon, A., Gilman, J. B., Kuster, W. C., Grand, N., Chevaillier, S., Colomb, A., Dolgorouky, C., Gros, V., Lopez, M., Sarda-Esteve, R., Holloway, J., Stutz, J., Petetin, H., McKeen, S., Beekmann, M., Warneke, C., Parrish, D. D. and De Gouw, J. A.: Emission ratios of anthropogenic volatile organic compounds in northern mid-latitude megacities: Observations versus emission inventories in Los Angeles and Paris, J. Geophys. Res. Atmos., 118(4), 2041–2057, doi:10.1002/jgrd.50059, 2013.

Bouzidi, H., Aslan, L., El Dib, G., Coddeville, P., Fittschen, C. and Tomas, A.: Investigation of the Gas-Phase Photolysis and Temperature-Dependent OH Reaction Kinetics of 4-Hydroxy-2-butanone, Environ. Sci. Technol., 49(20), 12178–12186, doi:10.1021/acs.est.5b02721, 2015.

Bouzidi, H., Laversin, H., Tomas, a., Coddeville, P., Fittschen, C., El Dib, G., Roth, E. and Chakir, a.: Reactivity of 3-hydroxy-3-methyl-2-butanone: Photolysis and OH reaction kinetics, Atmos. Environ., 98(3), 540–548, doi:10.1016/j.atmosenv.2014.09.033, 2014.

Calvert, J. G., Atkinson, R., Becker, K. H., Kamens, R. M., Seinfeld, J. H., Wallington, T. H. and Yarwood, G.: The Mechanisms of Atmospheric Oxidation of the Aromatic Hydrocarbons, Oxford University Press, USA. [online] Available from: https://books.google.com/books?id=P0basaLrxDMC, 2002.

Carlton, A. G., Wiedinmyer, C. and Kroll, J. H.: A review of Secondary Organic Aerosol (SOA) formation from isoprene, Atmos. Chem. Phys., 9(14), 4987–5005, doi:10.5194/acp-9-4987-2009, 2009.

Carter, W. P. L., Cocker, D. R., Fitz, D. R., Malkina, I. L., Bumiller, K., Sauer, C. G., Pisano, J. T., Bufalino, C. and Song, C.: A new environmental chamber for evaluation of gas-phase chemical mechanisms and secondary aerosol formation, Atmos. Environ., 39(40), 7768–7788, doi:10.1016/j.atmosenv.2005.08.040, 2005.

1112 Cocker, D. R., Flagan, R. C. and Seinfeld, J. H.: State-of-the-Art Chamber Facility for Studying Atmospheric
1113 Aerosol Chemistry, Environ. Sci. Technol., 35(12), 2594–2601, doi:10.1021/es0019169, 2001.

1114 Cours, T., Canneaux, S. and Bohr, F.: Features of the potential energy surface for the reaction of HO2
1115 radical with acetone, Int. J. Quantum Chem., 107(6), 1344–1354, doi:10.1002/qua.21269, 2007.

1116 Cubison, M. J., Ortega, a. M., Hayes, P. L., Farmer, D. K., Day, D., Lechner, M. J., Brune, W. H., Apel, E.,
1117 Diskin, G. S., Fisher, J. a., Fuelberg, H. E., Hecobian, a., Knapp, D. J., Mikoviny, T., Riemer, D., Sachse, G.
1118 W., Sessions, W., Weber, R. J., Weinheimer, a. J., Wisthaler, a. and Jimenez, J. L.: Effects of aging on
1119 organic aerosol from open biomass burning smoke in aircraft and laboratory studies, Atmos. Chem.
1120 Phys., 11(23), 12049–12064, doi:10.5194/acp-11-12049-2011, 2011.

1121 Damschen, D. E., Merritt, C. D., Perry, D. L., Scott, G. W. and Talley, L. D.: Intersystem Crossing Kinetics,
1122 J. Phys. Chem., 82(21), 2268–2272, doi:10.1021/j100510a002, 1978.

1123 Docherty, K. S., Wu, W., Lim, Y. Bin and Ziemann, P. J.: Contributions of Organic Peroxides to Secondary
1124 Aerosol Formed from Reactions of Monoterpenes with O3, Environ. Sci. Technol., 39(11), 4049–4059,
1125 doi:10.1021/es050228s, 2005.

1126 Dzepina, K., Volkamer, R. M., Madronich, S., Tulet, P., Ulbrich, I. M., Zhang, Q., Cappa, C. D., Ziemann, P.
1127 J. and Jimenez, J. L.: Evaluation of recently-proposed secondary organic aerosol models for a case study
1128 in Mexico City, Atmos. Chem. Phys., 9(15), 5681–5709, doi:10.5194/acp-9-5681-2009, 2009.

1129 Eisenberg, W. C., Taylor, K. and Murray, R. W.: Gas-Phase Kinetics of the Reaction of Singlet Oxygen with
1130 Olefins at Atmospheric Pressure, J. Phys. Chem., 90(20), 1945–1948, doi:10.1021/j100400a041, 1986.

1131 Epstein, S. A., Blair, S. L. and Nizkorodov, S. A.: Direct Photolysis of α-Pinene Ozonolysis Secondary
1132 Organic Aerosol: Effect on Particle Mass and Peroxide Content, Environ. Sci. Technol., 48(19), 11251–8,
1133 doi:10.1021/es502350u, 2014.

1134 Epstein, S. A., Shemesh, D., Tran, V. T., Nizkorodov, S. A. and Gerber, R. B.: Absorption Spectra and
1135 Photolysis of Methyl Peroxide in Liquid and Frozen Water, J. Phys. Chem. A, 116(24), 6068–6077,
1136 doi:10.1021/jp211304v, 2012.

1137 Evans, R. C., Douglas, P. and Burrow, H. D., Eds.: Applied Photochemistry, Springer Netherlands,
1138 Dordrecht., 2013.

1139 Fang, W. H. and Phillips, D. L.: The crucial role of the S1/T2/T1 intersection in the relaxation dynamics of
1140 aromatic carbonyl compounds upon n →π* excitation, ChemPhysChem, 3(10), 889–892,
1141 doi:10.1002/1439-7641(20021018)3:10<889::AID-CPHC889>3.0.CO;2-U, 2002.

1142 Foster, R.: Organic Charge-Transfer Complexes, Academic Press, New York., 1969.

1143 Francisco, J. S. and Eisfeld, W.: Atmospheric Oxidation Mechanism of Hydroxymethyl Hydroperoxide †,
1144 J. Phys. Chem. A, 113(26), 7593–7600, doi:10.1021/jp901735z, 2009.

1145 Gäb, S., Hellpointner, E., Turner, W. V. and Korte, F.: Hydroxymethyl hydroperoxide and
1146 bis(hydroxymethyl) peroxide from gas-phase ozonolysis of naturally occurring alkenes, Nature,
1147 316(6028), 535–536, doi:10.1038/316535a0, 1985.

1148 Gao, H. and Zepp, R. G.: Factors Influencing Photoreactions of Dissolved Organic Matter in a Coastal
1149 River of the Southeastern United States, Environ. Sci. Technol., 32(19), 2940–2946,
1150 doi:10.1021/es9803660, 1998.

1151 George, I. J., Vlasenko, A., Slowik, J. G., Broekhuizen, K. and Abbatt, J. P. D.: Heterogeneous oxidation of
1152 saturated organic aerosols by hydroxyl radicals: uptake kinetics, condensed-phase products, and particle
1153 size change, Atmos. Chem. Phys., 7(16), 4187–4201, doi:10.5194/acp-7-4187-2007, 2007.

1154 Gierczak, T. and Ravishankara, A. R.: Does the HO2 radical react with ketones?, Int. J. Chem. Kinet., 32(9),
1155 573–580, doi:10.1002/1097-4601(2000)32:9<573::AID-KIN7>3.0.CO;2-V, 2000.

1156 Goldstein, S., Aschengrau, D., Diamant, Y. and Rabani, J.: Photolysis of Aqueous H 2 O 2 : Quantum Yield
1157 and Applications for Polychromatic UV Actinometry in Photoreactors, Environ. Sci. Technol., 41(21),
1158 7486–7490, doi:10.1021/es071379t, 2007.

1159 Hallquist, M., Wenger, J. C., Baltensperger, U., Rudich, Y., Simpson, D., Claeys, M., Dommen, J., Donahue,
1160 N. M., George, C., Goldstein, A. H., Hamilton, J. F., Herrmann, H., Hoffmann, T., Iinuma, Y., Jang, M.,

1161 Jenkin, M. E., Jimenez, J. L., Kiendler-Scharr, A., Maenhaut, W., McFiggans, G., Mentel, T. F., Monod, A.,
1162 Prevot, A. S. H., Seinfeld, J. H., Surratt, J. D., Szmigielski, R. and Wildt, J.: The formation, properties and
1163 impact of secondary organic aerosol: current and emerging issues, Atmos. Chem. Phys., 9(14), 5155–
1164 5236 [online] Available from: <Go to ISI>://WOS:000268535500040, 2009.

1165 Hayes, P. L., Carlton, a. G., Baker, K. R., Ahmadov, R., Washenfelder, R. a., Alvarez, S., Rappenglück, B.,
1166 Gilman, J. B., Kuster, W. C., de Gouw, J. a., Zotter, P., Prévôt, a. S. H., Szidat, S., Kleindienst, T. E., Offenberg,
1167 J. H., Ma, P. K. and Jimenez, J. L.: Modeling the formation and aging of secondary organic aerosols in Los
1168 Angeles during CalNex 2010, Atmos. Chem. Phys., 15(10), 5773–5801, doi:10.5194/acp-15-5773-2015,
1169 2015.

1170 Hodzic, A., Madronich, S., Kasibhatla, P. S., Tyndall, G., Aumont, B., Jimenez, J. L., Lee-Taylor, J. and
1171 Orlando, J.: Organic photolysis reactions in tropospheric aerosols: effect on secondary organic aerosol
1172 formation and lifetime, Atmos. Chem. Phys., 15(16), 9253–9269, doi:10.5194/acp-15-9253-2015, 2015.

1173 Hoffmann, T., Odum, J. R., Bowman, F., Collins, D., Klockow, D., Flagan, R. C. and Seinfeld., J. H.:
1174 Formation of Organic Aerosols from the Oxidation of Biogenic Hydrocarbons, J. Atmos. Chem., 26(2),
1175 189–222, doi:10.1023/A:1005734301837, 1997.

1176 Hu, W. W., Campuzano-Jost, P., Palm, B. B., Day, D. A., Ortega, A. M., Hayes, P. L., Krechmer, J. E., Chen,
1177 Q., Kuwata, M., Liu, Y. J., de Sá, S. S., McKinney, K., Martin, S. T., Hu, M., Budisulistiorini, S. H., Riva, M.,
1178 Surratt, J. D., St. Clair, J. M., Isaacman-Van Wertz, G., Yee, L. D., Goldstein, A. H., Carbone, S., Brito, J.,
1179 Artaxo, P., de Gouw, J. A., Koss, A., Wisthaler, A., Mikoviny, T., Karl, T., Kaser, L., Jud, W., Hansel, A.,
1180 Docherty, K. S., Alexander, M. L., Robinson, N. H., Coe, H., Allan, J. D., Canagaratna, M. R., Paulot, F. and
1181 Jimenez, J. L.: Characterization of a real-time tracer for isoprene epoxydiols-derived secondary organic
1182 aerosol (IEPOX-SOA) from aerosol mass spectrometer measurements, Atmos. Chem. Phys., 15(20),
1183 11807–11833, doi:10.5194/acp-15-11807-2015, 2015.

1184 Huie, R. E. and Herron, J. T.: Kinetics of the reactions of singlet molecular oxygen (O21Dg) with organic
1185 compounds in the gas phase, Int. J. Chem. Kinet., 5(2), 197–211, doi:10.1002/kin.550050204, 1973.

1186 Jathar, S. H., Cappa, C. D., Wexler, a. S., Seinfeld, J. H. and Kleeman, M. J.: Multi-generational oxidation
1187 model to simulate secondary organic aerosol in a 3-D air quality model, Geosci. Model Dev., 8(8), 2553–
1188 2567, doi:10.5194/gmd-8-2553-2015, 2015.

1189 Johannessen, S. C. and Miller, W. L.: Quantum yield for the photochemical production of dissolved
1190 inorganic carbon in seawater, Mar. Chem., 76(4), 271–283, doi:10.1016/S0304-4203(01)00067-6, 2001.

1191 Johnson, M. S., Nilsson, E. J. K., Svensson, E. A. and Langer, S.: Gas-Phase Advanced Oxidation for
1192 Effective, Efficient in Situ Control of Pollution, Environ. Sci. Technol., 48(15), 8768–8776,
1193 doi:10.1021/es5012687, 2014.

1194 Kang, E., Root, M. J., Toohey, D. W. and Brune, W. H.: Introducing the concept of Potential Aerosol Mass
1195 (PAM), Atmos. Chem. Phys., 7(22), 5727–5744, doi:10.5194/acp-7-5727-2007, 2007.

1196 Kang, E., Toohey, D. W. and Brune, W. H.: Dependence of SOA oxidation on organic aerosol mass
1197 concentration and OH exposure: experimental PAM chamber studies, Atmos. Chem. Phys., 11(4), 1837–
1198 1852, doi:10.5194/acp-11-1837-2011, 2011.

1199 Keller-Rudek, H., Moortgat, G. K., Sander, R. and Sörensen, R.: The MPI-Mainz UV/VIS Spectral Atlas of
1200 Gaseous Molecules of Atmospheric Interest, [online] Available from: www.uv-vis-spectral-atlas-
1201 mainz.org, 2015.

1202 Klems, J. P., Lippa, K. a and McGivern, W. S.: Quantitative Evidence for Organic Peroxy Radical
1203 Photochemistry at 254 nm, J. Phys. Chem. A, 119(2), 344–351, doi:10.1021/jp509165x, 2015.

1204 Kumar, M. and Francisco, J. S.: Red-Light-Induced Decomposition of an Organic Peroxy Radical: A New
1205 Source of the HO 2 Radical, Angew. Chemie Int. Ed., doi:10.1002/anie.201509311, 2015.

1206 Kwok, E. and Atkinson, R.: Estimation of hydroxyl radical reaction rate constants for gas-phase organic
1207 compounds using a structure-reactivity relationship: An update, Atmos. Environ., 29(14), 1685–1695,
1208 doi:10.1016/1352-2310(95)00069-B, 1995.

1209 Lambe, A. T., Ahern, A. T., Williams, L. R., Slowik, J. G., Wong, J. P. S., Abbatt, J. P. D., Brune, W. H., Ng, N.
1210 L., Wright, J. P., Croasdale, D. R., Worsnop, D. R., Davidovits, P. and Onasch, T. B.: Characterization of
1211 aerosol photooxidation flow reactors: heterogeneous oxidation, secondary organic aerosol formation

1212 and cloud condensation nuclei activity measurements, Atmos. Meas. Tech., 4(3), 445–461,
1213 doi:10.5194/amt-4-445-2011, 2011a.

1214 Lambe, A. T., Cappa, C. D., Massoli, P., Onasch, T. B., Forestieri, S. D., Martin, A. T., Cummings, M. J.,
1215 Croasdale, D. R., Brune, W. H., Worsnop, D. R. and Davidovits, P.: Relationship between Oxidation Level
1216 and Optical Properties of Secondary Organic Aerosol, Environ. Sci. Technol., 47(12), 6349–6357,
1217 doi:10.1021/es401043j, 2013.

1218 Lambe, A. T., Chhabra, P. S., Onasch, T. B., Brune, W. H., Hunter, J. F., Kroll, J. H., Cummings, M. J., Brogan,
1219 J. F., Parmar, Y., Worsnop, D. R., Kolb, C. E. and Davidovits, P.: Effect of oxidant concentration, exposure
1220 time, and seed particles on secondary organic aerosol chemical composition and yield, Atmos. Chem.
1221 Phys., 15(6), 3063–3075, doi:10.5194/acp-15-3063-2015, 2015.

1222 Lambe, A. T., Onasch, T. B., Croasdale, D. R., Wright, J. P., Martin, A. T., Franklin, J. P., Massoli, P., Kroll, J.
1223 H., Canagaratna, M. R., Brune, W. H., Worsnop, D. R. and Davidovits, P.: Transitions from
1224 Functionalization to Fragmentation Reactions of Laboratory Secondary Organic Aerosol (SOA)
1225 Generated from the OH Oxidation of Alkane Precursors, Environ. Sci. Technol., 46(10), 5430–5437,
1226 doi:10.1021/es300274t, 2012.

1227 Lambe, A. T., Onasch, T. B., Massoli, P., Croasdale, D. R., Wright, J. P., Ahern, A. T., Williams, L. R., Worsnop,
1228 D. R., Brune, W. H. and Davidovits, P.: Laboratory studies of the chemical composition and cloud
1229 condensation nuclei (CCN) activity of secondary organic aerosol (SOA) and oxidized primary organic
1230 aerosol (OPOA), Atmos. Chem. Phys., 11(17), 8913–8928, doi:10.5194/acp-11-8913-2011, 2011b.

1231 Laue, T. and Plagens, A.: Named Organic Reactions, 2nd ed., John Wiley & Sons, Chichester, England,
1232 New York. [online] Available from: http://www.wiley.com/WileyCDA/WileyTitle/productCd-
1233 047001041X.html, 2005.

1234 Levy II, H.: Normal atmosphere: large radical and formaldehyde concentrations predicted., Science,
1235 173(3992), 141–143, doi:10.1126/science.173.3992.141, 1971.

1236 Li, R., Palm, B. B., Borbon, A., Graus, M., Warneke, C., Ortega, a M., Day, D. a, Brune, W. H., Jimenez, J.
1237 L. and de Gouw, J. a: Laboratory Studies on Secondary Organic Aerosol Formation from Crude Oil Vapors,
1238 Environ. Sci. Technol., 47(21), 12566–12574, doi:10.1021/es402265y, 2013.

1239 Li, R., Palm, B. B., Ortega, A. M., Hu, W., Peng, Z., Day, D. A., Knote, C., Brune, W. H., de Gouw, J. and
1240 Jimenez, J. L.: Modeling the radical chemistry in an Oxidation Flow Reactor (OFR): radical formation and
1241 recycling, sensitivities, and OH exposure estimation equation, J. Phys. Chem. A, 119(19), 4418–4432,
1242 doi:10.1021/jp509534k, 2015.

1243 Liu, P. F., Abdelmalki, N., Hung, H.-M., Wang, Y., Brune, W. H. and Martin, S. T.: Ultraviolet and visible
1244 complex refractive indices of secondary organic material produced by photooxidation of the aromatic
1245 compounds toluene and m-Xylene, Atmos. Chem. Phys., 15(3), 1435–1446, doi:10.5194/acp-15-1435-
1246 2015, 2015.

1247 Liu, P., Zhang, Y. and Martin, S. T.: Complex refractive indices of thin films of secondary organic materials
1248 by spectroscopic ellipsometry from 220 to 1200 nm, Environ. Sci. Technol., 47, 13594–13601,
1249 doi:10.1021/es403411e, 2013.

1250 Mao, J., Ren, X., Brune, W. H., Olson, J. R., Crawford, J. H., Fried, a., Huey, L. G., Cohen, R. C., Heikes, B.,
1251 Singh, H. B., Blake, D. R., Sachse, G. W., Diskin, G. S., Hall, S. R. and Shetter, R. E.: Airborne measurement
1252 of OH reactivity during INTEX-B, Atmos. Chem. Phys., 9(1), 163–173, doi:10.5194/acp-9-163-2009, 2009.

1253 Massoli, P., Lambe, A. T., Ahern, A. T., Williams, L. R., Ehn, M., Mikkilä, J., Canagaratna, M. R., Brune, W.
1254 H., Onasch, T. B., Jayne, J. T., Petäjä, T., Kulmala, M., Laaksonen, A., Kolb, C. E., Davidovits, P. and Worsnop,
1255 D. R.: Relationship between aerosol oxidation level and hygroscopic properties of laboratory generated
1256 secondary organic aerosol (SOA) particles, Geophys. Res. Lett., 37(24), L24801,
1257 doi:10.1029/2010GL045258, 2010.

1258 Matsunaga, A. and Ziemann, P. J.: Gas-Wall Partitioning of Organic Compounds in a Teflon Film Chamber
1259 and Potential Effects on Reaction Product and Aerosol Yield Measurements, Aerosol Sci. Technol., 44(10),
1260 881–892, doi:10.1080/02786826.2010.501044, 2010.

1261 Messaadia, L., El Dib, G., Ferhati, A. and Chakir, A.: UV–visible spectra and gas-phase rate coefficients
1262 for the reaction of 2,3-pentanedione and 2,4-pentanedione with OH radicals, Chem. Phys. Lett., 626,

73–79, doi:10.1016/j.cplett.2015.02.032, 2015.

Monks, P. S.: Gas-phase radical chemistry in the troposphere, Chem. Soc. Rev., 34, 376–395, doi:10.1039/b307982c, 2005.

Nakashima, N.: Laser photolysis of benzene. V. Formation of hot benzene, J. Chem. Phys., 77(12), 6040, doi:10.1063/1.443847, 1982.

Nakashima, N. and Yoshihara, K.: Laser flash photolysis of benzene. VIII. Formation of hot benzene from the S[sub 2] state and its collisional deactivation, J. Chem. Phys., 79(6), 2727–2735, doi:10.1063/1.446176, 1983.

Nguyen, T. B., Crounse, J. D., Schwantes, R. H., Teng, a. P., Bates, K. H., Zhang, X., St. Clair, J. M., Brune, W. H., Tyndall, G. S., Keutsch, F. N., Seinfeld, J. H. and Wennberg, P. O.: Overview of the Focused Isoprene eXperiment at the California Institute of Technology (FIXCIT): mechanistic chamber studies on the oxidation of biogenic compounds, Atmos. Chem. Phys., 14(24), 13531–13549, doi:10.5194/acp-14-13531-2014, 2014.

O'Sullivan, D. W., Neale, P. J., Coffin, R. B., Boyd, T. J. and Osburn, C. L.: Photochemical production of hydrogen peroxide and methylhydroperoxide in coastal waters, Mar. Chem., 97(1-2), 14–33, doi:10.1016/j.marchem.2005.04.003, 2005.

Odum, J. R., Hoffmann, T., Bowman, F., Collins, D., Flagan Richard, C. and Seinfeld John, H.: Gas particle partitioning and secondary organic aerosol yields, Environ. Sci. Technol., 30(8), 2580–2585, doi:10.1021/es950943+, 1996.

Ono, R., Nakagawa, Y., Tokumitsu, Y., Matsumoto, H. and Oda, T.: Effect of humidity on the production of ozone and other radicals by low-pressure mercury lamps, J. Photochem. Photobiol. A Chem., 274, 13–19, doi:10.1016/j.jphotochem.2013.09.012, 2014.

Ortega, A. M., Day, D. A., Cubison, M. J., Brune, W. H., Bon, D., de Gouw, J. A. and Jimenez, J. L.: Secondary organic aerosol formation and primary organic aerosol oxidation from biomass-burning smoke in a flow reactor during FLAME-3, Atmos. Chem. Phys., 13(22), 11551–11571, doi:10.5194/acp-13-11551-2013, 2013.

Ortega, A. M., Hayes, P. L., Peng, Z., Palm, B. B., Hu, W., Day, D. A., Li, R., Cubison, M. J., Brune, W. H., Graus, M., Warneke, C., Gilman, J. B., Kuster, W. C., de Gouw, J. A. and Jimenez, J. L.: Real-time measurements of secondary organic aerosol formation and aging from ambient air in an oxidation flow reactor in the Los Angeles area, Atmos. Chem. Phys. Discuss., 15(15), 21907–21958, doi:10.5194/acpd-15-21907-2015, 2015.

Osburn, C. L., Retamal, L. and Vincent, W. F.: Photoreactivity of chromophoric dissolved organic matter transported by the Mackenzie River to the Beaufort Sea, Mar. Chem., 115(1-2), 10–20, doi:10.1016/j.marchem.2009.05.003, 2009.

Palm, B. B., Campuzano-Jost, P., Ortega, A. M., Day, D. A., Kaser, L., Jud, W., Karl, T., Hansel, A., Hunter, J. F., Cross, E. S., Kroll, J. H., Peng, Z., Brune, W. H. and Jimenez, J. L.: In situ secondary organic aerosol formation from ambient pine forest air using an oxidation flow reactor, Atmos. Chem. Phys., 16(5), 2943–2970, doi:10.5194/acp-16-2943-2016, 2016.

Peng, Z., Day, D. A., Stark, H., Li, R., Lee-Taylor, J., Palm, B. B., Brune, W. H. and Jimenez, J. L.: HOx radical chemistry in oxidation flow reactors with low-pressure mercury lamps systematically examined by modeling, Atmos. Meas. Tech., 8(11), 4863–4890, doi:10.5194/amt-8-4863-2015, 2015.

Phillips, S. M. and Smith, G. D.: Light Absorption by Charge Transfer Complexes in Brown Carbon Aerosols, Environ. Sci. Technol. Lett., 1(10), 382–386, doi:10.1021/ez500263j, 2014.

Phillips, S. M. and Smith, G. D.: Further Evidence for Charge Transfer Complexes in Brown Carbon Aerosols from Excitation–Emission Matrix Fluorescence Spectroscopy, J. Phys. Chem. A, 119(19), 4545–4551, doi:10.1021/jp510709e, 2015.

Pitts, J. N. and Finlayson, B. J.: Mechanismen der photochemischen Luftverschmutzung, Angew. Chemie, 87(1), 18–33, doi:10.1002/ange.19750870103, 1975.

Platt, S. M., El Haddad, I., Zardini, a. a., Clairotte, M., Astorga, C., Wolf, R., Slowik, J. G., Temime-Roussel, B., Marchand, N., Ježek, I., Drinovec, L., Močnik, G., Möhler, O., Richter, R., Barmet, P., Bianchi, F.,

1313 Baltensperger, U. and Prévôt, a. S. H.: Secondary organic aerosol formation from gasoline vehicle
1314 emissions in a new mobile environmental reaction chamber, Atmos. Chem. Phys., 13(18), 9141–9158,
1315 doi:10.5194/acp-13-9141-2013, 2013.

1316 Presto, A. A., Huff Hartz, K. E. and Donahue, N. M.: Secondary Organic Aerosol Production from Terpene
1317 Ozonolysis. 1. Effect of UV Radiation, Environ. Sci. Technol., 39(18), 7036–7045, doi:10.1021/es050174m,
1318 2005.

1319 Pretsch, E., Bühlmann, P. and Badertscher, M.: Structure Determination of Organic Compounds, Springer
1320 Berlin Heidelberg, Berlin, Heidelberg., 2009.

1321 Renlund, A. M. and Trott, W. M.: ArF Laser-induced decomposition of simple energetic niolecules, Chem.
1322 Phys. Lett., 107(6), 555–560, doi:10.1016/S0009-2614(84)85155-6, 1984.

1323 Roberts, J. M. and Fajer, R. W.: UV absorption cross sections of organic nitrates of potential atmospheric
1324 importance and estimation of atmospheric lifetimes, Environ. Sci. Technol., 23(8), 945–951, 1989.

1325 Romonosky, D. E., Ali, N. N., Saiduddin, M. N., Wu, M., Lee, H. J. (Julie), Aiona, P. K. and Nizkorodov, S.
1326 A.: Effective absorption cross sections and photolysis rates of anthropogenic and biogenic secondary
1327 organic aerosols, Atmos. Environ., 130, 172–179, doi:10.1016/j.atmosenv.2015.10.019, 2016.

1328 Romonosky, D. E., Laskin, A., Laskin, J. and Nizkorodov, S. A.: High-Resolution Mass Spectrometry and
1329 Molecular Characterization of Aqueous Photochemistry Products of Common Types of Secondary
1330 Organic Aerosols, J. Phys. Chem. A, 119(11), 2594–2606, doi:10.1021/jp509476r, 2015.

1331 Sander, S. P., Friedl, R. R., Barker, J. R., Golden, D. M., Kurylo, M. J., Wine, P. H., Abbatt, J. P. D., Burkholder,
1332 J. B., Kolb, C. E., Moortgat, G. K., Huie, R. E. and Orkin, V. L.: Chemical Kinetics and Photochemical Data
1333 for Use in Atmospheric Studies Evaluation Number 17., 2011.

1334 Saukko, E., Lambe, A. T., Massoli, P., Koop, T., Wright, J. P., Croasdale, D. R., Pedernera, D. A., Onasch, T.
1335 B., Laaksonen, A., Davidovits, P., Worsnop, D. R. and Virtanen, A.: Humidity-dependent phase state of
1336 SOA particles from biogenic and anthropogenic precursors, Atmos. Chem. Phys., 12(16), 7517–7529,
1337 doi:10.5194/acp-12-7517-2012, 2012.

1338 Schmidt, G. a, Kelley, M., Nazarenko, L., Ruedy, R., Russell, G. L., Aleinov, I., Bauer, M., Bauer, S. E., Bhat,
1339 M. K., Bleck, R., Canuto, V., Chen, Y., Cheng, Y., Clune, T. L., Del Genio, A., de Fainchtein, R., Faluvegi, G.,
1340 Hansen, J. E., Healy, R. J., Kiang, N. Y., Koch, D., Lacis, A. a, LeGrande, A. N., Lerner, J., Lo, K. K., Matthews,
1341 E. E., Menon, S., Miller, R. L., Oinas, V., Oloso, A. O., Perlwitz, J. P., Puma, M. J., Putman, W. M., Rind, D.,
1342 Romanou, A., Sato, M., Shindell, D. T., Sun, S., Syed, R. A., Tausnev, N., Tsigaridis, K., Unger, N.,
1343 Voulgarakis, A., Yao, M.-S. and Zhang, J.: Configuration and assessment of the GISS ModelE2
1344 contributions to the CMIP5 archive, J. Adv. Model. Earth Syst., 6(1), 141–184,
1345 doi:10.1002/2013MS000265, 2014.

1346 Seakins, P. W.: A brief review of the use of environmental chambers for gas phase studies of kinetics,
1347 chemical mechanisms and characterisation of field instruments, EPJ Web Conf., 9, 143–163,
1348 doi:10.1051/epjconf/201009012, 2010.

1349 Sharpless, C. M. and Blough, N. V: The importance of charge-transfer interactions in determining
1350 chromophoric dissolved organic matter (CDOM) optical and photochemical properties, Environ. Sci.
1351 Process. Impacts, 16(4), 654, doi:10.1039/c3em00573a, 2014.

1352 da Silva, G. and Bozzelli, J. W.: Role of the α-hydroxyethylperoxy radical in the reactions of acetaldehyde
1353 and vinyl alcohol with HO2, Chem. Phys. Lett., 483(1-3), 25–29, doi:10.1016/j.cplett.2009.10.045, 2009.

1354 Smith, J. D., Kroll, J. H., Cappa, C. D., Che, D. L., Liu, C. L., Ahmed, M., Leone, S. R., Worsnop, D. R. and
1355 Wilson, K. R.: The heterogeneous reaction of hydroxyl radicals with sub-micron squalane particles: a
1356 model system for understanding the oxidative aging of ambient aerosols, Atmos. Chem. Phys., 9(9),
1357 3209–3222, doi:10.5194/acp-9-3209-2009, 2009.

1358 Strollo, C. M. and Ziemann, P. J.: Products and mechanism of secondary organic aerosol formation from
1359 the reaction of 3-methylfuran with OH radicals in the presence of NOx, Atmos. Environ., 77, 534–543,
1360 doi:10.1016/j.atmosenv.2013.05.033, 2013.

1361 Tkacik, D. S., Lambe, A. T., Jathar, S., Li, X., Presto, A. A., Zhao, Y., Blake, D., Meinardi, S., Jayne, J. T.,
1362 Croteau, P. L. and Robinson, A. L.: Secondary Organic Aerosol Formation from in-Use Motor Vehicle
1363 Emissions Using a Potential Aerosol Mass Reactor, Environ. Sci. Technol., 48(19), 11235–11242,

doi:10.1021/es502239v, 2014.

Tsang, W.: Chemical kinetic data base for combustion chemistry part V. Propene, J. Phys. Chem. Ref. data, 20(2), 221–274, doi:10.1063/1.555880, 1991.

Turro, N. J., Ramamurthy, V. and Scaiano, J. C.: Principles of Molecular Photochemistry: An Introduction, University Science Books, Sausalito, CA, USA. [online] Available from: http://www.uscibooks.com/turro2.htm, 2009.

Updyke, K. M., Nguyen, T. B. and Nizkorodov, S. a.: Formation of brown carbon via reactions of ammonia with secondary organic aerosols from biogenic and anthropogenic precursors, Atmos. Environ., 63, 22–31, doi:10.1016/j.atmosenv.2012.09.012, 2012.

Wang, B., Lambe, A. T., Massoli, P., Onasch, T. B., Davidovits, P., Worsnop, D. R. and Knopf, D. a.: The deposition ice nucleation and immersion freezing potential of amorphous secondary organic aerosol: Pathways for ice and mixed-phase cloud formation, J. Geophys. Res., 117(D16), D16209, doi:10.1029/2012JD018063, 2012.

Wang, J., Doussin, J. F., Perrier, S., Perraudin, E., Katrib, Y., Pangui, E. and Picquet-Varrault, B.: Design of a new multi-phase experimental simulation chamber for atmospheric photosmog, aerosol and cloud chemistry research, Atmos. Meas. Tech., 4(11), 2465–2494, doi:10.5194/amt-4-2465-2011, 2011.

Warneke, C., Roberts, J. M., Veres, P., Gilman, J., Kuster, W. C., Burling, I., Yokelson, R. and de Gouw, J. a.: VOC identification and inter-comparison from laboratory biomass burning using PTR-MS and PIT-MS, Int. J. Mass Spectrom., 303(1), 6–14, doi:10.1016/j.ijms.2010.12.002, 2011.

Wong, J. P. S., Zhou, S. and Abbatt, J. P. D.: Changes in Secondary Organic Aerosol Composition and Mass due to Photolysis: Relative Humidity Dependence, J. Phys. Chem. A, 119(19), 4309–4316, doi:10.1021/jp506898c, 2015.

Zhang, X., Cappa, C. D., Jathar, S. H., McVay, R. C., Ensberg, J. J., Kleeman, M. J. and Seinfeld, J. H.: Influence of vapor wall loss in laboratory chambers on yields of secondary organic aerosol., Proc. Natl. Acad. Sci. U. S. A., 111(16), 5802–7, doi:10.1073/pnas.1404727111, 2014.

Zhang, Y., Xie, H. and Chen, G.: Factors Affecting the Efficiency of Carbon Monoxide Photoproduction in the St. Lawrence Estuarine System (Canada), Environ. Sci. Technol., 40(24), 7771–7777, doi:10.1021/es0615268, 2006.

Ziemann, P. and Atkinson, R.: Kinetics, products, and mechanisms of secondary organic aerosol formation, Chem. Soc. Rev., 41(19), 6582, doi:10.1039/c2cs35122f, 2012.

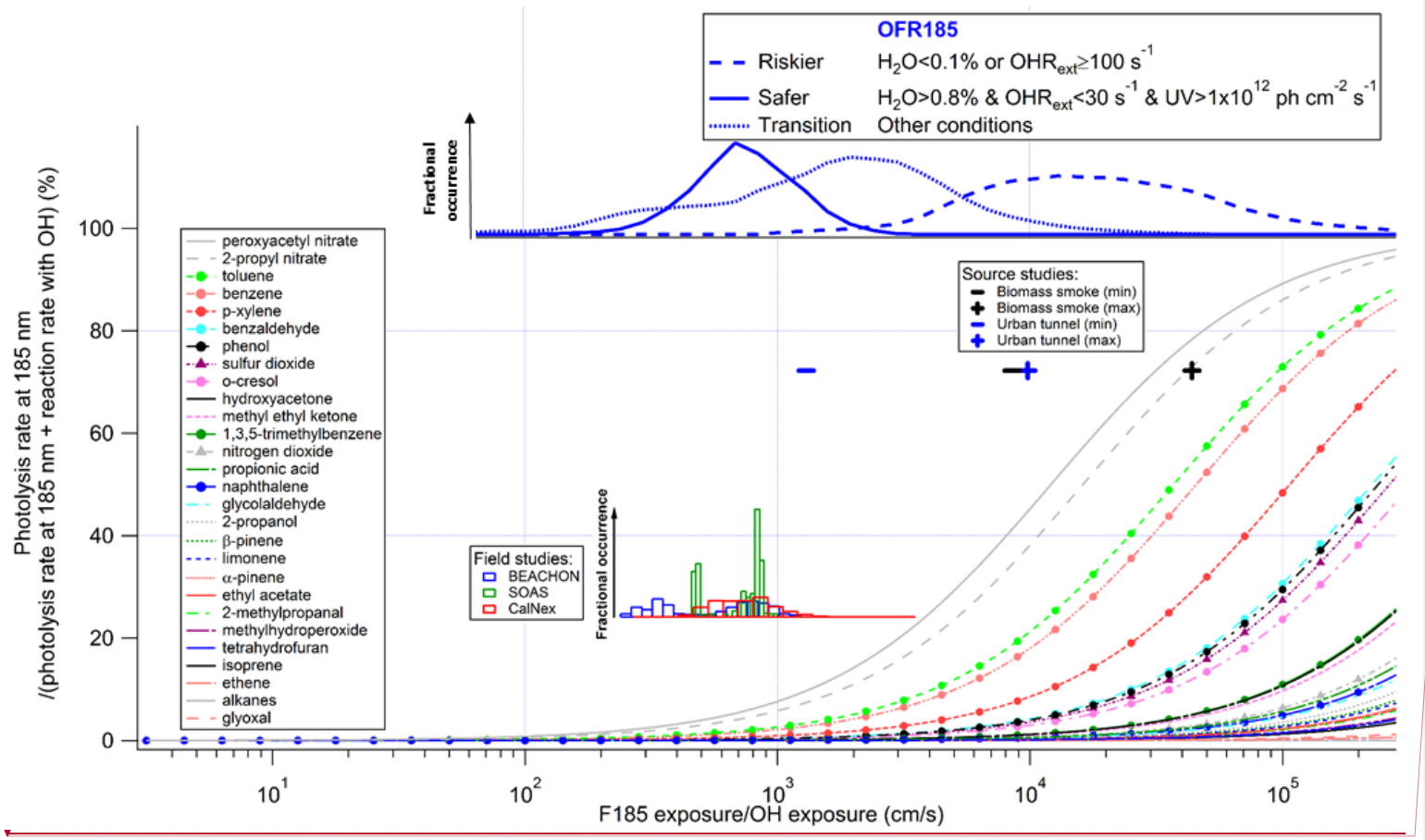

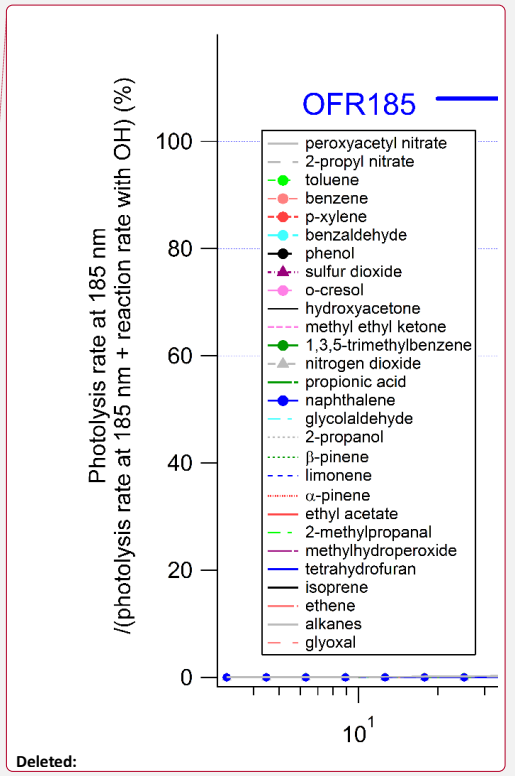

Deleted:

1397

Figure 1. Fractional importance of the photolysis rate at 185 nm of several species of interest vs. the reaction rate with OH, as a function of the ratio of exposure to 185 nm photons (F185) and OH. F185 exposure (in photons cm^{-2}) is the product of 185 nm photon flux (in photons cm^{-2} s^{-1}) and time (in s). F185 exposure / OH exposure is thus in cm s^{-1}. The modeled frequency distributions of ratios of 185 nm photon exposure to OH exposure under riskier, safer, and transition conditions for OFR185 are also shown. The curves of aromatics and inorganic gases are highlighted by solid dots and upward triangles, respectively. The lower inset shows histograms of model-estimated F185/OH exposures for three field studies where OFR185 was used to process ambient air. Their ordinate is the fractional occurrence of a given condition (X_{exp}/OH_{exp}). All histograms are normalized to be of identical total area (i.e., total probability of 1). The upper inset (black and blue markers) shows similar information for source studies of biomass smoke (FLAME-3; Ortega et al., 2013) and an urban tunnel (Tkacik et al., 2014). All curves, markers, and histograms in this figure share the same abscissa.

Deleted: . Fractional importance of the photolysis rate at 185 nm of several species of interest vs. the reaction rate with OH, as a function of the ratio of exposure to 185 nm photons (F185) and OH. The modeled range for OFR185 and for pathological conditions for OFR185 are also shown. The curves of aromatics and inorganic gases are highlighted by solid dots and upward triangles, respectively. The lower inset shows histograms of model-estimated F185/OH exposures for three field studies where OFR185 was used to process ambient air. The upper inset (black and blue markers) shows the same information for source studies of biomass smoke (FLAME-3; Ortega et al., 2013) and an urban tunnel (Tkacik et al., 2014). All curves, markers, and histograms share the same abscissa.

Page Break

¶

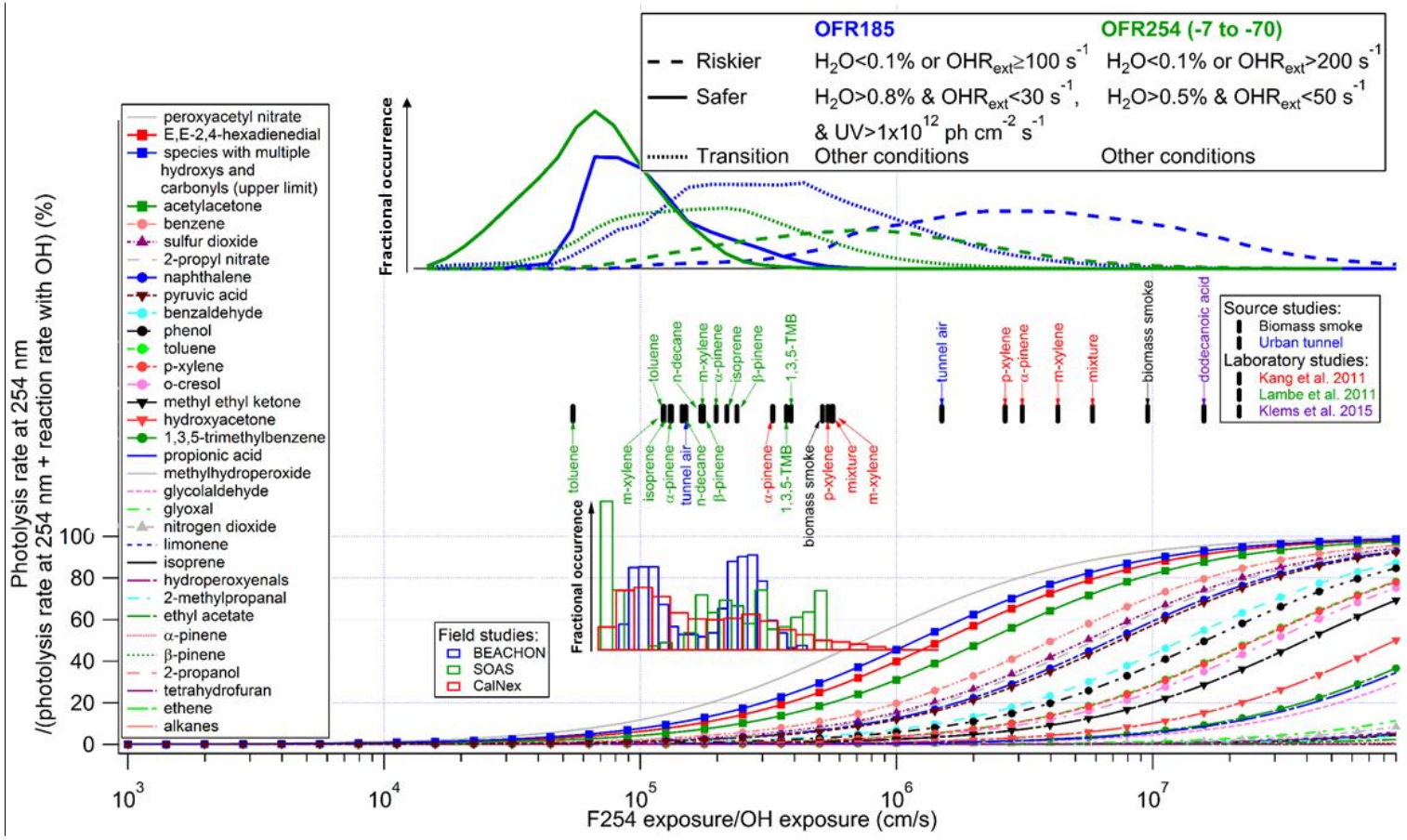
OFR185
OFR254 (-7 to -70)
Riskier
H2O<0.1% or OHRext≥100 s-1
H2O<0.1% or OHRext>200 s-1
Safer
H2O>0.8% & OHRext<30 s-1, & UV>1x10^12 ph cm-2 s-1
H2O>0.5% & OHRext<50 s-1
Transition
Other conditions
Other conditions
Fractional occurrence
peroxyacetyl nitrate
E,E-2,4-hexadienedial
species with multiple hydroxys and carbonyls (upper limit)
acetylacetone
benzene
sulfur dioxide
2-propyl nitrate
naphthalene
pyruvic acid
benzaldehyde
phenol
toluene
p-xylene
o-cresol
methyl ethyl ketone
hydroxyacetone
1,3,5-trimethylbenzene
propionic acid
methylhydroperoxide
glycolaldehyde
glyoxal
nitrogen dioxide
limonene
isoprene
hydroperoxyenals
2-methylpropanal
ethyl acetate
α-pinene
β-pinene
2-propanol
tetrahydrofuran
ethene
alkanes
Photolysis rate at 254 nm /(photolysis rate at 254 nm + reaction rate with OH) (%)
Source studies:
Biomass smoke
Urban tunnel
Laboratory studies:
Kang et al. 2011
Lambe et al. 2011
Klems et al. 2015
toluene
n-decane
m-xylene
α-pinene
isoprene
β-pinene
1,3,5-TMB
tunnel air
p-xylene
α-pinene
m-xylene
mixture
biomass smoke
dodecanoic acid
Field studies:
BEACHON
SOAS
CalNex
F254 exposure/OH exposure (cm/s)

1437

Figure 2. Same format as Fig. 1, but for the fractional importance of the photolysis rate at 254 nm vs. the reaction rate with OH as a function of the ratio of exposure to 254 nm (F254) and OH. The modeled frequency distributions of ratios of 254 nm photon exposure to OH exposure under riskier, safer, and transition conditions for OFR185 and OFR254 (-7 to -70) are also shown. The curves of saturated carbonyl compounds and possible highly absorbing oxidation intermediates are highlighted by downward triangles and squares, respectively. The insets show histograms of model-estimated F254/OH exposures for three field studies where OFR185 was used to process ambient air. In addition to source studies of biomass smoke (FLAME-3) and urban tunnel (Tkacik et al., 2014), F254 exposure/OH exposure ratios in two laboratory studies (Kang et al., 2011; Lambe et al., 2011b) are shown in the upper inset. Colored tags indicate species used in the laboratory experiments. The lower and upper limits of F254 exposure/OH exposure ratios in the experiments with a certain source in a certain study are denoted by tags below and above the markers, respectively.

Deleted: range for OFR254-70

Deleted: OFR254-7 and for corresponding pathological

Deleted: ketones

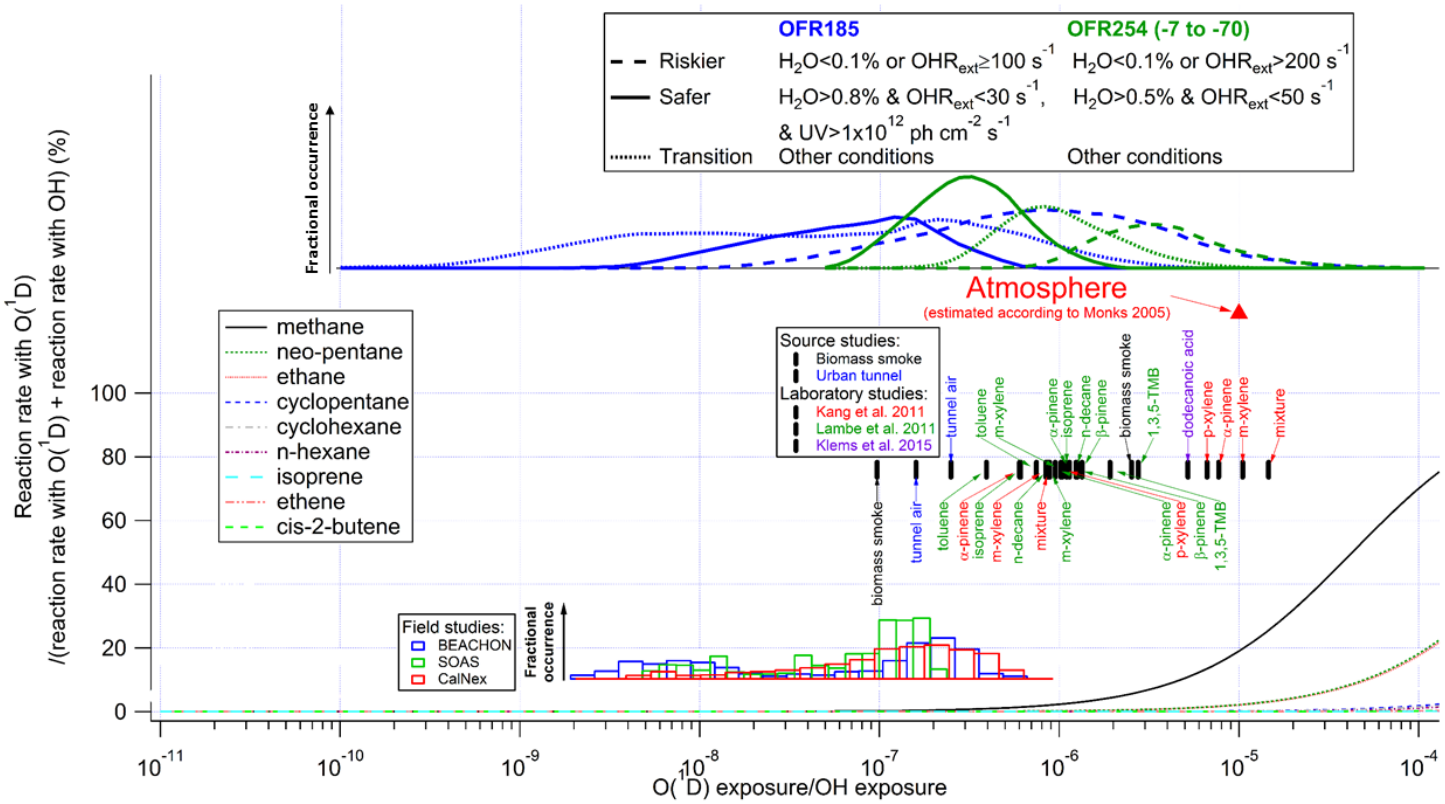

Figure 3. Same format as Fig. 2, but for the ratio of the reaction rate with $O(^1D)$ vs. OH as a function of the relative exposure to $O(^1D)$ and OH. A typical value of the relative exposure of $O(^1D)$ and OH in the troposphere estimated according to Monks (2005) is also shown.

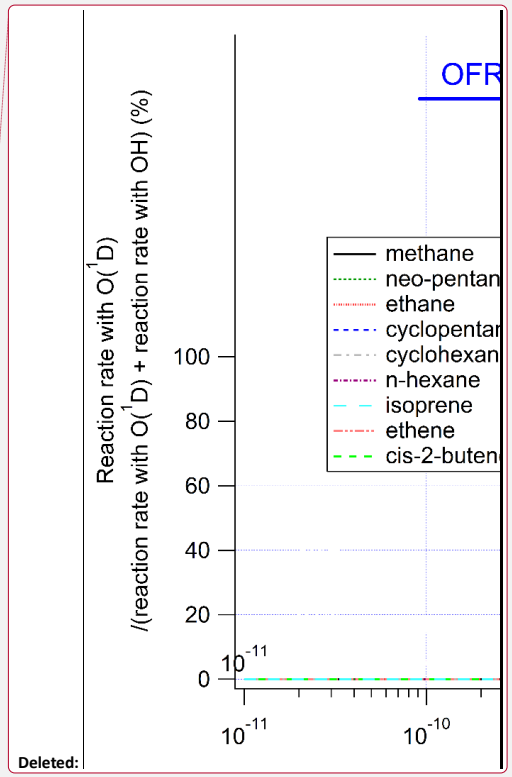

Deleted:

Formatted: Font: (Default) SimSun

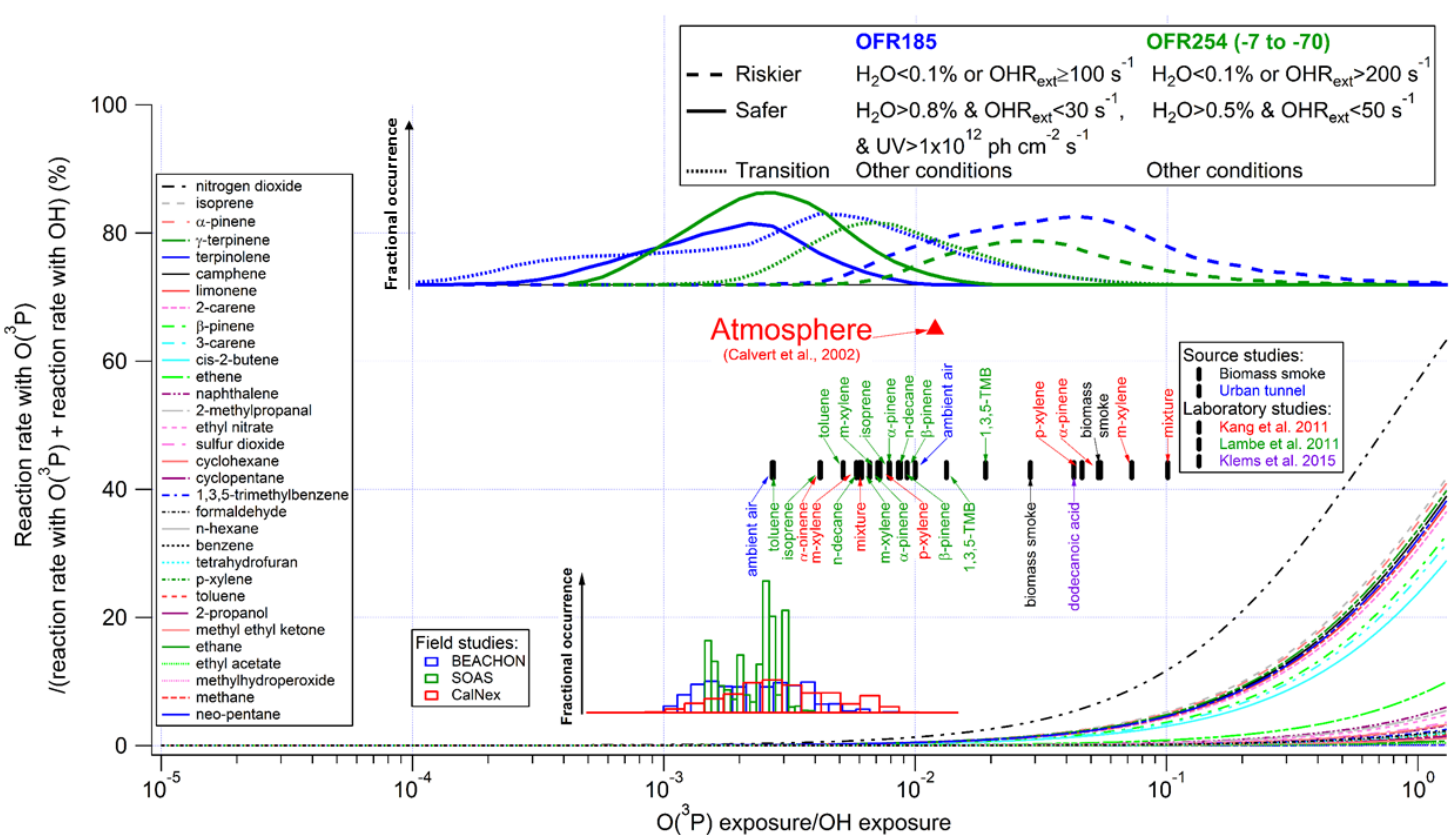

Figure 4. Same format as Fig. 3, but for the ratio of the reaction rate with $O(^3P)$ vs. OH as a function of the relative exposure of $O(^3P)$ and OH. A typical value of the relative exposure of $O(^3P)$ and OH in the troposphere from Calvert et al. (2002) is also shown.

Deleted: Page Break

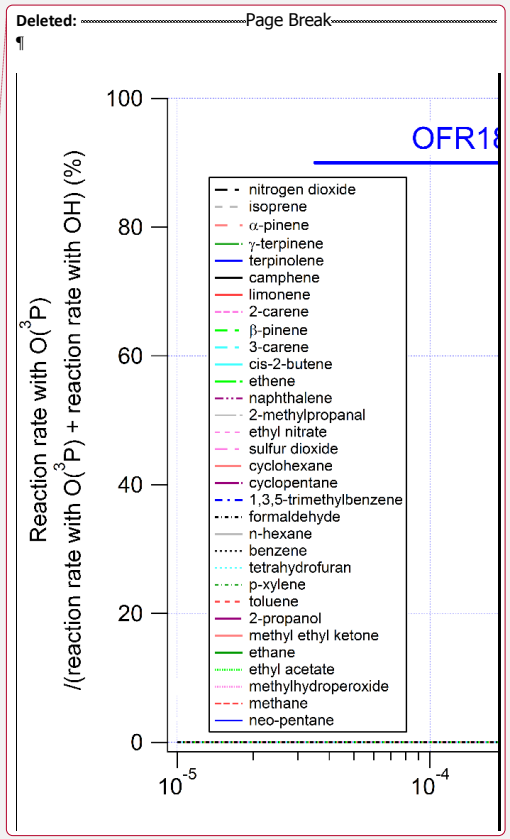

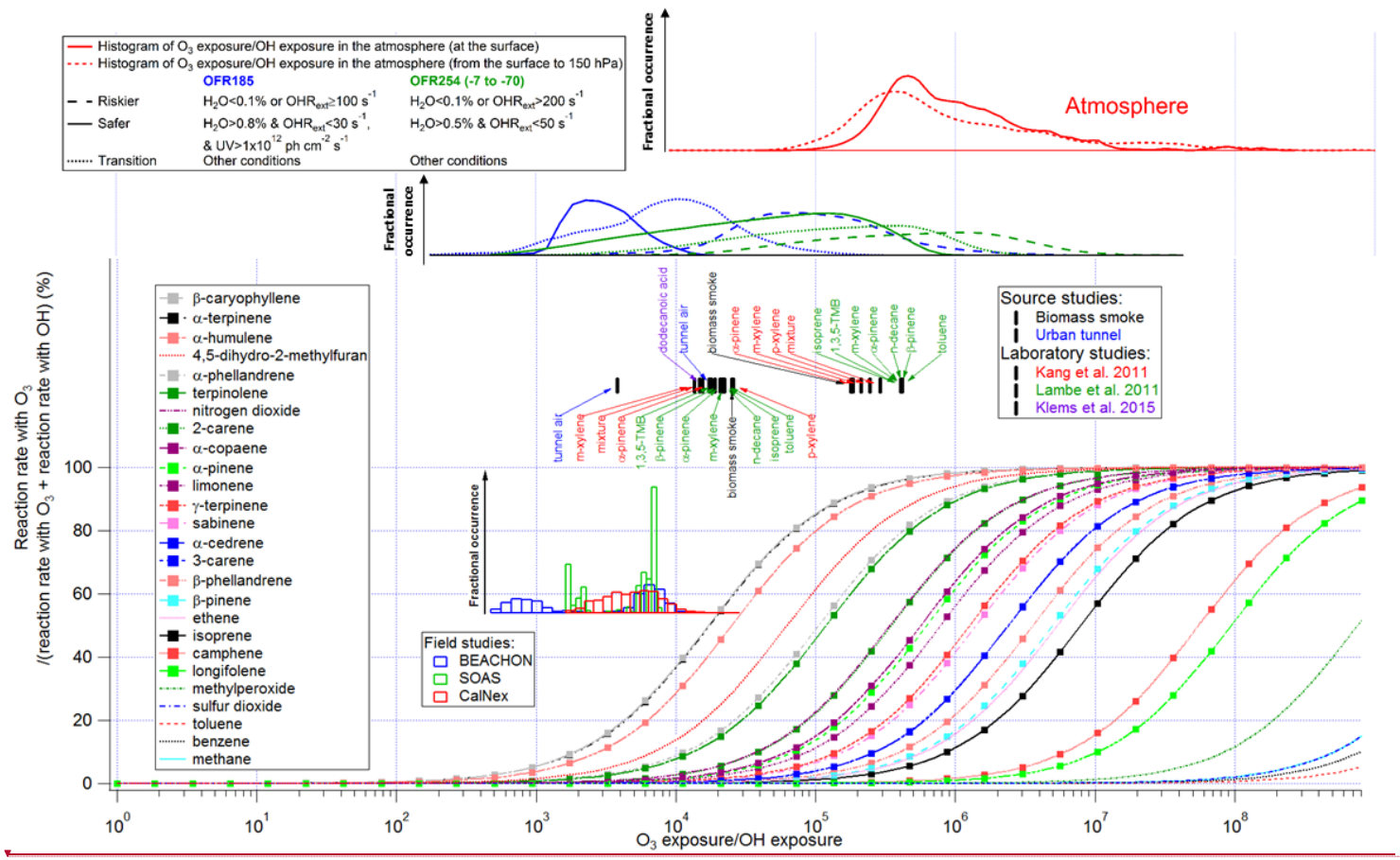
Histogram of O3 exposure/OH exposure in the atmosphere (at the surface)
Histogram of O3 exposure/OH exposure in the atmosphere (from the surface to 150 hPa)
OFR185
OFR254 (-7 to -70)
Riskier
H2O<0.1% or OHRext≥100 s-1
H2O<0.1% or OHRext>200 s-1
Safer
H2O>0.8% & OHRext<30 s-1, & UV>1x10^12 ph cm-2 s-1
H2O>0.5% & OHRext<50 s-1
Transition
Other conditions
Other conditions
Fractional occurrence
Atmosphere
Fractional occurrence
Source studies:
Biomass smoke
Urban tunnel
Laboratory studies:
Kang et al. 2011
Lambe et al. 2011
Klems et al. 2015
Field studies:
BEACHON
SOAS
CalNex
Fractional occurrence
β-caryophyllene
α-terpinene
α-humulene
4,5-dihydro-2-methylfuran
α-phellandrene
terpinolene
nitrogen dioxide
2-carene
α-copaene
α-pinene
limonene
γ-terpinene
sabinene
α-cedrene
3-carene
β-phellandrene
β-pinene
ethene
isoprene
camphene
longifolene
methylperoxide
sulfur dioxide
toluene
benzene
methane
Reaction rate with O3 /(reaction rate with O3 + reaction rate with OH) (%)
O3 exposure/OH exposure

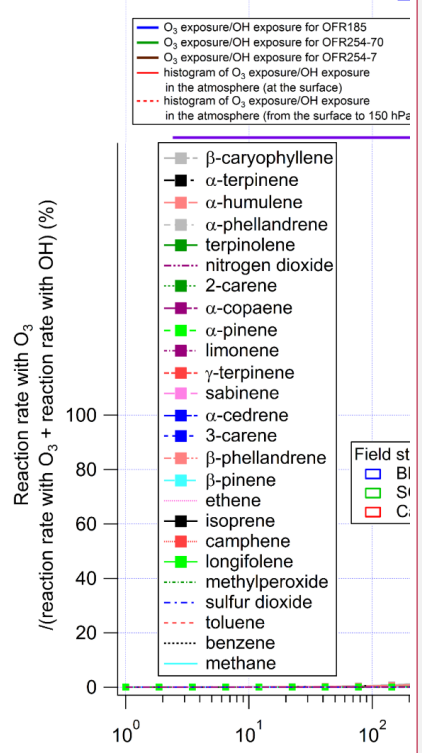
O3 exposure/OH exposure for OFR185
O3 exposure/OH exposure for OFR254-70
O3 exposure/OH exposure for OFR254-7
histogram of O3 exposure/OH exposure in the atmosphere (at the surface)
histogram of O3 exposure/OH exposure in the atmosphere (from the surface to 150 hPa
β-caryophyllene
α-terpinene
α-humulene
α-phellandrene
terpinolene
nitrogen dioxide
2-carene
α-copaene
α-pinene
limonene
γ-terpinene
sabinene
α-cedrene
3-carene
β-phellandrene
β-pinene
ethene
isoprene
camphene
longifolene
methylperoxide
sulfur dioxide
toluene
benzene
methane
Reaction rate with O3 /(reaction rate with O3 + reaction rate with OH) (%)

Deleted:

1461 **Figure 5**. Same format as Fig. 2, but for the fractional importance of the reaction rate with O_3 vs. OH as a function of the relative exposure of O_3 and OH. The curves of biogenics
1462 are highlighted by squares. Also shown are modeled distributions of the relative exposure of O_3 and OH at the Earth's surface (solid line) and throughout the column from the
1463 surface to a height with a pressure of 150 hPa (dashed line). The distributions were calculated from the mean daily concentrations of O_3 and OH as simulated by the GISS
1464 ModelE2.

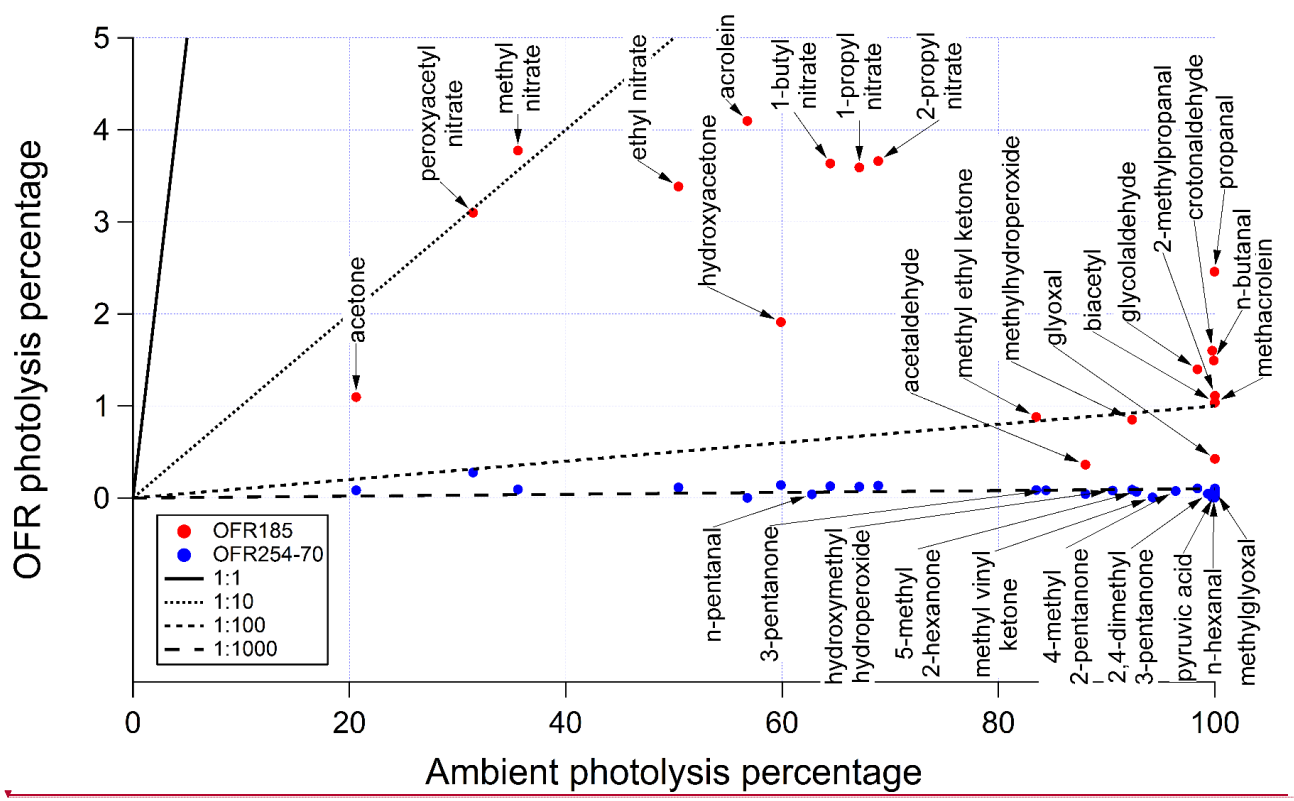

Figure 6. Ambient photolysis fractions of secondary species in a week (calculated from photolysis rates reported in Hodzic et al. (2015)) vs. photolysis fractions of those species in OFR185 and OFR254-70 when reaching the same photochemical age (ambient OH concentration of 1.5×10^6 molecules cm^{-3} assumed) under conditions of 70% relative humidity (water vapor mixing ratio of 1.4%) and 25 s^{-1} initial OHR_{ext}. If the points of a certain species for both OFR185 and OFR254-70 are available, the species name is tagged on the OFR185 point (downward arrow), otherwise on the OFR254-70 point (upward arrow). The 1:1, 1:10, 1:100, and 1:1000 lines are also shown for comparison.

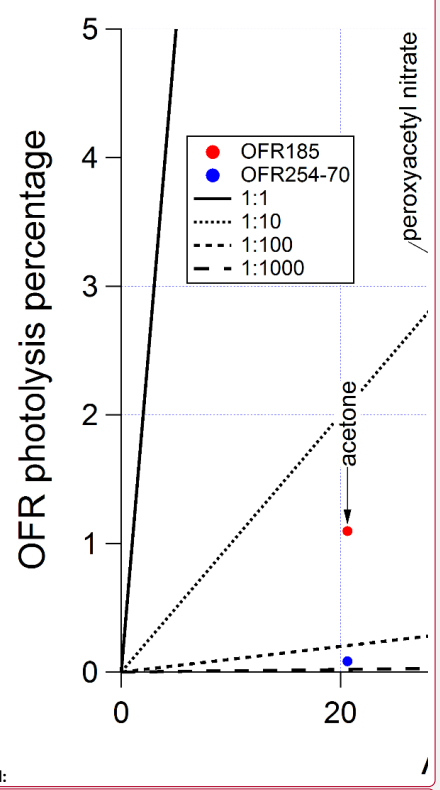

Deleted:

Deleted: . Ambient photolysis percentages of secondary species in a week (calculated from photolysis rates reported in Hodzic et al. (2015)) vs. photolysis percentages of those species in OFR185 and OFR254-70 reaching the same photochemical age (ambient OH concentration of 1.5×10^6 molecules cm^{-3} assumed) under the condition of 70% relative humidity and 25 s^{-1} initial OHR_{ext}. If the points of a certain species for both OFR185 and OFR254-70 are available, the species name is tagged on the OFR185 point, otherwise on the OFR254-70 point. The 1:1, 1:10, 1:100, and 1:1000 lines are also shown for comparison.¶

Page Break

¶

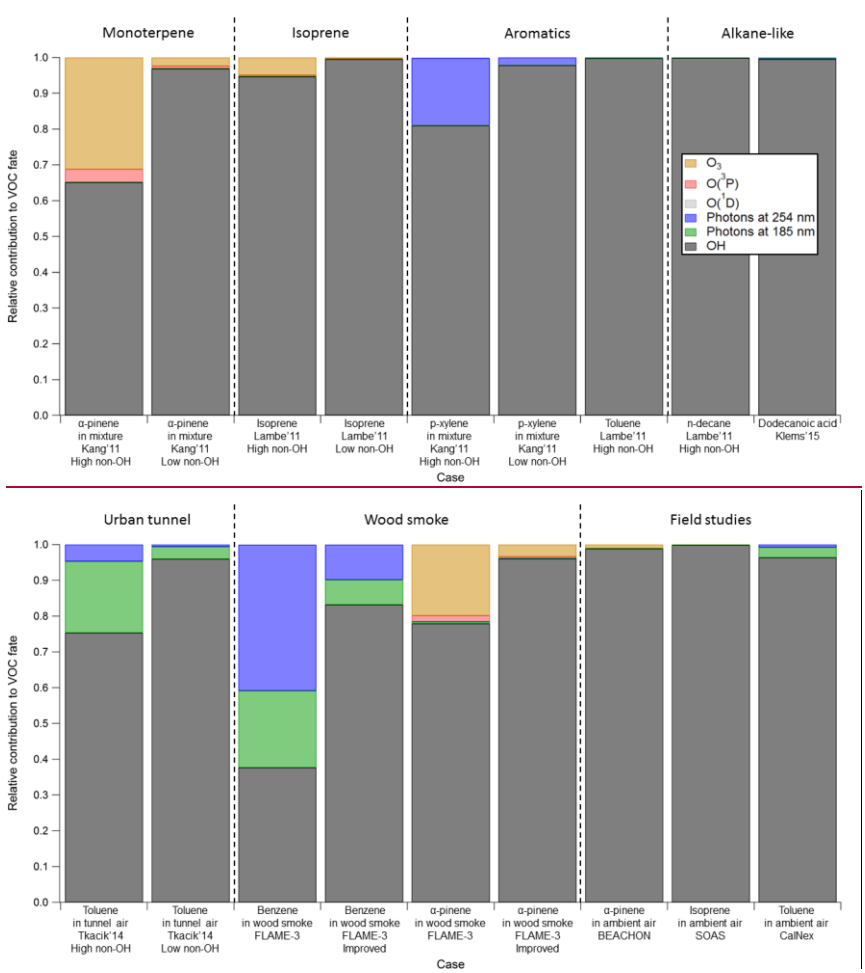

Figure 7. VOC fate in several representative cases of the laboratory, source, and field studies examined in this work. More details on VOC fate in these studies can be found in Table S4.

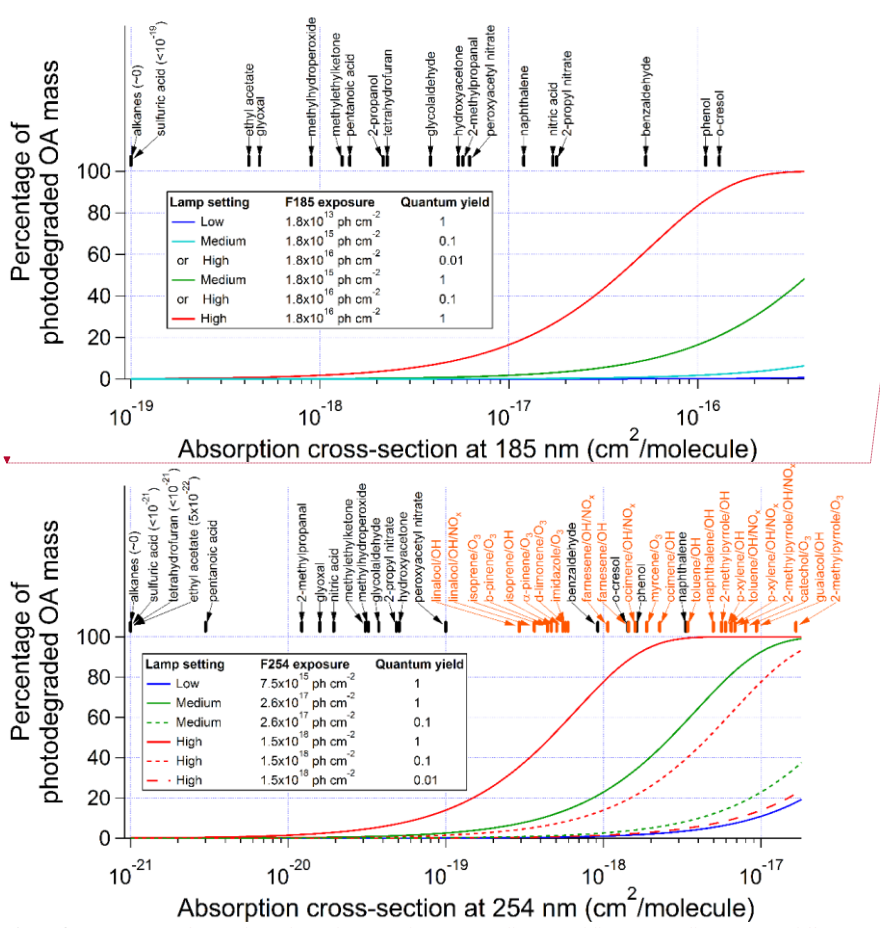

Figure 8. Percentage of SOA photodegradation at (upper panel) 185 and (lower panel) 254 nm at different UV levels as a function of absorption cross-section under the assumptions of quantum yields of 1, 0.1, and 0.01. Absorption cross-sections of some SOA component surrogates (black tag) and SOA samples (orange tag; calculated from data in Lambe et al. (2013) and Romonosky et al. (2015a)) are also shown.

Deleted:

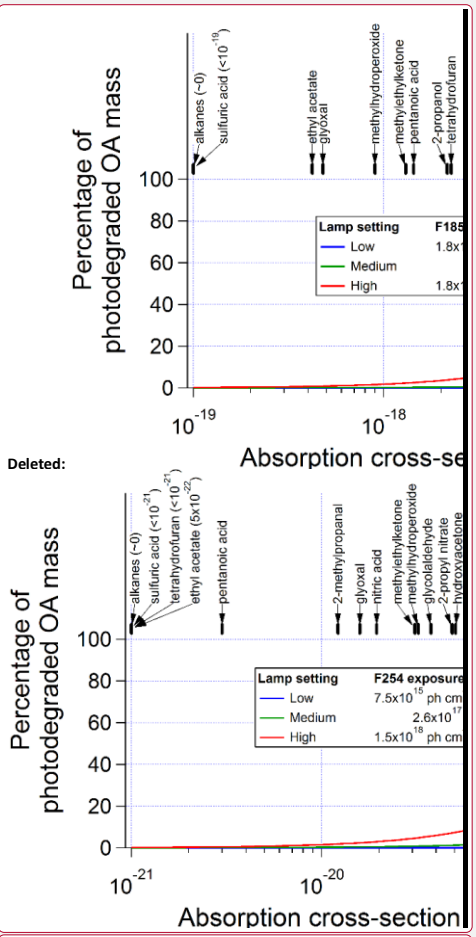

Deleted: . Percentage of SOA photodegradation at (upper) 185 and (lower) 254 nm at different UV levels as a function of absorption cross-section under the assumption of unity quantum yield. Absorption cross-sections of some representative SOA components are also shown.

Table 1. Code of the labels of typical cases. A case label is composed of three characters denoting the water mixing ratio, the photon flux, and the external OH reactivity, respectively.

	Water mixing ratio	Photon flux	External OH reactivity
Options	L=low (0.07%)	L=low (10^{11} photons cm^{-2} s^{-1} at 185 nm; $4.17x10^{13}$ photons.cm^{-2} s^{-1} at 254 nm)	0
	M=medium (1%)	M=medium (10^{13} photons cm^{-2} s^{-1} at 185 nm; $1.45x10^{15}$ photons cm^{-2} s^{-1} at 254 nm)	L=low (10 s^{-1}) typically for remote or clean urban air
	H=high (2.3%)	H=high (10^{14} photons cm^{-2} s^{-1} at 185 nm; $8.51x10^{15}$ photons cm^{-2} s^{-1} at 254 nm)	H=high (100 s^{-1}) typically for polluted urban air
		"L"=lowest in Li et al. (2015)'s PAM ($7.9x10^{11}$ photons cm^{-2} s^{-1} at 185 nm; 2.04 $x10^{14}$ photons.cm^{-2} s^{-1} at 254 nm)	V=very high (1000 s^{-1}) only for laboratory experiments
Example	LH0:	low water mixing ratio, high photon flux, no external OH reactivity	